Some aspects of the theory of transport in disordered systems

Kuljinder S. Chase

Thesis submitted for the degree of
Doctor of Philosophy of the University
of London and the Diploma of
Imperial College

Solid state Theory group
Department of Physics
The Blackett Laboratory
Imperial College of Science and Technology
London SW7 2BZ

September 1986

Abstract

The statistical behaviour of the conductance in two and three dimensional disordered systems is considered by numerical means.

Following a brief review of some concepts in the theory of localization relevant to this work, a numerical algorithm used to study the statistics of the conductance is discussed, and its derivation illustrated for the density of states.

The statistical behaviour of the conductance is examined and it is found that in any dimension, if the eigenstates are localized then the conductance is a non self-averaging quantity. The variance of the logarithm of the conductance is found to scale with the mean of the logarithm of the conductance <lng>.

The scaling theory of localization is verified in two dimensions by direct calculation of the beta function.

The connection between fluctuations in the density of states and fluctuations in the conductance is explored, by introducing a simplified model consisting of a disordered unit cell periodically continued to infinity in one direction. It is found that fluctuations in the conductance of this model, are qualitatively similar to those found before. The density of states of such a system is shown to be discrete and some preliminary investigations into the nature of the fluctuations in one dimension are presented.

We conclude by examining the electronic properties of the one dimensional quasicrystal. The band structure is shown to be a Cantor set, and the wavefunctions found to be selfsimilar. It is shown that states at the band centre cannot be localized.

Table of contents

Abstract 2

Figure captions 4

Acknowledgements 9

1. Introduction and survey 11

2. Review 16

3. A numerical algorithm for investigating the electronic properties of random systems. .. 34

4. The statistics of the conductance in two and three dimensions 60

5. Scaling of the conductance in two dimensions 82

6. A study of the measure of the spectrum and its connection to the statistics of the conductance 90

7. The electronic properties of the one dimensional quasicrystal. 124

References 163

Figure captions

Fig 2.1 The average density of states of a disordered system. The mobility edges are indicated by E_c

Fig 2.2 The form of the beta function dlng/dlnL, in one two and three dimensions.

Fig 3.1 The sample is composed of slices, labeled by integers N. Its size is increased by adding additional slices.

Fig 3.2 The density of states of a disordered chain of 100 atoms at disorder unity, as a function of energy.

Fig 3.3 The density of states of a disordered chain of 250 atoms at disorder unity. Notice that the structure is sharper then in the diagram above.

Fig 4.1 The logarithm of the variance V of Lng plotted against the average of Lng, in two dimensions.

Fig 4.2 The variance V of Lng plotted against the average of Lng, in two dimensions.

Fig 4.3 The variance V of Lng plotted against the average of Lng, in three dimensions.

Fig 4.4 The variance V of Lng plotted as a function of system size in three dimensions. For clarity only some typical error bars are shown.

Fig 4.5 The variance V of Lng plotted against the average of Lng, in one dimension.

Fig 5.1 The beta function, defined as d<lng>/dlnL ,plotted against the average of lng. The dashed line is the perturbative prediction $\beta(g) = -1/g$. The points that deviate most from this line, correspond to small systems at low disorders.

Fig 5.2 The two different beta functions obtained from eqn{5.2} and eqn{5.3} respectively.

Fig 5.3 The beta function of fig[5.1] after the approximate correction outlined in the text. The agreement with the scaling prediction is now much better.

Fig 6.1a The density of states of a three dimensional cube of dimension 4^3, at a disorder W = 5.

Fig 6.1b Same as in fig[6.1a] but now for a cube of dimension 8^3. Notice that density of states is getting smoother.

Fig 6.2 The density of states of a system consisting of a disordered unit cell periodically continued to infinity in one direction, calculated using the algorithm of section 6.3.

Fig 6.3 The proportion of band P plotted against the size of the unit cell, for a one dimensional system at disorder W = 1. The error bars are not significant.

Fig 6.4 The modulus of the logarithm of P plotted against the unit cell dimension for one dimensional systems at disorders W = 1 and W = 2.

Fig 6.5 The proportion of band P plotted against unit cell dimension, for a two dimensional system at various values of the disorder parameter W.

Fig 6.6 The modulus of the logarithm of P plotted against the unit cell dimension for a two dimensional systems at disorder W = 10.

Fig 6.7 The proportion of band P plotted against unit cell dimension, for a three dimensional system at various values of the disorder parameter W.

Fig 6.8 Plots of the density of states and conductance vs the position of the Fermi-level, for a one dimensional system consisting of one hundred atoms at disorder W = 1.

Fig 6.9 Plots of the density of states and conductance vs the position of the Fermi-level, for a one dimensional system consisting of two hundred and fifty atoms at disorder W = 1.

Fig 6.10 The density of states of a one dimensional system whose length is ten times the localization length. Some peak values of the density of states and conductance, obtained by increasing resolution, until no more change was detected are labeled.

Fig 6.11 The inverse participation number P^{-1} as a function of energy, for one dimensional chains of 1000 atoms at disorders W = 1 and W = 4.

Fig 7.1 The grid projection method. All points within the window formed by the solid and dashed parallel lines are projected perpendicularly onto the solid line.

Fig 7.2 The rational approximants to the irrational golden mean.

Fig 7.3 The density of states of a one dimensional quasicrystal, under increasing energy resolution.

Fig 7.4 The spectrum of successive periodic approximations to the quasicrystal.

Fig 7.5 a, b and c. The modulus of the wavefunction as a function of position at the band centre, for V_S/V_L = 2 and several different system sizes.

Fig 7.6 The Logarithm of the inverse participation number plotted against the logarithm of the number of sites, at the band centre, for different values of V_S/V_L.

Fig 7.7a The modulus of the wavefunction as a function of position, at the edge of the spectrum. $V_S/V_L = 2$.

Fig 7.7b The modulus of the wavefunction as a function of position, at the inner edge of the outermost sub-band of W_3. Notice that fig[7.7a] is at the outer edge of this sub-band.

Fig 7.7c Same as Fig 7.7a but on an expanded scale to show that the self-similarity, holds to the smallest length scales.

Fig 7.7d Same as 7.7b but at the edge of the middle sub-band of W_3.

Fig 7.8 The Logarithm of the inverse participation number plotted against the logarithm of the number of sites, at the edge of the spectrum, V_S/V_L. = 2.

Fig 7.9 A Localized wavefunction, in the spectrum of the quasicrystal.

Fig 7.10 The standard map. Two typical trajectories are illustrated; A) a trajectory which starts within the band and cycles and B) a trajectory which starts outside the band and escapes.

Fig 7.11 Decimating the quasicrystal. The three different situations are illustrated and the site to be decimated is circled in each case.

Fig A2.7.1 The manifold upon which the trace mapping moves (from the paper of Kohmoto).

Fig A2.7.2 The manifold for a perfectly ordered system.

Acknowledgements

It gives me great pleasure to acknowledge the many people, whose support and encouragement have made my three years as a research student both enjoyable and memorable.

In particular I would like to express my gratitude to Dr Angus MacKinnon, for many hours of patient, cheerful and enthusiastic supervision, and for his expert assistance during my many duels with the computer.

I should also like to take this opportunity to thank :-

Dr David Elderfield, Dr Dimitri VVedensky, Dr Nick Rivier and Dr Paul Goldbart for many stimulating and enthusiastic explanations,
Dr Elle Castano for reading, and providing a sympathetic ear during the writing of this thesis,
Tony Lawerence for his interest and many useful discussions on the contents of chapter 7,
Professor J. B. Pendry for useful comments,
James Maclaren and Philip Rous for their help with the Cray, and their ability to find the humorous side of even the gravest situation, and SERC for financial support.

On the non academic front, I am deeply indebted to Dr K. Frimpong Ansah, Dr Alan Kwabwe, Kumar Singarajah and Chandra Patni, who have ensured that life was always interesting during my years at Imperial College.

A statistican waded confidently into a river of average depth one metre. He drowned.

G. Bomans

Chapter 1

Introduction and survey

Disorder has a spectacular effect upon the electronic properties of physical systems. Localization of the eigenstates leads to corrections to the classical conductivity, which can turn what may have been good conductors into insulators, and makes possible the observation of phenomena such as the Quantum Hall effect.

Since the pioneering work of Anderson(1958) which predicted that localization of eigenstates was possible and related its onset to a critical degree of disorder, there has been much effort expended in trying to include quantum mechanics into a microscopic theory of transport. See Thouless(1974) for a review. Amongst the notable early successes was the prediction by Mott and Twose(1961) that all states were localized for an infinitesimal amount of disorder in one dimension, and the concept of a mobility edge separating localized and extended states, Mott(1968).

However the physics of disordered systems is now known to be much richer then was at first thought, so it is not surprising that a coherent theory of transport in random systems did not surface until recently. A scaling theory which emphasized the role of the dimensionless conductance as the only relevant coupling was formulated by Abrahams, Anderson, Licciardello and Ramakrishnan(1979), and Wegner(1979), and is to date the most widely accepted theory of localization. Since the original formulation a whole multitude of effects have been incorporated into the scaling framework and, it now constitutes the most systematic theory of transport in random systems. It is still however based upon a hypothesis, that the dimensionless conductance is the only relevant variable, which has only partially been confirmed by perturbative calculations in the weak disorder limit, Wegner(1979), Gorkov et al(1979) and by numerical

simulations, Mackinnon and Kramer(1981), and is still a subject of some controversy.

Because of the complications introduced by disorder, much of the work to date has concentrated on calculating averages with the tacit assumption that the quantities of interest self-average. It was realized by Anderson et al(1980) that in one dimension this assumption was incorrect, the resistance did not self-average and further more its distribution expanded with system size. Thus simple averages were not meaningful, but they managed to show that the logarithm of the resistance was a self-averaging quantity. Much work has since been done in one dimension mainly through the use of transfer matrix techniques, through which it is possible to obtain the whole distribution, Kirkman and Pendry(1984). These techniques are however difficult to extend to two and three dimensional systems. It was generally believed that non self-averaging was a peculiarity of one dimension, and that the distributions would be much better behaved in higher dimensions.

This thesis constitutes an attempt to study the behaviour of the probability distributions of the conductance in two and three dimensions. As analytical work is particularly difficult, we have chosen to examine the distributions numerically using a particularly efficient algorithm, MacKinnon(1985), which allows reasonably large systems to be examined. Such a study has two purposes:-

1) To investigate whether non self-averaging fluctuations are solely a feature of dimensionality and,
2) If not what is the nature of these fluctuations and what consequences do they have for the scaling theory of localization.

The level of sophistication of recent experiments, on thin films and MOSFET's, of dimensions small enough to observe the effects of electron localization suggests that

experimental investigations into the sample to sample behaviour of the transport coefficients are now feasible.

Whilst the majority of this thesis is concerned with fluctuations of transport coefficients, there is one slightly anomalous chapter, which investigates the electronic properties of one dimensional quasicrystals. These are similar to the much studied incommensurate systems, Sokoloff(1985) but differ fundamentally in that there is a minimal separation between points, and they are composed from a finite number of units, which repeat in an almost periodic manner. The study of these systems is motivated by the discovery by Shechtman et al(1984) of an icosahedral phase in an alloy of Aluminium and Manganese, which is the three dimensional counterpart of the system we study, and the construction by Merlin et al(1985) of a quasicrystalline superlattice structure. Further the eigenstates of incommensurate systems in general are thought to be characteristic of states at the mobility edge, so we may learn something about real disordered systems.

The layout of this thesis is as follows. Chapter 2 contains a brief review of some central ideas in the physics of disordered systems, which are important to the content of this thesis. More extensive discussions can be found in the recent reviews of Lee and Ramakrishnan(1985) and Thouless(1985).

In chapter 3 we discuss in some detail the algorithm we shall use in later chapters to examine certain features of the probability distributions of the conductance. The derivation of the algorithm is illustrated for the density of states. Particular attention is paid to the problems of trying to study finite systems and the resolution of these difficulties by embedding the disordered sample in a perfect medium.

A study of the variance of the conductance in two and three dimensions, calculated over an ensemble of systems, using the algorithm of chapter 3 forms the content of chapter 4. The self-averaging properties of the conductance are discussed and the consequences of these upon the scaling theory of localization examined. Our results are compared with the recent predictions of Lee and Stone(1985) and Altshuler(1985) concerning universal conductance fluctuations. Most of the results of this chapter have appeared in Chase and MacKinnon(1985).

Chapter 5 is a short chapter in which we explicitly check the predictions of the scaling theory of localization, in two dimensions, by direct evaluation of the beta function, using the algorithm of chapter 3. This has several advantages over previous numerical verifications of scaling in that we deal with real two dimensional systems rather then quasi one dimensional strips. Some recent objections to scaling are discussed.

In chapter 6 we explore the connections between fluctuations in the density of states and those in the conductance. A simplified model consisting of a

disordered unit cell periodically continued to infinity in one direction, which allows us to study the measure of the spectrum is introduced and an algorithm for its study derived. It is shown that fluctuations in this model are similar to those observed in chapter 4, and some differences between this model and real disordered systems discussed. Finally some preliminary investigations into the nature of these fluctuations are presented.

The electronic properties of the one dimensional Quasicrystal are investigated in chapter 7. It is shown that the band structure of such a system is very singular and self-similar. The properties of the wavefunctions at the centre of the band are investigated in detail and it is shown that they cannot be localized. Wavefunctions at other points of the band are briefly discussed, and are also found to be self-similar. Finally in Appendix 7.1 we discuss properties of the transfer matrices for this system and in Appendix 7.2 show how our model can be mapped onto a model studied by Kohmoto et al(1983).

All equations are numbered sequentially within each chapter and most diagrams appear opposite or immediately after the page upon which they are referred.

Chapter 2

Review

In this chapter we give a brief review of some key concepts and ideas, which form the basis of our present understanding of the localization problem, and which are either used, or referred to, in this thesis. Localization has been a field of much activity over the past twenty five years or so, and there exists a vast amount of literature on the subject. We shall not try to review all the important ideas, but shall concentrate on those most relevant to the subject of this thesis, and refer the reader to the excellent review of Lee and Ramakrishnan(1985), for a more complete picture.

2.1 Models of disorder

There are several ways of introducing disorder into an otherwise perfect system. We can start with an ordered lattice and replace atoms at random, whilst retaining the underlying structure of the lattice. This is known as substitutional disorder and is an example of the type of disorder found in alloys. Alternatively instead of changing atoms, we can change the topological structure of the lattice by cutting bonds at random. This is known as topological disorder and is found for example in amorphous materials such as silicon. The vast majority of work has concentrated on substitutionally disordered systems because the underlying lattice allows for a relatively simple formulation. By contrast topologically disordered systems are much more difficult to analyze and their electronic properties are generally assumed to be similar to those of substitutionally disordered systems, but this may not be true. Indeed it is known that their bands do not have purely exponential tails.

In common with most other work on localization we shall concentrate on substitutional disorder in this

thesis and further will consider only the simplest Hamiltonian necessary to observe the effects we are interested in. Effects such as electron-electron interaction, electron-phonon interaction, spin-orbit scattering, etc will be ignored. These are no doubt important but are rather complicated and their effects on even the average conductance is not yet fully understood, and besides systems in which these effects are small are experimentally realized.

The Hamiltonian we shall study is the tight binding Anderson Hamiltonian

$$H = \Sigma \; |i\rangle \varepsilon_i \langle i| + \Sigma \; |i\rangle V_{ij} \langle j|$$

Where the $|i\rangle$'s are Wannier functions located at the sites of a regular lattice. ε_i are random site energies and the V_{ij}'s are matrix elements connecting sites i and j. We shall take these to be constant and between nearest neighbours. We shall refer to two variations of this Hamiltonian in this thesis. The diagonally disordered model in which the hopping elements are constant and the off diagonal disorder model in which the site energies are fixed and the hopping elements allowed to vary.

2.2 The density of states of random systems

Disorder as well as effecting the transport properties has a dramatic effect upon the density of states. The average density of states is a well studied quantity and is known to be smooth and continuous. The Van Hove singularities of the corresponding ordered system are rounded off and for sufficient disorder vanish altogether. Moreover the band edges are no longer sharp, the bands develop exponential tails, a point first considered by Liftshitz(1964). These arise from deep potential fluctuations, and are a non perturbative effect. The exact form of these tails has been calculated by Brèzin and Parisi(1983) using instanton methods. The

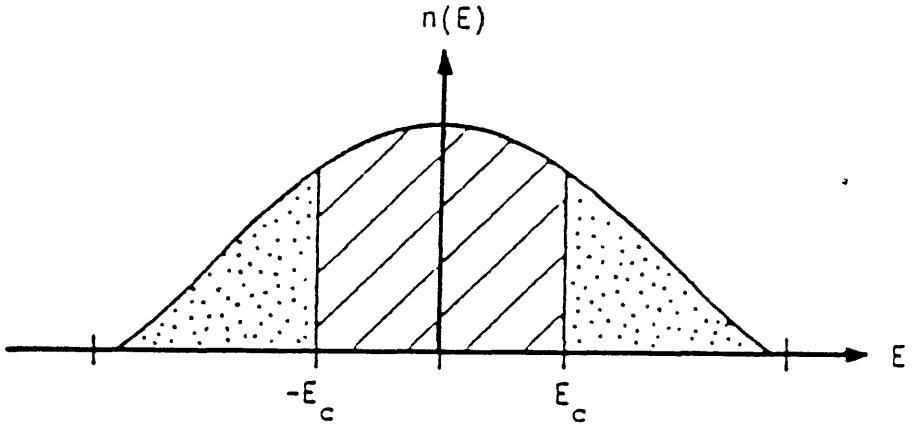


Fig 2.1 The average density of states of a disordered system. The mobility edges are indicated by E_c

states in the tails of the band are more likely to be localized as they arise from deep potential fluctuations. Mott has argued that localized and extended states must be separated in energy by a mobility edge, because localized and extended states cannot coexist. The expected form of the average density of states is illustrated in fig[2.1].

The average density of states though contains no information about localization and has been proven to be analytic across the mobility edge, Wegner(1981).

However the unaveraged local density of states contains much information on localization. In the thermodynamic limit it is known to be continuous on the energy interval for which the eigenstates are extended, and consist of a dense distribution of poles, on the interval where the eigenstates are localized, Economou(1983). In fact this is closely related to the original criterion used by Anderson(1958) to distinguish between localized and extended states. Sect 2.4.

The form of the unaveraged total density of states does not seem to be clear from the literature, some authors believe it to be smooth and self-averaging, whilst rigorous studies of localization, Kunz and Soulliard(1980), distinguish between localized and extended states by studying the analytic nature of the spectrum. Extended states correspond to the continuous part of the spectrum, whilst localized states correspond to the discrete part.

In this thesis we shall take a physicist's point of view and instead of considering infinite systems, we shall consider the physical situation of a random system coupled to perfect leads. Whenever we refer to the density of states we mean that obtained by taking the sum of the local density of states over the disordered region only. For this system the density of states appears to become discrete as the system size is increased when the eigenstates are expected to be localized. Sect 3.6. In

this sense we would agree with the idea of a discrete spectrum in the thermodynamic limit. This is an important point for it implies that an electron in the leads, which have a continuous spectrum, will in general not find a state in the disordered sample of the same energy, and will in effect have to tunnel through it. We shall explore this in more detail in chapter 6.

2.3 Electron localization

Before 1958 it was thought that the sole effect of disorder on the electronic wavefunctions was to cause a loss of phase coherence over distances of the order of the mean free path, and that the amplitude of the wavefunctions was relatively uneffected in that they remained extended throughout the system. These arguments were based upon classical transport theory and gave a conductivity which behaved as

$$\sigma = ne^2\tau/m$$

Where n is the electron density and τ the mean free time.

In 1958 Anderson, by working from the opposite extreme of weakly interacting tightly bound orbitals and treating the coupling as a perturbation, pointed out that if the disorder was sufficiently strong the eigenstates may become localized in that the envelope of the wavefunction decays exponentially from some point in space.

$$|\Phi(r)|^2 \sim \exp(\alpha|r-r_0|)$$

The length scale α^{-1} associated with this decay is known as the localization length. These states are normalizable, and hence cannot carry a current. The original work of Anderson was rather complicated and relied on probabilistic arguments to determine the convergence of the self-energy. Subsequently these ideas

were given much physical basis by the work of Mott, who proved the very important result that all states were localized in one dimension for arbitary disorder, and introduced the idea of a mobility edge, which separates localized and extended states in higher dimensions. The next major breakthrough did not come until the mid seventies when Thouless and coworkers began to lay down the initial ideas for what was to become the scaling theory of localization, which we discuss below. A review of these ideas can be found in Thouless(1979).

2.4 Some ways of studying Localization

Direct evaluation of the conductance

There are many different ways of examining the properties of localized states, of which perhaps the most useful have been those that evaluate the conductance, as this turns out in the scaling theory to be the only characteristic quantity. Localized states are normalizable and hence do not carry a significant current whilst extended states can. The conductivity is usually calculated within the linear response regime where the transport properties of a system are probed by examining its response to infinitesimal external fields, without changing the nature of the eigenstates. This is usually achieved by using the Kubo formula which relates the linear response to the equilibrium properties of the system. The Kubo formula and its many variations, Mahan(1981), form the basis of almost all perturbative calculations and numerical simulations. The conductivity can be expressed in terms of the two particle Green's function, the disorder average of which, can be perturbatively calculated by using standard many-body theory, or by mapping onto an equivalent field theory, Wegner(1979). Numerical methods rely on iterative schemes to calculate the conductivity. An example of such a scheme is discussed in Chapter 3, and used extensively in this thesis.

Another method which has been particularly useful in one dimension is to view the problem as that of transmission through a potential barrier. The conductance of the barrier g can be related to the transmission coefficient T, via the Landauer relation, Landauer(1970).

$$g \sim T/(1-T) \qquad \{1.2\}$$

The use of transfer matrix techniques to calculate the transmission coefficient, have proved to be particularly powerful in one dimension. The behaviour of T can be deduced either by using limit theorems for products of random matrices, Johnston and Kunz(1983), or by symmetry reduction, using properties of the symmetric group, Pendry(1982). Using these methods limiting forms for the probability distributions of the resistance and the conductance, have been evaluated, Kirkman and Pendry(1984). An extensive review of transfer matrix techniques can be found in Erdös and Herndon(1982).

Despite the success of these methods in one dimension, extension to higher dimensions has not proved easy. The increase in the number of channels, complicates the relationship between conductivity and transmission probabilities. These appear to depend upon the definition of a channel and are still in much debate, Landauer(1985). In addition the transfer matrices become larger, which complicates their manipulation. However see Pendry(1984).

Analytical properties of the Green's function

The unaveraged local single particle Green's function also contains information about localization. This can be written as

$$G_{00}(E + i\Gamma) = [E + i\Gamma - \varepsilon_0 + \Sigma(E)]^{-1} \qquad \{2.2\}$$

Where $\Sigma(E)$ is the self-energy. Fourier transforming this it is seen that $G_{00}(t)$ decays in time if Σ has a finite imaginary part on the real axis, which is equivalent to Σ having a branch cut. If $G_{00}(t)$ decays in time then so does the probability of finding the particle at the origin, given that it was there at t=0. This clearly means the state is extended. Thus states are extended if the self-energy possesses a branch cut on the real axis.

The original paper of Anderson examined the convergence of the renormalized perturbation expansion of the self-energy, which cannot converge if the self-energy possesses a branch cut.

The analytic properties of the Green's function are identical to those of the self-energy, and it can be shown, Economou(1983) that whilst extended states correspond to that part of the real axis that has a branch cut, localized states are represented by a natural boundary which is a dense distribution of poles for which the side limits $\mathrm{Lim}_{\Gamma->0}\ G(E + i\Gamma)$ do not exist.

We shall use this criterion in chapter 7 to study the properties of the eigenstates at the band centre of a quasicrystal.

The participation number

The participation number P was introduced by Bell and Dean(1970), as a way of distinguishing between localized and extended states directly from the eigenstates. The inverse participation number is defined as

$$P^{-1} = \Sigma\ |\ a_i\ |^4\ /(\Sigma|\ a_i\ |^2\ )^2 \qquad \{3.2\}$$

and is effectively a measure of the volume occupied by the wavefunction. a_i is the amplitude of the wavefunction at site i. For extended states all the a_i are of order $1/\sqrt{N}$ so that the inverse participation number vanishes. For localized states which are localized over a few sites P^{-1} tends to a constant as the system size tends to infinity.

This criterion has been used extensively by Economou and Soukoulis(1984) and Schreiber(1985) who define a fractal dimension d via

$$P \sim N^d \qquad \{4.2\}$$

and study the behaviour of P as a function of system size. For extended states d is expected to be equal to the space dimension, whilst d=0 for localized states.

Economou and Soukoulis(1984) find that at the mobility edge in three dimensions d has a value of 2, and have suggested that the states are fractal, in that they show large amplitude fluctuations. This has also been suggested by Wegner(1979) and by Castellani and Peliti(1986) using field theoretic methods. Schreiber has analyzed the system size behaviour of P and finds that the eigenstates have a powerlaw decay over short length scales.

We shall use this to study the wavefunctions of the one dimensional quasicrystal in chapter 7, where the energy bands have a Cantor set structure, which makes the use of other methods problematic. More generally the measure of the spectrum is found to vanish for localized states, chapter 6, so that methods which rely on direct computation of the conductance are probably measuring properties of the gap. The participation number checks the properties of eigenstates explicitly. A closely related quantity which is often used is the participation ratio, which is essentially the participation number divided by the volume of the system L^d, and measures the fraction of states which contribute to a state.

2.5 The scaling theory of localization

The scaling theory of localization is currently the most widely accepted explanation for the behaviour of non-interacting electrons, in random systems. Originally a hypothesis of Abrahams, Anderson, Licciardello and

Ramakrishnan (1979), based upon some earlier ideas of Thouless(1974) the theory has since been reinforced by much analytical and numerical work.

The essence of the scaling hypothesis is that the change in the dimensionless conductance, $g = G/(e^2/h)$, when the length scale is varied depends only upon the conductance at the previous length scale.ie

$$d\ln g/d\ln L = \beta(g) \qquad \{5.2\}$$

This hypothesis was prompted by considering the system to be made up of many blocks, coupled together by an effective interaction, rather like the ideas of real space renormalization. In such a picture, there will in general, because of the disorder, be a mismatch between energy levels in neighbouring blocks. The chances of an electron being able to pass from one block to another, depend upon the probability of it being able to find a complementary level in a neighbouring block. This is determined by the ratio of the average width of a level, to the spacing between levels. $\delta E/\delta W$. Thouless(1974) has shown that δE can be approximated by the average shift in energy of a level, when boundary conditions are changed from periodic to antiperiodic. δW is just the inverse density of states. In addition Edwards and Thouless(1972) showed that the conductance of a block, was essentially given by the same quantity $\delta E/\delta W$. Thus the coupling between blocks is determined by the conductance of an individual block.

Now it is reasonable to assume that the conductance of the composite system will be determined by the coupling between blocks, which by the arguments outlined above is itself given by the conductance of a block. Hence the conductance of the composite system is determined only by the conductance of a block. For infinitesimal changes in scale this relationship can be expressed in the form of eqn{5.2}.

Although the arguments outlined above are rather tenuous, the scaling form has been supported by

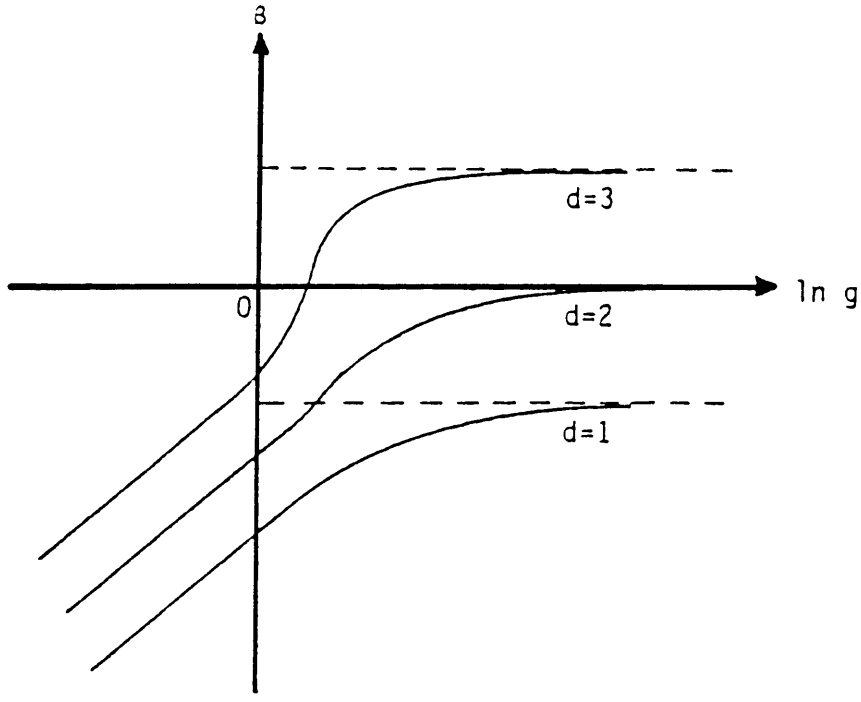


Fig 2.2 The form of the beta function dlng/dlnL, in one two and three dimensions.

perturbative calculations, Anderson, Abrahams and Ramakrishnan(1979) and Gorkov, Larkin and Khmelnitskii(1979) in the weak disorder limit, and by the mapping of the localization problem onto an equivalent field theory, Wegner(1979). The scaling form appears naturally in the field theoretic formulation where it turns out that g, the dimensionless conductance, is the only relevant coupling.

The dominant contribution to the corrections to the conductance, in the perturbative expansions comes from the maximally crossed diagrams, which depict those events in which an electron and a hole scatter off the same set of impurities in the same order. This implies a change in momentum of p to -p for the electron and -p to p for the hole, and has been interpreted as correlated backscattering by Bergmann(1984), who has shown that these terms are a result of quantum interference, rather like the Aharanov Bohm effect. This has been demonstrated in the experiment of Sharvin and Sharvin(1981}, who showed that the conductance oscillated as a function of an applied magnetic field, and the numerous experiments on small metal rings since, Büttiker et al(1985).

The form of the scaling function $\beta(g)$ in the asymptotic limits of weak and strong disorder can be easily deduced. In the metallic regime we expect that Ohms law is valid so that $g = \sigma L^{d-2}$. This leads to $\beta(g) = (d-2)$. In the strong disorder limit we expect that states are exponentially localized so that g decreases exponentially with system size $g \sim \exp(-\alpha L)$. In this limit $\beta(g) = \ln g$. The weak disorder regime is accessible to perturbation theory and leads to

$$\beta(g) = (d-2) - a/g \qquad \{6.2\}$$

Thus the form of the scaling functions is expected to be that shown in fig[2.2].

In one and two dimensions $\beta(g)$ is always negative and hence one always scales towards weak coupling and localized states. Thus we are led to the surprising result that in two as well as in one dimension all states are localized.

In three dimensions $\beta(g)$ changes sign at some critical conductance g_c and thus we have a nontrivial fixed point. Furthermore the fixed point is repulsive so that there are two regimes. For $g > g_c$ one scales towards the Ohmic regime and extended states, whilst for $g < g_c$ one scales toward weak coupling and localized states. The critical disorder, which characterises the point at which all states are localized, is now accepted to be around $W = 14$ to $W = 16$, and the critical exponent with which the conductance goes to zero is generally agreed to be unity, although there is still some controversy over this point. Furthermore the conductivity goes to zero continuously at the mobility edge so that the transition is of second order.

The scale dependence of the conductance in the weak disorder limit can be obtained from eqn{6.2}, which gives

$$\sigma(L) = \sigma_0 - (e^2/h\pi)[L - m] \qquad d = 1$$

$$\sigma(L) = \sigma_0 - (e^2/h\pi^2)\ln[\tfrac{L}{m}] \qquad d = 2 \qquad \{7.2\}$$

and

$$\sigma(L) = \sigma_0 - (e^2/h\pi^3)[\tfrac{1}{m} - \tfrac{1}{L}] \qquad d = 3$$

where m is the lower length scale cutoff. L is the smallest of the upper length scale cutoffs, which at T=0 is given by the system size. At finite temperatures it is the inelastic scattering length. Inelastic scattering suppresses localization because it allows electrons in localized states to be scattered into other localized states close in energy.

Besides perturbation theory, numerical simulations have been instrumental in providing justification for

scaling. These normally use finite size scaling on long strips to study the behaviour of the smallest Lyapunov exponent, which determines the localization length, MacKinnon and Kramer(1981) and Pichard and Sarma(1981).

We should mention that scaling is still a conjecture which has only been partially verified, and there are still objections in the literature, Efetov(1985), Ioffe et al(1985}. We shall examine the scaling hypothesis in two dimensions by numerical means, in chapter 5, and shall discuss some of the objections there.

2.6 Fluctuations and non self-averaging

Statistical mechanics aims to deduce the macroscopic properties of complex many particle systems from the microscopic behaviour of their constituents.

For a system in thermodynamic equilibrium physical quantities are time averages over an appropriate interval of time, and determination of, for example, the pressure or suceptibility are normally made over time intervals during which the configuration of the system changes randomly due to collisions or thermal fluctuations. These time averages are rather difficult to calculate as it is unfeasible to follow the time development of 10^{23} particles let alone specify initial conditions. So following Gibbs, one usually introduces an ensemble of systems, each suitably randomised and averages over the ensemble at a fixed time. For ergodic systems the two averages are identical.

One also has to calculate fluctuations around these averages, and if the averages are to be meaningful ie correspond to what is physically observed, the relative fluctuations must be small. This is true in general for almost all thermodynamic quantities, in the absence of quantum effects, where the fluctuations decrease as the number of particles in the system increases. These

systems are said to be self-averaging. In general relative fluctuations in physical quantities decrease as $1/\sqrt{N}$ for classical systems, and this is usually a consequence of the central limit theorem.

When quantum effects become important self-averaging may fail due to correlations between particles. An example of this is the case of fluctuations in density of a Bose gas within the grandcanonical ensemble. The relative fluctuations go as

$$\delta n/\langle n\rangle = (1 + 1/\langle n\rangle)^{1/2} \qquad \{8.2\}$$

and so even in the thermodynamic limit the fluctuations are comparable to the number of particles. These fluctuations have been observed in photon beams and are a result of interference between photons. Essentially when the photon density is high the probability of interference between them is also high. This results in destructive or constructive interference between them, depending upon their phase relationship, so that the interference of two photons leads to somewhere between zero and four times the intensity.

On introducing quenched disorder into the system we are faced with a problem somewhat similar to that discussed above. We cannot specify the value of the disorder parameter at each point, only some global parameter such as its average or its distribution, so we suppose that the precise nature of the randomness is irrelevant and average over the disorder. If the disorder is uncorrelated at each point and its value selected from a distribution $P[\{\varepsilon\}]$ the disorder average is given by

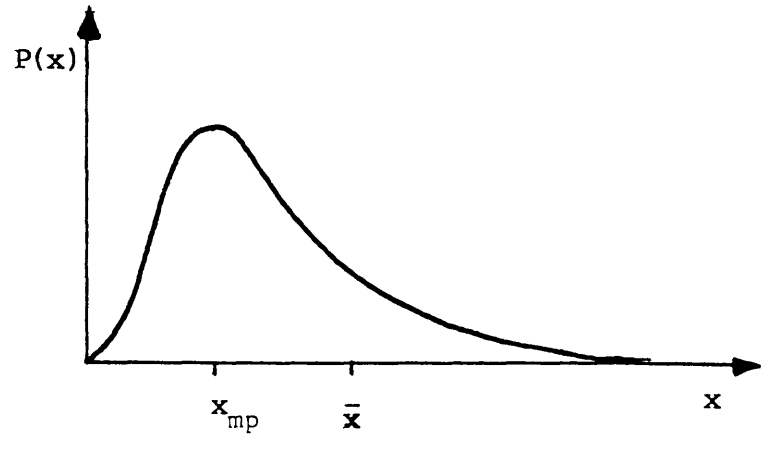
$$\langle F\rangle = \int D\varepsilon\ P[\{\varepsilon\}]\ F[\{\varepsilon\}] \qquad \{9.2\}$$

This is analagous to the Gibbs procedure of introducing an ensemble which contains systems with all realizations of disorder. Any real solid is a member of this ensemble.

As in the statistical mechanics of undisordered systems we must calculate fluctuations to check whether the ensemble averaged quantities are physically realized for any one system. These fluctuations have turned out to be very difficult to calculate, so there has been a tendency to rely on heuristic arguments for self-averaging such as the following:-

Any macroscopic system can be partitioned into a large number of subsystems, each of which is large enough for statistical mechanics to apply. Each subsystem has a different realization of the disorder and if the quantities we wish to calculate do not depend on long range correlations the system will, in the thermodynamic limit, explore all realizations of the disorder and therefore self average.

The first indication that this argument might fail, for response functions came with the development, over the last few years, of more rigorous methods for dealing with one dimensional systems. Anderson et al (1980) showed, using transfer matrix methods, that the relative fluctuations in the resistance increased with system size. The probability distribution of the resistance was found to have long tails which biased the average, and the width of the distribution increased with increasing system size or disorder. Thus the resistance of a disordered chain is extremely sensitive to the precise details of the disorder, and furthermore the presence of long tails in its distribution means that the average will differ markedly from a typical resistance.



A typical resistance is the most probable.

The probability distributions of the resistance and conductance have been determined in the weak and strong disorder limits by Kirkman and Pendry(1984).

From a scaling point of view the situation was highly unsatisfactory as $\langle R \rangle \neq 1/\langle g \rangle$ and furthermore no simple scaling relationship for the conductance could be found. Clearly what was required was some quantity which was characteristic of the ensemble. In their same paper Anderson et al were able to show that $\mathrm{Ln}(1+R)/L$ the inverse localization length was such a quantity, its distribution obeyed a weak form of the central limit theorem, so that in the thermodynamic limit it was the same for each member of the ensemble. They called the resistance defined by $\langle \mathrm{Ln}(1+R)/L \rangle$ a scale resistance. It is in some sense the most probable value of the resistance, as it is essentially the geometric mean which, for distributions with long tails at infinity, is always closer to the peak of the distribution then the arithmetic mean.

In higher dimensions the situation is not as clear, mainly because analytical results are much more difficult to obtain, and it was generally believed that the conductance and resistance would self-average. One dimensional systems were viewed as being slightly pathological in that the electron had to scatter from all the impurities, in traversing the sample. We shall examine this more closely in chapter 4, and show that non self-averaging is characteristic of localized states and not a peculiarity of one dimension.

Other recent work includes that of Altshuler(1985) and Lee and Stone(1985), who have extended the impurity diagram technique to calculate the fluctuations in the conductance, in the weakly localized regime. These authors find that the fluctuations are scale invariant, ie

independent of disorder or system size in this regime, which has been dubbed the 'mesoscopic' regime. We shall compare our results with theirs in chapters 4 and 6. In the strongly localized regime investigations have previously been limited to one dimension.

Azbel(1983) has examined the nature of the fluctuations, in one dimension and developed a qualitative theory based upon resonant conduction. He finds that the conductance as a function of energy consists of a series of sharp peaks, in the vicinity of which the conductance rises relative to an exponentially small value elsewhere, and that the most dominant peaks, ie those which contribute most to the average conductance, correspond to eigenstates localized near the centre of the sample. The number of peaks of transmission unity, and their width in energy, decreases with system size and thus the fluctuations in the conductance diverge. We shall report on some similar investigations in the last part of chapter 6, and shall discuss his theory in more detail there.

Chapter 3

A numerical algorithm for investigating the electronic properties of random systems.

3.1 Introduction

The investigation of the electronic properties of disordered systems is particularly difficult due to the lack of any simplifying symmetries such as translational or rotational invariance. There is no equivalent to Bloch's theorem which allows one to diagonalize the Hamiltonian of an ordered system relatively easily. Analytical methods have been developed in recent years which have predicted many unexpected features such as the absence of extended states in two dimensions, but experimental verification has been very difficult due to the presence of other competing effects that exist in real solids. Even for very simple models these theories involve approximations, the validity of which is usually based on physical intuition rather than mathematical rigour.

Computational methods provide a means of testing these theories for simplified models and are useful for probing effects such as strong localization which are inaccessible to perturbation theory. However numerical methods are not easy to implement because, even in the absence of many body or finite temperature effects, the sizes of systems that can be examined is rather small due to restrictions imposed by computer storage.

Brute force diagonalization for a system of N atoms requires the storage of N^2 quantities which prohibits the study of three dimensional systems of more then about 5^3 atoms, whilst approximate methods for dealing with larger systems have proven ineffective as far as transport properties are concerned. Any approximate scheme must take into account the non perturbative nature of localized states. Localization can only be observed within perturbation theory by summing over an infinite set of terms.

In this chapter we discuss an algorithm which allows us to calculate the conductivity of fairly large systems exactly. This algorithm is originally due to MacKinnon (1985) and various versions have been used in the past to study the scaling behaviour of the conductance, the quantum Hall effect and other properties of non-interacting electrons in disordered systems. We shall use this algorithm extensively to study the statistical behaviour of the conductivity in later chapters. In this thesis we shall only deal with systems which are time reversal invariant. More general versions of this algorithm can be found in the paper by MacKinnon.

The most important feature of this algorithm is that it is recursive and hence places no storage restrictions on the size of systems that can be treated. The systems are however very anisotropic with cross-sections of less than a hundred atoms.

The basis of this algorithm is the Kubo-Greenwood formula for the D.C. conductivity of non-interacting electrons. As discussed in chapter 1 the transport properties of the eigenstates of a system can be probed by their response to infinitesimal external fields. Kubo and others have shown that the conductivity under these conditions can be expressed in terms of the equilibrium correlation functions of the system.

$$\sigma_{\alpha\beta} = \frac{1}{w} \int_0^\infty dt\ e^{iwt} \langle [j_\alpha^+(t), j_\beta(t)] \rangle \qquad \{1.3\}$$

We shall only be concerned with the D.C conductivity of non-interacting electrons at zero temperature. In this limit the Kubo formula simplifies to

$$\sigma_{xx} = \lim_{\Gamma \to 0} \frac{2e^2\hbar}{m^2\pi\Omega} \mathrm{Tr}\{P\,\mathrm{Im}G(E+i\Gamma)P\,\mathrm{Im}G(E+i\Gamma)\} \qquad \{2.3\}$$

for the diagonal component. E is the Fermi energy, V is the volume of the system, P is the momentum operator and G is the one particle Green's function. The imaginary part to the energy is required to define the Green's functions

unambigiously and is normally associated with the adiabatic switching of the perturbation.(Nozières and Pines)

For systems of finite size one has to be very careful as the spectrum is discrete, so that at zero temperature the D.C conductivity will be zero as the Fermi level will almost certainly lie in a gap. Several authors in the past MacKinnon(1980), Thouless and Kirkpatrick(1980) have circumvented this problem by working with a finite imaginary part to the energy. A finite imaginary part in the energy is generally associated with inelastic scattering, or dissipation effects and tends to broaden the spectrum into a continuum. The effects of this on the conductivity are not clearly understood and furthermore the induced broadening of states may change the nature of the spectrum in a fundamental way.

To avoid these difficulties we shall make the system effectively infinite by embedding it in a perfectly ordered medium. This is perfectly physical because in any experiment one has to attach leads to the system to measure its conductivity anyway. The effects of this will be discussed later.

3.2 A recursive algorithm for calculating the conductivity and density of states

In this section we give a brief description of the algorithm. The derivation for the conductance is rather complicated so I shall illustrate the method only for the density of states, and refer the reader to the paper by MacKinnon for the derivation of the conductance.

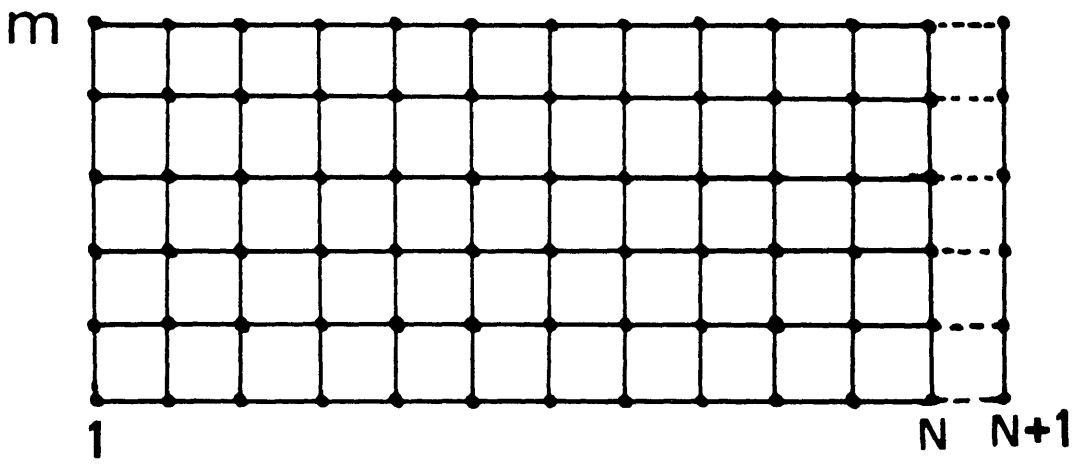


Fig 3.1 The sample is composed of slices, labeled by integers N. Its size is increased by adding additional slices.

Consider the tight binding Anderson model which is defined by the following Hamiltonian.

$$H = \Sigma\ |\underline{i}>\varepsilon_i<\underline{i}| + \Sigma\ |\underline{i}>V_{ij}<\underline{j}| \qquad \{3.3\}$$

The ε_i are site energies and V_{ij} are hopping elements which allow an electron to hop from site i to site j. We assume we have only nearest neighbour hopping so that <ij> means sum over nearest neighbours. The $|\underline{i}>$'s are Wannier functions located at the sites of a regular lattice. The disorder enters through the site energies ε and the hopping elements V, which can be selected from some distribution. From now on we shall label $V_{N,N+1}$ as V_N for simplicity, so that V_i is the hopping element which connects site i and i+1. For simplicity we shall also take V to be real, as we do not deal with magnetic field effects.

The Anderson Hamiltonian has been extensively used to study the electronic properties of random systems and despite its apparent simplicity has been shown to contain the essential features of the localization problem.

We shall work in the site representation, as the Hamiltonian has a particularly simple form. By using the commutation relation [x,H] = 2ihP, and the definition of the Green's function operator $g^{\pm} = (E \pm i\Gamma - H)^{-1}$ the Kubo formula eqn {2.3} can be written in the form

$$\sigma_{xx}(E+i\Gamma) = \frac{4e^2}{NMh}\{\Gamma^2\Sigma g^+_{\underline{i}\underline{j}}X_{\underline{j}}g^-_{\underline{j}\underline{i}}X_{\underline{i}} - i\frac{\Gamma}{2}\Sigma(g^+_{\underline{i}\underline{i}} - g^-_{\underline{i}\underline{i}})X^2_{\underline{i}}\} \qquad \{4.3\}$$

The trace is now simple in the site representation as the X's are diagonal.

Divide the lattice into slices along one lattice direction, and label these slices by integers. Our system is then composed of slices and we may increase its size by adding additional slices, fig[3.1].

In any dimension we can represent the Hamiltonian of the system in a convenient way if rewrite {3.3} in a semi-matrix form.

$$H = \Sigma\ |N\rangle\varepsilon_N\langle N| + \Sigma\ |N\rangle V_N\langle N+1|$$

The N's are integers labelling a slice. The $|N\rangle$'s are vectors in the subspace of a slice. They are of dimension m, where m is the number of atoms in a slice.

$$|N\rangle = \begin{bmatrix} |N1\rangle \\ \cdot \\ \cdot \\ \cdot \\ |Nm\rangle \end{bmatrix}$$

The ε_N's and V_N's are matrices which operate in the subspace of a slice and are of dimension m .

$$\varepsilon_N = \begin{bmatrix} \varepsilon_{N1} & V & & & 0 \\ V & \cdot & & & \\ & & \cdot & & \\ & & & \cdot & V \\ 0 & & & V & \varepsilon_{Nm} \end{bmatrix}$$

The Green's function may be written as

$$(ZI-H)_{ii}G_{ij} - H_{ii+1}G_{i+1j} - H_{ii-1}G_{i-1j} = I\delta_{ij} \qquad \{5.3\}$$

Where the G_{ij}'s are submatrices of the full Green's function and $Z = E + i\Gamma$ is a complex energy.

$$G_{jk} = \begin{bmatrix} g_{j1,k1} & \cdots & g_{j1,km} \\ \cdot & & \\ \cdot & & \\ \cdot & & \\ g_{jm,k1} & & g_{jm,km} \end{bmatrix}$$

and $g_{j1,k1}$ is the element of the Green's function between the site (j1) and the site (k1). Since our Hamiltonian is real it follows that G is symmetric. $g_{ij} = g_{ji}$ and $G^+ = (G^-)^*$

Consider the effect of adding an extra slice to the system of length N. The Hamiltonian for the new system can be written as

$$H^{N+1} = H^{N} + H^{0}_{N+1} + V_N \qquad \{6.3\}$$

Where H^N is the Hamiltonian for the system of length N, H^0_{N+1} is the Hamiltonian of the uncoupled $N+1^{th}$ slice and the V_N's are the hopping elements coupling the $N+1^{th}$ slice to the rest of the system.

We can obtain the Green's function for the system of size N+1 by treating V_N as a perturbation and using Dyson's equation

$$G = G^0 + G^0 V G \qquad \{7.3\}$$

Where $$G^0 = G^N + |N+1\rangle (ZI - H^0_{N+1})^{-1} \langle N+1| \qquad \{8.3\}$$

I is the unit matrix. Thus we have for the matrix elements of G

$$G^{N+1}_{ij} = G^0_{ij} + G^0_{iN} V_N G^{N+1}_{N+1j} + G^0_{i,N+1} V_N G^{N+1}_{Nj} \qquad \{9.3\}$$

In particular

$$G^{N+1}_{ij} = G^N_{ij} + G^N_{iN} V_N G^{N+1}_{N+1,N+1} V_N G^N_{Nj} \qquad 0<i,j<N \qquad \{10.3a\}$$

$$G^{N+1}_{i,N+1} = G^N_{iN} V G^{N+1}_{N+1,N+1} \qquad i<N \qquad \{10.3b\}$$

$$G^{N+1}_{N+1,j} = G^{N+1}_{N+1,N+1} V_N G^N_{N,j} \qquad j<N \qquad \{10.3c\}$$

$$G^{N+1}_{N+1,N+1} = [Z - H^0_{N+1} - V_N G^N_{NN} V_N]^{-1} \qquad \{10.3d\}$$

will be very useful

3.3 The density of states

The density of states is defined as

$$\rho = \frac{-1}{NM\pi} \mathrm{Im}\ \Sigma\ \mathrm{Tr}\ G_{ii} \qquad \{11.3\}$$

Let $$S^N = \sum^{N} \mathrm{Tr}\ G^N_{ii} \qquad \{12.3\}$$

Then $$S^{N+1} = \mathrm{Tr} \sum^{N+1} G^{N+1}_{ii}$$

$$= \mathrm{Tr}\ \left(\sum^{N} G^{N+1}_{ii} + G^{N+1}_{N+1,N+1} \right)$$

using {10.3}

$$S^{N+1} = \mathrm{Tr} \sum^{N} G^N_{ii} + \mathrm{Tr}(\Sigma V_N G^N_{Ni} G^N_{iN} V_N R_{N+1} + R_{N+1}) \qquad \{13.3\}$$

Where we have defined $G^{N+1}_{N+1,N+1} = R_{N+1}$

The first term is just S^N

Let $$F_N = V_N \left[\sum^{N} G^N_{Ni} G^N_{iN} \right] V_N \qquad \{14.3\}$$

Then $$S^{N+1} = S^N + \mathrm{Tr}\left(R_{N+1} [\ F_N + I\ ] \right) \qquad \{15.3\}$$

We now show that F_{N+1} can be also be obtained by recursion

$$F_{N+1} = V_{N+1} \left[\sum^{N+1} G^{N+1}_{N+1,i} G^{N+1}_{i,N+1} \right] V_{N+1}$$

$$= V_{N+1} \left[\sum^{N} G^{N+1}_{N+1,i} G^{N+1}_{i,N+1} + R_{N+1} R_{N+1} \right] V_{N+1}$$

using {10.3}

$$F_{N+1} = V_{N+1} \left[R_{N+1} (\ F_N + I) R_{N+1} \right] V_{N+1} \qquad \{16.3\}$$

With initial conditions $F_0 = 0$

This completes the derivation of the algorithm for the density of states. The closed set of relations {17.3} allow the density of states to be calculated iteratively

$$\rho = \frac{-1}{NM\pi} \text{Im} \sum^{N} \text{Tr}\, G_{ii}$$

$$S^{N+1} = S^{N} + \text{Tr}(R_{N+1}[F_N + I]) \qquad \{17.3\}$$

$$F_{N+1} = V_{N+1}[R_{N+1}(F_N + I)R_{N+1}]V_{N+1}$$

$$R_{N+1} = [Z - H^{0}_{N+1} - V_N R_N V_N]^{-1}$$

Storage requirements are determined only by the number of atoms in a slice because at each stage of the calculation we need only store the latest R and F, which are matrices of size M. Thus starting from a single slice we may obtain the density of states of a system of arbitary length by using the set of equations {17.3}.

Boundary conditions

As mentioned before although the length of the system is arbitary its cross-section is rather small, so that we may wish to impose periodic boundary conditions in the transverse directions to eliminate surface effects. This is easily done by introducing terms in the Hamiltonian of a slice which couple opposite end of the slice.

3.4 The conductivity

A recursive procedure similar to that for the density of states {17.3} can also be developed for the conductivity but its derivation is much more complicated. We quote only the results here, and refer the reader to the paper by MacKinnon for their derivation.

Let us define $$S^{N}_{xx} = \frac{NMh}{4e^2}\sigma^{N}_{xx} \qquad \{18.3\}$$

$$B_N = \Gamma V_N[\sum^{N} G^{N}_{Nj} X_j (2\Gamma G^{N}_{ji} - iI\delta_{ij}) X_i G^{N}_{jN}]V_N$$

$$C_N = \Gamma V_N[\sum^{N} G^{N}_{Nj} X_j G^{N*}_{jN}]V_N$$

Then it can be shown that

$$S_{xx}^{N+1} = \mathrm{Tr}\,[\mathrm{Re}(B_N R_{N+1}) + C_N R_{N+1} C_N^* R_{N+1}] \qquad \{19.3\}$$

Where $$B_{N+1} = V_{N+1} R_{N+1} [B_N + 2\, C_N R_{N+1} C_N^*] R_{N+1} V_{N+1}$$

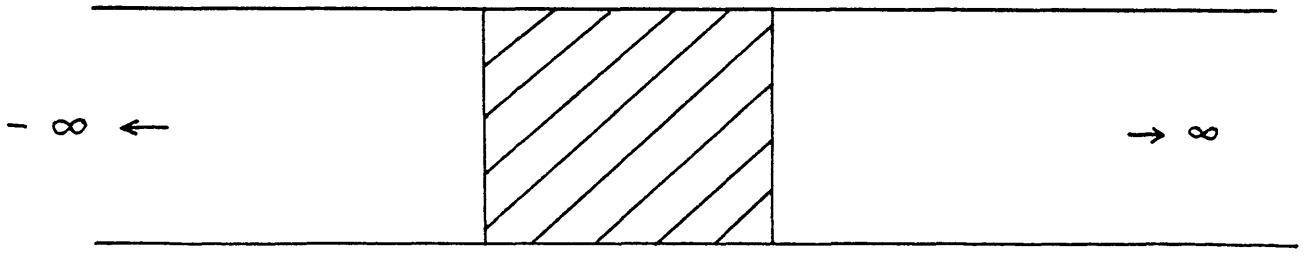
$$C_{N+1} = V_{N+1} R_{N+1} C_N R_{N+1} V_{N+1}$$

In deriving these equations it is assumed that the new slice is always added at the origin $X_j = 0$. This is done because it simplifies the expressions for the conductance appreciably, in that, terms containing X vanish in the iteration. In effect this involves a shift of origin after each slice is added, which clearly cannot effect the conductivity as it is independent of the choice of origin.

The set of equations {19.3} are quite remarkable in that they allow us to calculate the conductivity in an iterative manner. All the matrices defined above are limited in size only by the cross-section of the system. Thus it is possible to treat very long systems without running into storage problems. The restriction on the width of systems that can be studied is not really a hinderance as we can study the behaviour of the conductivity of long systems as a function of their width in analogy with the ideas of finite size scaling.

3.5 Embedding the system in a perfect medium

To avoid the problems of calculating the D.C. conductivity of a finite system we shall consider making the system effectively infinite by attaching perfectly ordered systems to the ends of the sample.



Although attaching perfectly ordered strips (metals) to the ends of the sample solves the finite size problems, it destroys the homogeneity of the the system, which means that the Kubo formula in the form of eqn{1.3} is not strictly valid. This difficulty arises because although the Kubo formula in its most general form establishes a non-local relationship between the electric field and current density, it is only in the case of a homogeneous electric field and current density that the conductivity can be extracted in the simple form of eqn {1.3}.

Economou and Soukoulis(1981) have suggested that the Kubo formula can be used over the disordered region only, and the effect of the metals is solely to provide boundary conditions, since the electric field in the metals will be zero due to their infinite conductance. This procedure is however physically unsatisfactory, as it results in a non zero resistance for a perfectly ordered system.

Thouless(1981) and Langreth and Abrahams(1981) have pointed out that one has to be very careful when using linear response theory on this arrangement. The problem arises during the switching on of the perturbation. If this is applied to the disordered region only, then during the switching on process, current pulses will be generated in the leads, which will lead to charge density oscillations and not result in the required steady state.

To reach the required steady state, in which the perturbation acts only over the disordered region, they show that an additional field must be applied to the leads to cancel these oscillations. This leads to the physically reasonable result of zero resistance for an ordered system.

In one dimension the Economou-Soukoulis procedure yields a resistance defined as

$$R \sim 1/T \qquad \{20.3\}$$

in terms of the transmission coefficient T, whereas the Thouless-Langreth method leads to

$$R \sim 1/T - 1 \qquad \{21.3\}$$

This is the Landauer result, Sec 2.4, which can be obtained by considering waves traveling in the leads to be incident upon the disordered medium. In this derivation the potential across the sample is determined self consistently and for this to be possible there must be some inelastic mechanism in the leads to equiliberate the electrons. Such a mechanism could physically be provided by electron-electron interactions. If one does not allow the electrons to equiliberate one obtains the Economou-Soukoulis result {20.3}. The two results differ by a constant, which is the zero disorder resistance as given by eqn{20.3}.

As to which procedure corresponds most closely to the experimental situation is not clear, and depends crucially upon the definition of the leads, but the Landauer result appears to be physically 'more' correct as it leads to the expected zero disorder limit.

We have not found a way of evaluating the Kubo formula correctly, in dimensions greater then one, so we shall use the Economou-Soukoulis procedure. Fisher and Lee(1981), and Langreth and Abrahams(1981) have derived multi-channel Landauer type formulae for two and three dimensional systems, and have shown that the Economou-Soukoulis procedure yields a conductance defined as

$$g \sim Tr(tt^{+}) \qquad \{22.3\}$$

where t is the transmission matrix. Many general multi-channel versions of the Landauer formula exist, Anderson(1981), Bütticker et al(1985) and there is much variation between them, but they all agree that in the limit of a large number of channels or large disorder the conductance reduces to eqn{22.3}.

Thus for large systems or small conductances the the differences between the different definitions of the conductance are expected to be small.

3.5.1 Procedure for attaching Metals

In this section we discuss the modifications required to incorporate infinite metals into the algorithm of section 3.2. Again we shall use the density of states as an example. As discussed in the last section we shall use the metals merely to provide boundary conditions and restrict the trace in the various quantities required to evaluate the conductivity and density of states, to the disordered region.

Let the submatrix of the Green's function at the end of a semi-infinite strip be denoted by G^{∞}_{00} . We shall show how to calculate this in appendix 1.

Attaching a semi-infinite metal to the lower edge is easy, we simply use G^{∞}_{00} as our starting value for R. The various quantities in the recursion scheme for the density of states would then have the initial values

$$R_0 = G^{\infty}_{00} \ , \ F_0 = 0 \text{ and } S_0 = 0 \qquad \{24.3\}$$

using these we then iterate the set of equations {17.3} until we reach the required length. At this point we have the density of states of our sample with a semi-infinite metal attached to one edge. Let us denote the various quantities at this point with a apostrophe.

We now consider coupling a semi-infinite metal to the other edge. The Green's function of the composite system can be calculated by treating the coupling as a perturbation. This gives

$$G_{ii} = G'_{ii} + G'_{iN} V_N G_{Ni}$$

Which leads to

$$G_{ii} = G'_{ii} + G'_{iN} V_N K_N V_N G'_{Ni} \quad 0 < i < N \qquad \{25.3\}$$

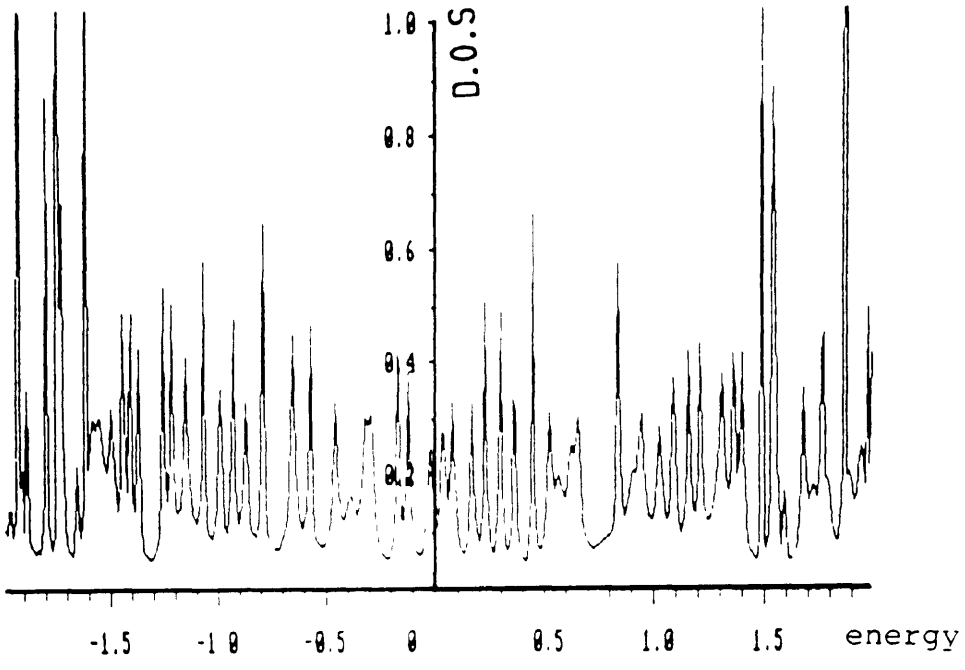


Fig 3.2 The density of states of a disordered chain of 100 atoms at disorder unity, as a function of energy.

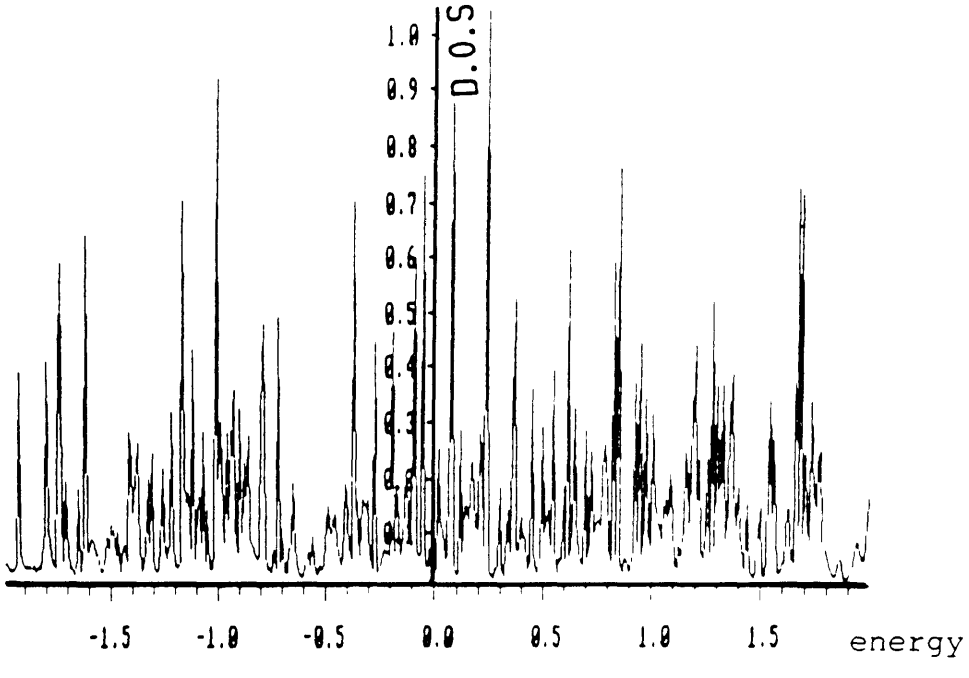


Fig 3.3 The density of states of a disordered chain of 250 atoms at disorder unity. Notice that the structure is sharper then in the diagram above.

Where we have defined $K_N = [(G^{\infty}_{00})^{-1} - VG^{0}_{NN}V]^{-1}$

Taking the trace gives the density of states.

$$S_N = S'_N + F'_N K_N \qquad \{26.3\}$$

Similarly for the conductivity.

$$S^N_{xx} = S^{N'}_{xx} + Tr[Re(R'_N C'_N)Re(R'_N C'_N) + Im(R'_N C'_N)Im(R'_N C'_N) + Re(K'_N)Re(B'_N) - Im(K'_N)Im(B'_N)]$$

3.6 The effect of the metals on the density of states

Figs[3.2] and[3.3] show the density of states of systems of various lengths at a disorder W=1 in one dimension. The density of states is that obtained by summing over the disordered region only, and in this sense is a sort of local density of states. The metals have made the density of states continuous. This is analagous to the broadening of a discrete level when coupled to a continuum. However there is still a lot of structure which becomes sharper as the system becomes longer. This reflects a decrease in the strength of the coupling between the states of the metals and those of the system, because the states are becoming more localized. The spectrum appears to becomes discrete in the limit of infinite length and the data shows that the influence of the metals diminishes with increasing system size. We shall demonstrate in chapter 6 that the spectrum is discrete for localized states so that the metals do not change the nature of the spectrum, in contrast to a finite imaginary part to the energy which broadens states irrespective of their physical properties. We shall discuss this point further in chapter 6.

Appendix 3.1 The submatrix of the Green's function at the end of a semi-infinite ordered strip.

Since the Green's function at the end of a semi-infinite metal is independent of the position of the origin it can be obtained by setting $G^{N+1}_{N+1,N+1} = G^{N}_{NN}$ in equation {10.3d}. This leads to

$$g = [ZI - H - g]^{-1} \qquad \{A1.3\}$$

Where we have set V = 1 for simplicity and defined g to be the submatrix of the Green's function at the end of a semi-infinite metal. H is the Hamiltonian of an ordered slice. Thus we have to solve the matrix quadratic equation

$$g^2 - (ZI - H)g + I = 0 \qquad \{A2.3\}$$

There are at least 2^N solutions to this equation, and there is no systematic way of obtaining them but we can select the physically relevant one by transforming to k space, since this will diagonalize both g and H. This follows from Bloch's theorem.

The transformation to k space is a unitary transformation effected by the eigenvectors U of the Hamiltonian H. This leads to

$$U^{+}gUU^{+}gU - (ZI - D)U^{+}gU + I = 0 \qquad \{A3.3\}$$

Since $U^{+}U = 1$. D is the matrix of eigenvalues of H.

If we denote $U^{+}gU$ by the diagonal matrix A then

$$A^2 - (ZI - D)A + I = 0 \qquad \{A4.3\}$$

This is an uncoupled set of N scalar quadratic equations which can be trivially solved. Let us denote the solution by the diagonal matrix B. Then the submatrix of the Green's function in the basis of a slice can be obtained by the back transformation

$$g = UBU^{+} \qquad \{A5.3\}$$

The advantage of this method is that H can normally be diagonalized by hand, thus providing a saving on computer time. When this is not possible an alternative and more elegant method is the following.

For an ordered system eqn{5.3} of chapter 3 reduces to

$$(ZI-H_0)G_{ij} - VG_{i-1j} - VG_{i+1j} = I\delta_{ij} \qquad \{A6.3\}$$

We can write this as

$$\begin{bmatrix} V & 0 \\ 0 & V^{-1} \end{bmatrix}\begin{bmatrix} G_{i+1j} \\ VG_{ij} \end{bmatrix} = \begin{bmatrix} Z-H_0 & -I \\ I & 0 \end{bmatrix}\begin{bmatrix} G_{ij} \\ VG_{i-1j} \end{bmatrix} - \begin{bmatrix} \delta_{ij} \\ 0 \end{bmatrix} \qquad \{A7.3\}$$

This is an inhomogeneous equation whose solutions can be expressed as linear combinations of the solutions of the associated homogeneous problem.

$$\begin{bmatrix} V & 0 \\ 0 & V^{-1} \end{bmatrix}\begin{bmatrix} G_{i+1j} \\ VG_{ij} \end{bmatrix} = \begin{bmatrix} Z-H_0 & -I \\ I & 0 \end{bmatrix}\begin{bmatrix} G_{ij} \\ VG_{i-1j} \end{bmatrix} \qquad \{A8.3\}$$

Using Bloch's theorem $G_{i+1j} = \alpha G_{ij}$ this takes the form of the generalized eigenvalue problem

$$\alpha \begin{bmatrix} V & 0 \\ 0 & V^{-1} \end{bmatrix}\begin{bmatrix} U^a \\ U^b \end{bmatrix} = \begin{bmatrix} Z-H_0 & -I \\ I & 0 \end{bmatrix}\begin{bmatrix} U^a \\ U^b \end{bmatrix} \qquad \{A9.3\}$$

U is the matrix of eigenvectors and α the matrix of eigenvalues. These can be obtained by the use of standard numerical routines.

Consider first a $-\infty$ -> 0 strip. For $i < j$ the columns of G_{ij} are linear combinations of those columns of U^a corresponding to those eigenvalues with modulus greater then

unity, $|\alpha| > 1$, since the solutions must decay into the strip. ie

$$G_{ij} = U^a \alpha^{i-j} A \qquad \{A8.3\}$$

Where A is the matrix of coefficients. This can be determined by demanding that this solution satisfies the inhomogeneous equation. At the end of an infinite strip the inhomogeneous equation leads to the pair of equations

$$0 = (Z-H_0)G_{00} - VG_{-10} - 1$$

and $\qquad \{A9.3\}$

$$VG_{00} = (Z-H_0)G_{-10} - VG_{-20}$$

Eliminating $(Z-H_0)$ between these and substituting for G from above leads to

$$VU^a\alpha A = 1 \qquad \{A10.3\}$$

Hence the Green's function at the end of a $-\infty$ --> 0 strip is given by

$$G_{00}^{-\infty} = U^a A = U^a\alpha^{-1}[U^a]^{-1}V^{-1} \qquad \{A11.3\}$$

Similarly for a 0 -->∞ strip it can be shown that

$$G_{00}^{+\infty} = U^a\alpha[U^a]^{-1}V^{-1} \qquad \{A12.3\}$$

<u>The Limit Γ --> 0</u>

For a perfectly ordered system one has to be careful when setting the imaginary part of the energy to zero, because the eigenvalues of {A9.3} are all of modulus unity, so that the division between those of modulus greater then ,or less then, unity is no longer clear. The correct set of eigenvectors can then be selected by considering the derivative $\frac{d\alpha}{d\Gamma}$, which would tell us which way the eigenvalues split under perturbation by a finite Γ. This is discussed in the paper by MacKinnon. Alternatively we may

keep Γ infinitesimally small $\sim 10^{-10}$, which is easily within the accuracy of most computers, and splits the eigenvalues. Such small values of Γ do not effect the quantities we wish to examine.

Appendix 3.2 Sample program

```
C*************************************************************
C       PROGRAM CDEN2D CALCULATES THE DENSITY OF STATES AND
C       CONDUCTIVITY OF TWO DIMENSIONAL SQUARES
C
C*************************************************************
C       DEFINE VARIABLES
C
C
        PROGRAM CDEN2D(INPUT,OUTPUT,TAPE5=INPUT,TAPE6=OUTPUT)
        PARAMETER(NX=32)
        COMPLEX BP(NX,NX),CP(NX,NX),EP(NX,NX)
        COMPLEX GP(NX,NX),GE(NX,NX),EH(NX,NX)
        COMPLEX FP(NX,NX),GPFP(NX,NX)
        COMPLEX GPBP(NX,NX),GPCP(NX,NX)
        COMPLEX CX,CY,EH1,G0,DCX,DCY,SP,DF
        REAL G
        LOGICAL STRIP
C
C       READ IN PARAMETERS FREE FORMAT
C
C-------------------------------------------------------------
C        N1        = STRIP WIDTH
C        GAMMA     = IMAGINARY PART OF ENERGY
C        W         = DISORDER
C        NA        = DIMENSIONS OF SQUARE
C        STRIP     = .TRUE.-STRIP GEOMETRY
C                    .FALSE.-CYLINDERICAL GEOMETRY
C        NPRINT    = RESULTS PRINTED EVERY NPRINT STEPS
C        NBC       =   =0-FINITE LENGHT STRIP
C                      =1-[1D] METALS ON BOTH ENDS
C                      =2-[2D] METALS ON BOTH ENDS
C.
 1      READ(5,*,END=9999)N1,GAMMA,W,EF,NA,STRIP,NBC
        WRITE(6,999)N1,GAMMA,W,EF,NA,STRIP
 999    FORMAT(//' N1=',I2,'  GAMMA=',G8.2,'  W=',F5.2,
     +  '   EF=',F5.2,'  NA=',I4,'  STRIP=',L2,' NB =',I1)
C
C-------------------------------------------------------------
C
C
C         INITIALISATION SEQUENCE
C
          DS=0E0
          SX=0E0
          SY=0E0
          SSX=0E0
          ADD=0E0
          PI=3.141592654
          VIER=4.0/(PI*FLOAT(N1))
          N1H=N1-1
          E1=EF+0.5*W
C
C        INITIALISATION OF SECONDARY QUANTITIES
C
        DO 10 K=1,N1
        DO 10 J=1,N1
```

```
              BP(J,K)=(0E0,0E0)
              CP(J,K)=(0E0,0E0)
              FP(J,K)=(0E0,0E0)
   10         GP(J,K)=(0E0,0E0)
C
C       THIS PART FOR [1D] METALS
C
          IF(NBC-1)25,11,20
    11    ETA=GAMMA
          IF(ETA.EQ.0.0)ETA=1E-100
          CX=CMPLX(EF,ETA)
          CY=CSQRT(CX*CX-4.0)
          IF(SIGN(ETA,AIMAG(CX)+AIMAG(CY)).EQ.ETA)CY=-CY
          G0=0.5*(CX+CY)
          EH1=1.0/G0
          DO 19 K=1,N1
   19          GP(K,K)=G0
          GOTO 25
C
C         THIS PART FOR [2D] METALS
C
   20     CALL GMET2D(NX,N1,EF,GAMMA,EP,STRIP)
          DO 21 K=1,N1
          DO 21 J=1,N1
   21          GP(J,K)=EP(J,K)
          CALL INVERT(N1,EP,EH,NX)
C
C         INITIALISE CONDUCTIVITY AND VARIENCE SUMS
C
    25    NS=0
          N=0
          S=0E0
          SS=0E0
          SP=0E0
C
C>>>>>> LOOP OVER STRIP >>>>>>>>>>>>>>>>>>>>>>>>>>>>>>>>>>>>
C
   900    DO 901 IZ=1,N1
C
C       INCREASE STRIP STRIP LENGHT
          N=N+1
C
C         SHIFT ORIGIN
C
          DO 40 K=1,N1
                IF(K.EQ.N1)GOTO 39
                K1=K+1
             DO 38 J=K1,N1
                   CX=CP(J,K)+CONJG(CP(J,K))
                   Y=AIMAG(GP(J,K))
                   CY=BP(J,K)+CMPLX(-AIMAG(CX),REAL(CX)+Y)
                   BP(J,K)=CY
                   BP(K,J)=CY
                   CY=CMPLX(REAL(CP(J,K))+Y,AIMAG(CP(J,K)))
                   CP(J,K)=CY
    38             CP(K,J)=CONJG(CY)
    39          Y=AIMAG(GP(K,K))
                X=REAL(CP(K,K))
             BP(K,K)=CMPLX(REAL(BP(K,K)),AIMAG(BP(K,K))+X+X+Y)
```

```
   40      CP(K,K)=CMPLX(REAL(CP(K,K))+Y,0.0)
C
C
        DO 324 K=1,N1
 324            FP(K,K)=FP(K,K)+1.0
C
C        CALCULATE NEW GP
C
        DO 30 K=1,N1
        DO 29 J=1,N1
   29          EP(J,K)=-GP(J,K)
   30          EP(K,K)=EP(K,K)+CMPLX(E1-W*RANF(),GAMMA)
        IF (N1.EQ.1) GOTO 112
        DO 100 J=1,N1H
               EP(J,J+1)=EP(J,J+1)-1.0
  100          EP(J+1,J)=EP(J+1,J)-1.0
C
        IF(STRIP) GOTO 112
               EP(N1,1)=EP(N1,1)-1.0
               EP(1,N1)=EP(1,N1)-1.0
C       CALL MATRIX INVERSION
 112    CALL INVERT(N1,EP,GP,NX)
C
C        CALCULATE VARIOUS PRODUCTS
C
        DO 300 K=1,N1
        DO 298 J=1,N1
               GPBP(J,K)=(0E0,0E0)
               GPFP(J,K)=(0E0,0E0)
 298           GPCP(J,K)=(0E0,0E0)
C

       DO 300 L=1,N1
        DO 300 J=1,N1
               GPBP(J,K)=GPBP(J,K)+(GP(J,L)*BP(L,K))
               GPFP(J,K)=GPFP(J,K)+(GP(J,L)*FP(L,K))
 300           GPCP(J,K)=GPCP(J,K)+(GP(J,L)*CP(L,K))
C
C        CALCULATE NEW CONTRIBUTION TO CONDUCTIVITY
C
        DX=0E0
        DO 310 K=1,N1
        DO 309 L=1,N1
 309            DX=DX+(REAL(GPCP(K,L))*REAL(GPCP(L,K))+
     +                 AIMAG(GPCP(K,L))*AIMAG(GPCP(L,K)))
  310           DX=DX+REAL(GPBP(K,K))
        S1=S1-DX
C
C        CALCULATE NEW CONTRIBUTION TO DENSITY OF STATES
C
        DF=0E0
        DO 534 K=1,N1
 534            DF=DF+GPFP(K,K)
        SP=SP+DF
C
C        CALCULATE NEW VALUES OF CP AND CM
C
        DO 319 K=1,N1
               IF(K.EQ.N1)GOTO 318
```

```
              K1=K+1
        DO 315 J=K1,N1
 315            CP(J,K)=(0E0,0E0)
        DO 316 L=1,N1
        DO 316 J=K1,N1
 316            CP(J,K)=CP(J,K)+(GPCP(J,L)*CONJG(GP(L,K)))
        DO 317 J=K1,N1
 317            CP(K,J)=CONJG(CP(J,K))
 318            CP(K,K)=(0E0,0E0)
        DO 319 L=1,N1
 319          CP(K,K)=CP(K,K)+(REAL(GPCP(K,L))*REAL(GP(K,L))+
     +                    AIMAG(GPCP(K,L))*AIMAG(GP(K,L)))
C
C        CALCULATE NEW VALUE OF BP
C
        DO 330 K=1,N1
        DO 331 J=K,N1
 331            BP(J,K)=(0E0,0E0)
        DO 330 L=1,N1
        DO 330 J=K,N1
  330           BP(J,K)=BP(J,K)+(GPBP(J,L)*GP(L,K))+
     +                              2*(GPCP(J,L)*CONJG(CP(L,K)))
        DO 332 K=1,N1H
              K1=K+1
        DO 332 J=K1,N1
 332            BP(K,J)=BP(J,K)
C
C CALCULATE NEW VALUE OF FP
C
        DO 544 K=1,N1
        DO 566 J=1,N1
 566            GPFP(J,K)=(0E0,0E0)
C
        DO 544 L=1,N1
        DO 544 J=1,N1
 544            GPFP(J,K)=GPFP(J,K)+(GP(J,L)*FP(L,K))
C
         DO 533 K=1,N1
         DO 577 J=1,N1
  577             FP(J,K)=(0E0,0E0)
C
        DO 533 L=1,N1
        DO 533 J=1,N1
 533            FP(J,K)=FP(J,K)+(GPFP(J,L)*GP(L,K))
C
C<<<<<<<<<<< END OF MAIN LOOP <<<<<<<<<<<<<<<<<<<<<<<<<<<<<<
C
  901  CONTINUE
C
C      THIS PART FOR [1D] METALS
C
        DX=0E0
        DF=0E0
        IF(NBC-1)440,410,420
 410    DO 412 K=1,N1
        DO 412 J=1,N1
               EP(J,K)=-GP(J,K)
 412           EP(K,K)=EP(K,K)+EH1
        GOTO 430
```

```
C
C         THIS PART FOR [2D] METALS
C
  420    DO 422 K=1,N1
         DO 422 J=1,N1
  422           EP(J,K)=EH(J,K)-GP(J,K)
C
C        THIS PART FOR [1D] AND [2D] METALS
C
 430     CALL INVERT(N1,EP,GE,NX)
         DO 432 K=1,N1
         DO 439 J=1,N1
 439           GPCP(J,K)=(0.0,0.0)
         DO 432 L=1,N1
         DO 432 J=1,N1
 432           GPCP(J,K)=GPCP(J,K)+(GE(J,L)*CP(L,K))
         DO 433 K=1,N1
         DO 433 J=1,N1
 433           DX=DX+(REAL(GPCP(K,J))*REAL(GPCP(J,K))+
     +          AIMAG(GPCP(K,J))*AIMAG(GPCP(J,K))+
     +         REAL(GE(K,J))*REAL(BP(J,K))
     +        -AIMAG(GE(K,J))*AIMAG(BP(J,K)))
C
C      CALCULATE CONDUCTANCE AND DENSITY OF STATES
C
        DO 757 K=1,N1
        DO 757 J=1,N1
 757           DF=DF+(GE(K,J)*FP(J,K))
C
  440 NS=NS+1
      S1=S1-DX
      X=S1
      S=S+X
      SS=SS+X*X
      S1=DX
      X=S
      IF(X.LT.0.0) WRITE(6,*) X
      CONDXX=VIER*X/FLOAT(N)
      G=CONDXX
      SP=SP+DF
      Y=AIMAG(SP)
      DENSIT=-1.0*(VIER*Y/4.0)/FLOAT(N)
      WRITE(6,*)G,DENSIT
      GOTO 1
 9999  STOP
       END
C

C
C$$$$$$$$$$$$$ END OF MAIN PROGRAM $$$$$$$$$$$$$$$$$$$$$$$$$
C
C
C
C*************** SUBROUTINES ******************************
C
       SUBROUTINE INVERT(N,A,B,NX)
       DIMENSION RINT(32)
       COMPLEX A(NX,NX),B(NX,NX)
       INTEGER I,J,IR,IB,IA,ID,IFAIL,N
```

```
      IR=N
      DO 10 I=1,N
      DO 20 J=1,N
 20         B(I,J)=(0.0,0.0)
 10         B(I,I)=(1.0,0.0)
      IA=32
      IB=32
      IFAIL=0
      CALL F03AHF(N,A,IA,DETR,DETI,ID,RINT,IFAIL)
      CALL F04AKF(N,IR,A,IA,RINT,B,IB)
      RETURN
      END

      SUBROUTINE GMET2D(NN,N1,EF,GAMMA,GP,STRIP)
C -------------------------------------------------------------
C
C     GMET2D CALCULATES THE ELEMENTS OF THE GREEN'S
C     FUNCTION AT THE END OF A SEMI-INFINITE 2D METAL
C
C-------------------------------------------------------------
      COMPLEX GP(NN,NN),CX,CY,DC,DCX,DCY
      COMPLEX GGO(32)
      REAL U(32,32),D(32)
      LOGICAL STRIP
C
C     DIAGONALISATION OF HAMILTONIAN OF ONE SLICE
C
      DK=6.283185308/FLOAT(N1)
      OK=3.1415927/FLOAT(N1+1)
      VECK=(0E0)
      IF(STRIP)THEN
               A=OK
               VO=0
      ELSE
               A=DK
               VO=0.7853981634
      ENDIF
      DO 10 I=1,N1
              V=VO
              VECK=VECK+A
              S=0
              D(I)=(EF-2*COS(VECK))
      DO 8 J=1,N1
              V=V+VECK
              X=SIN(V)
              U(J,I)=X
  8           S=S+X*X
              X=1/SQRT(S)
      DO 9 J=1,N1
  9           U(J,I)=U(J,I)*X
C
 10   CONTINUE
C
C     CALCULATION OF THE GREEN'S FUNCTION ELEMENTS IN THE
C     BASIS OF THE EIGENFUNCTIONS OF A SLICE
C
      ETA=GAMMA
      IF(ABS(ETA).EQ.0.0)ETA=1E-100
      DO 30 I=1,N1
```

```
              CX=0.5*CMPLX(D(I),ETA)
              CY=CSQRT(CX*CX-1.0)
              IF(SIGN(ETA,AIMAG(CX)+AIMAG(CY)).EQ.ETA)CY=-CY
   30         GGO(I)=CX+CY
C
C       BACK TRANSFORMATION
C
        DO 39 J=1,N1
        DO 38 I=1,N1
   38         GP(J,I)=(0E0,0E0)
        DO 39 K=1,N1
        DO 39 I=1,N1
   39         GP(J,I)=GP(J,I)+(U(I,K)*U(J,K))*GGO(K)
        DO 41 I=2,N1
              K=I-1
        DO 41 J=1,K
   41         GP(J,I)=GP(I,J)
        RETURN
        END
```

Chapter 4

The statistics of the conductance in two and three dimensions

4.1 Introduction

In the past the study of averages has dominated, investigations into the properties of disordered systems, partly because of an intuitive belief that the quantities of interest self-averaged, and partly because the complications introduced by disorder make the calculation of fluctuations very difficult. However it has recently begun to emerge that the properties of disordered systems, are rather subtle and that simple averages are not enough to describe the systems of interest. Instead we need to study probability distributions, as was emphasized by Anderson as early as 1978, Anderson(1978).

In the context of localization extensive studies in one dimension, Anderson et al(1980), have shown that quantities such as the resistance and conductance do not self-average, in that the relative fluctuations in these quantities diverge with increasing system size in contrast to normal thermodynamic variables, for which the fluctuations decrease as $1/\sqrt{L}$. See section 2.6.

Instead the distributions are characterized by the logarithm of the resistance, or conductance, and are asymptotically log normal, Pendry(1982).

We can understand why LnR self averages whilst R may not by considering the following example. Kapitulnik and Shapir (1983) have shown that the problem of an electron in a one dimensional random potential can be mapped onto the partition function of the Yang-Lee Hamiltonian, which is essentially a one dimensional Ising model with random couplings, and random imaginary local fields. The resistance can be expressed as $R=|R_L|^2$

where $R_L \sim \sum_1^L \exp\{\Sigma K_l S_l S_{l-1} - \frac{i}{2}\Sigma h_l (S_l + S_{l-1})\}$ {1.4}

S_l are spin variables, that take the values ± 1 and K_l are random independent variables related to the random potential at site l. Meaningful statistics can only be extracted from additive quantities like free energies, which the resistance is not. If we choose our potential, such that $\{h_l\} = 0$ then we have the normal Ising model. Performing the sum we obtain

$$R_L \sim \prod_{l}^{L} \cosh(K_l) \qquad \{2.4\}$$

R is a product of random variables whose statistics we cannot comment on but if we take the log

$$\mathrm{Ln}R_L \sim \sum_{l}^{L} \cosh(K_l) \qquad \{3.4\}$$

LnR is sum of random independent variables and so the central limit theorem applies. For this model the distribution of LnR is gaussian and LnR/L self averages. In general the distributions are only weakly log normal. See Kirkman(1984) for a detailed discussion.

In higher dimensions, no such analytical results exist as the transfer matrix methods used so successfully in one dimension become more difficult.(See however Pendry(1984)). The general feeling was that the one dimensional systems were pathological and that the distributions would be much better behaved in higher dimensions, because electrons would have a greater number of paths for getting from one point to another. These systems were seen as lots of one dimensional chains in parallel so it was thought that fluctuations would be relatively unimportant.

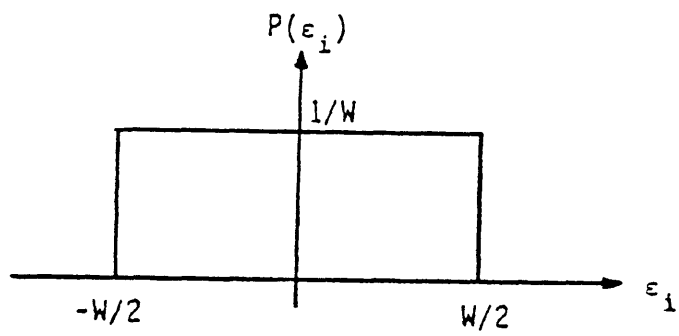
In this chapter we examine the behaviour of the probability distribution of the conductance in two and three dimensions by numerical means, and show that non self-averaging, of the conductance, is an intrinsic property of localized states irrespective of dimensionality. Furthermore in two and three dimensions two regimes can be identified. At sufficiently low

disorder in 2-D and near the mobility edge in 3-D the conductance fluctuations are approximately scale independent in agreement with the recent predictions of Altshuler(1985) and Lee and Stone (1985). At the other extreme, where states are strongly localized the fluctuations increase exponentially with system size, on a length scale of the order of the localization length. It is found that the fluctuations are governed by one parameter, the conductance, in any regime. We take this to be further evidence for the validity of one parameter scaling.

4.2 A numerical study of the statistics

In order to see whether the conductance is a self-averaging quantity or not in two and three dimensions, we have used the algorithm of chapter three to calculate the conductance of a large ensemble of systems of dimension N^d embedded in a perfect medium. Embedding the sample in a perfect medium allows us to use the Kubo formula on finite systems, and does not change the nature of the eigenstates. See ch3 and ch6.

The model we employ is the tight binding Anderson model with random site energies and constant nearest neighbour hopping. The disorder is specified by the width W of the distribution from which the site energies are selected. We shall take this to be a top hat distribution



The exact details of the distribution used are not expected to be important, as long as it is continuous, because the scaling regime is thought to be universal. The random site energies only enter the algorithm in the calculation of the quantity R_N, eqn{17.3}, which is just the Green's function at the end of a system of length N.

The quantity we choose to examine is the logarithm of the dimensionless conductance Lng, because as discussed in the introduction it is expected to be statistically much better behaved then the conductance itself. We show in section 4.4 that if the standard deviation of Lng increases with system size then so does the relative error

in g itself. Thus Lng can be used to study fluctuations, and non self-averaging. We calculate the ensemble average of the logarithm of the conductance <Lng> and enough higher moments to allow us to accurately determine the behaviour of the variance V of Lng

$$V = \langle (Lng)^2 \rangle - \langle Lng \rangle^2 \qquad \{4.4\}$$

and repeat the calculation for different values of the disorder W and system size N.

In two dimensions the range of the disorder parameter was chosen to cover the regimes of both strong and weak localization, W=1 to W=20 was found to be sufficient. In three dimensions W ranged from 10 to 25 and covered the extended and localized regions. The range of system sizes that could be examined was limited by restrictions on computer time. In three dimensions all the matrices in the algorithm are of dimension N^2 by N^2 , and so a system of dimension N=6 would require the manipulation of 36 by 36 complex matrices.

Since we require good statistics we need to average over fairly large ensembles so that the systems we can look at cannot be too large. In two dimensions the system sizes ranged from N=4 to N=16,and in three dimensions from N=4 to N=6, whilst the sizes of the ensembles were 1000 and 300 respectively. These values of parameters were found to be sufficient to give a clear answer to the self-averaging problem. The calculations were performed on the Cray 1 computer, of the university of London, whose vector facilities allowed a significant decrease in computational time.

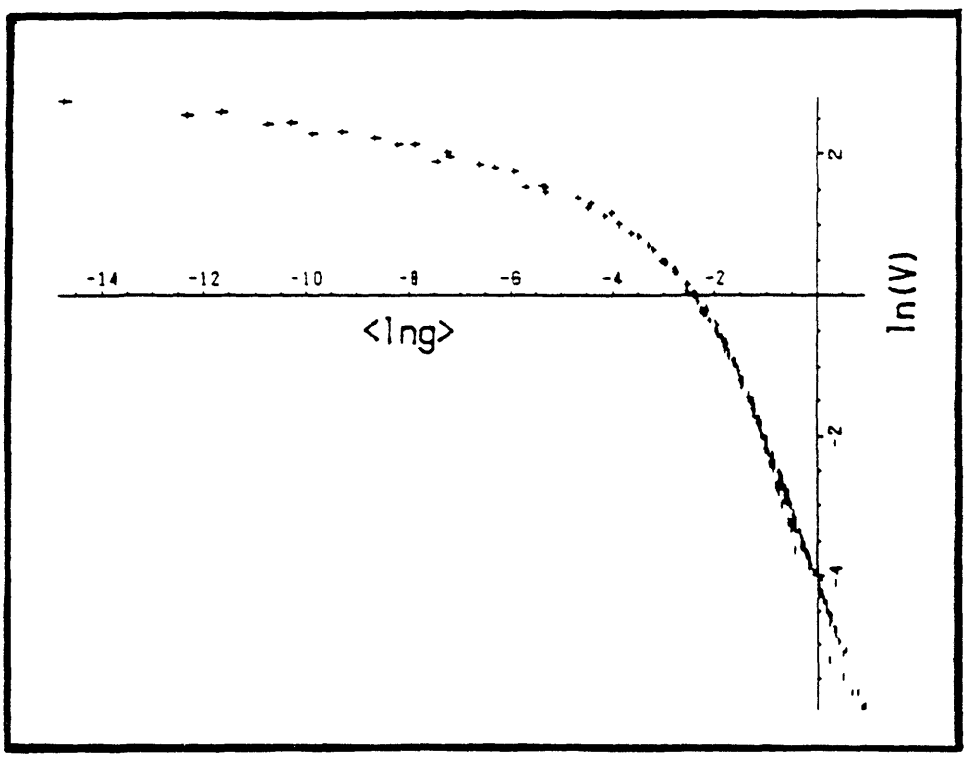


Fig 4.1 The logarithm of the variance V of Lng plotted against the average of Lng, in two dimensions.

4.3 Results

Figures [4.1] to [4.5] show the behaviour of the variance as a function of the average of the logarithm of the conductance <Lng> in one,two and three dimensions. We plot the results as a function of <Lng> because the conductance is supposed to be the only relevant parameter in the scaling theory of localization. An important feature to notice about these curves is that the variance appears to scale with the mean, independent of system size and disorder.

$$V=V(<Lng>) \qquad \{4.4\}$$

4.3.1 Analysis of 2D results

a) Low disorder

Fig [4.1] shows a plot of the logarithm of the variance of Lng vs <Lng>. For large g or low disorder the curve is linear on this scale which allows us to write

$$LnV = \alpha - \beta<Lng> \qquad \alpha \sim -4 \qquad \beta \sim 2 \qquad \{4.5\}$$

Now in the weak disorder limit the conductance is known to behave in a logarithmic manner with system size, eqn{7.2}.

$$g = g_o - ALn(L/L_o) \quad \text{with } g_o >> ALn(L/L_o)$$

The results of chapter 5 show that the beta function calculated using the average of the logarithm of the conductance d<lng>/dlnL, fig[5.3], is very similar to that predicted by scaling theory, which is calculated using the average of the conductance. Hence we may write

$$<Lng> = Ln\{g_o - ALn(L/L_o)\} \qquad \{4.6\}$$

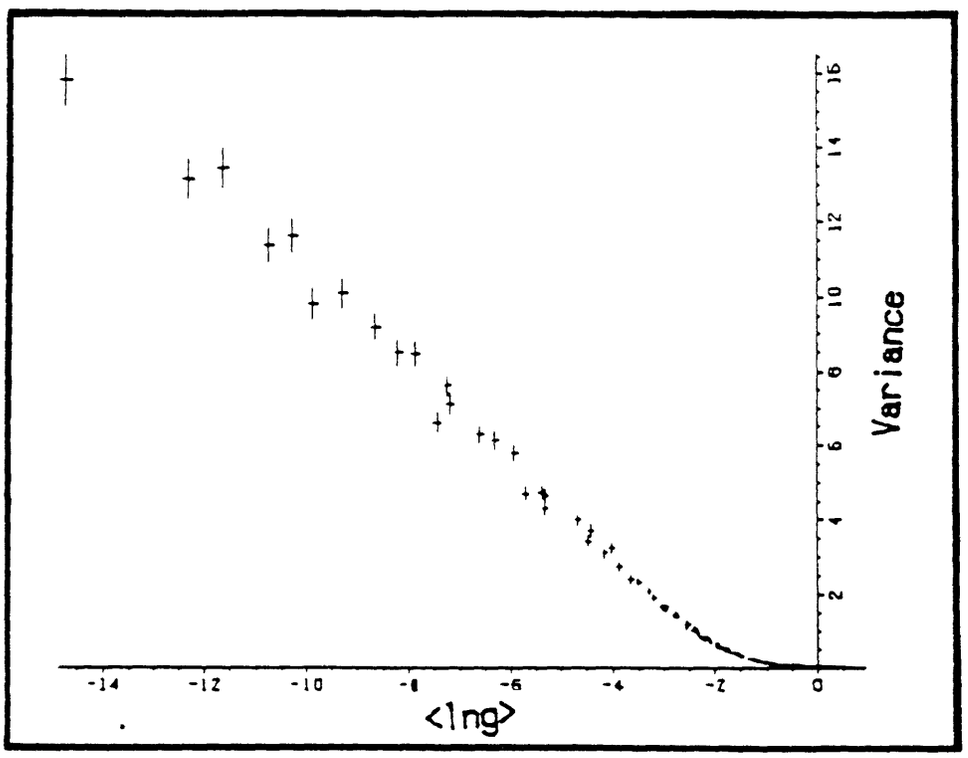


Fig 4.2 The variance V of Lng plotted against the average of Lng, in two dimensions.

Substituting this into eqn {4.5} gives

$$LnV = \alpha - \beta Ln\{g_o - ALn(L/L_o)\}$$

or

$$V \approx e^{\alpha}/g_o^2 + 2e^{\alpha}g_o^{-3}ALn(L/L_o) \qquad \{4.7\}$$

Hence V ~ Ln L and increases with increasing system size.

b) <u>High disorder</u>

The high disorder behaviour can be deduced from fig [4.2] which shows a plot of the variance V against <Lng>. On this curve the relationship is linear in the low conductance regime

$$V = A - B\langle Lng\rangle \qquad A \sim -2 \qquad B \sim 1 \qquad \{4.8\}$$

For high disorder the states are almost surely exponentially localized. We can express this as

$$\exp(\langle Lng\rangle) \sim g_o\exp(-\alpha L)$$

Where α^{-1} is the localization length. Eqn{4.8} then becomes

$$V = A - BLng_o + \alpha BL \qquad \{4.9\}$$

Again V increases with system size, but now much faster then in the low disorder limit.

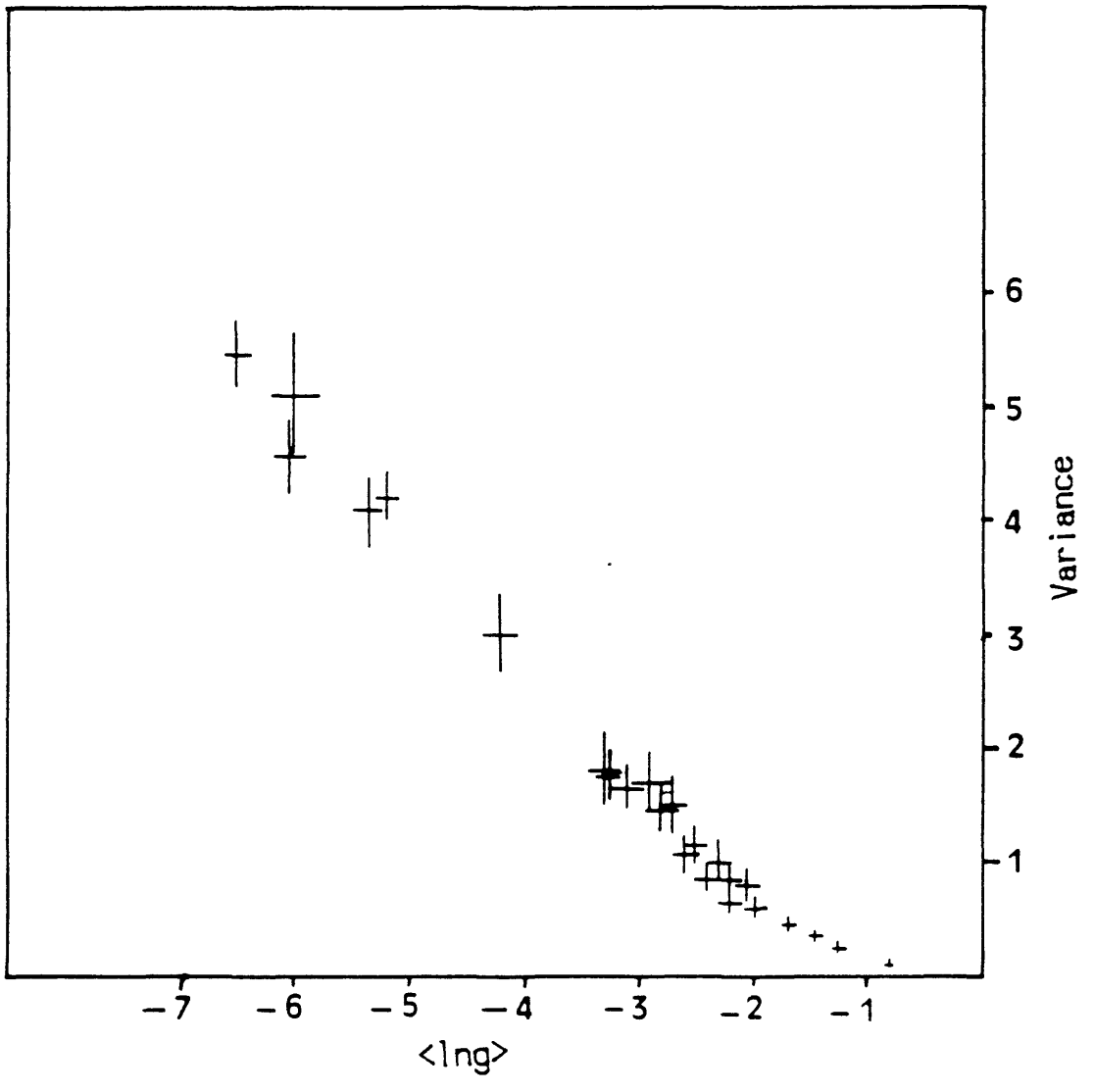


Fig 4.3 The variance V of Lng plotted against the average of Lng, in three dimensions.

4.3.2 Analysis of 3D results

Fig[4.3] shows a plot of the variance against <Lng> and on the face of it looks very similar to the one and 2D curves fig[4.5] and fig[4.2]. However the behaviour with system size is rather different as can be seen from fig [4.4] where we have plotted the variance as a function of system size for different values of the disorder.

Above W=18 the variance clearly increases with system size whereas below W=14 it does the opposite. W=16 is the accepted value of the disorder at which the Anderson transition takes place, so clearly there is a difference in the behaviour of the statistics for extended and localized states. We can deduce the behaviour of the statistics in the strong disorder limit where fig[4.3] is linear

$$V = A - B\langle Lng\rangle \qquad A \sim -1.5 \quad B \sim 1 \qquad \{4.9\}$$

As before states are exponentially localized in this regime

$$g \sim \exp(-\alpha L)$$

Therefore $$V \sim \alpha L \qquad \{4.10\}$$

We do not have enough data to analyze the low disorder behaviour but fig[4.4] clearly shows the variance decreasing with system size.

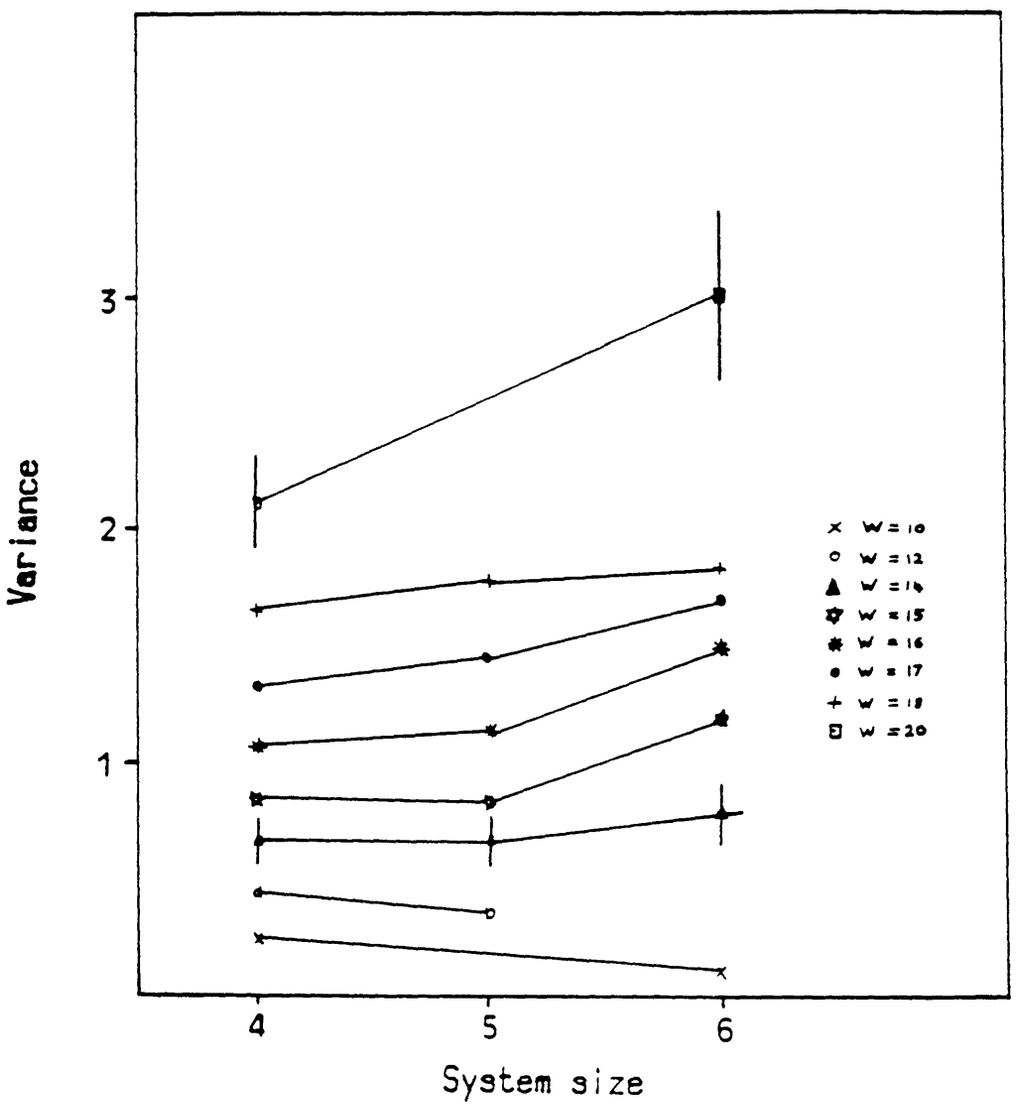


Fig 4.4 The variance V of Lng plotted as a function of system size in three dimensions. For clarity only some typical error bars are shown.

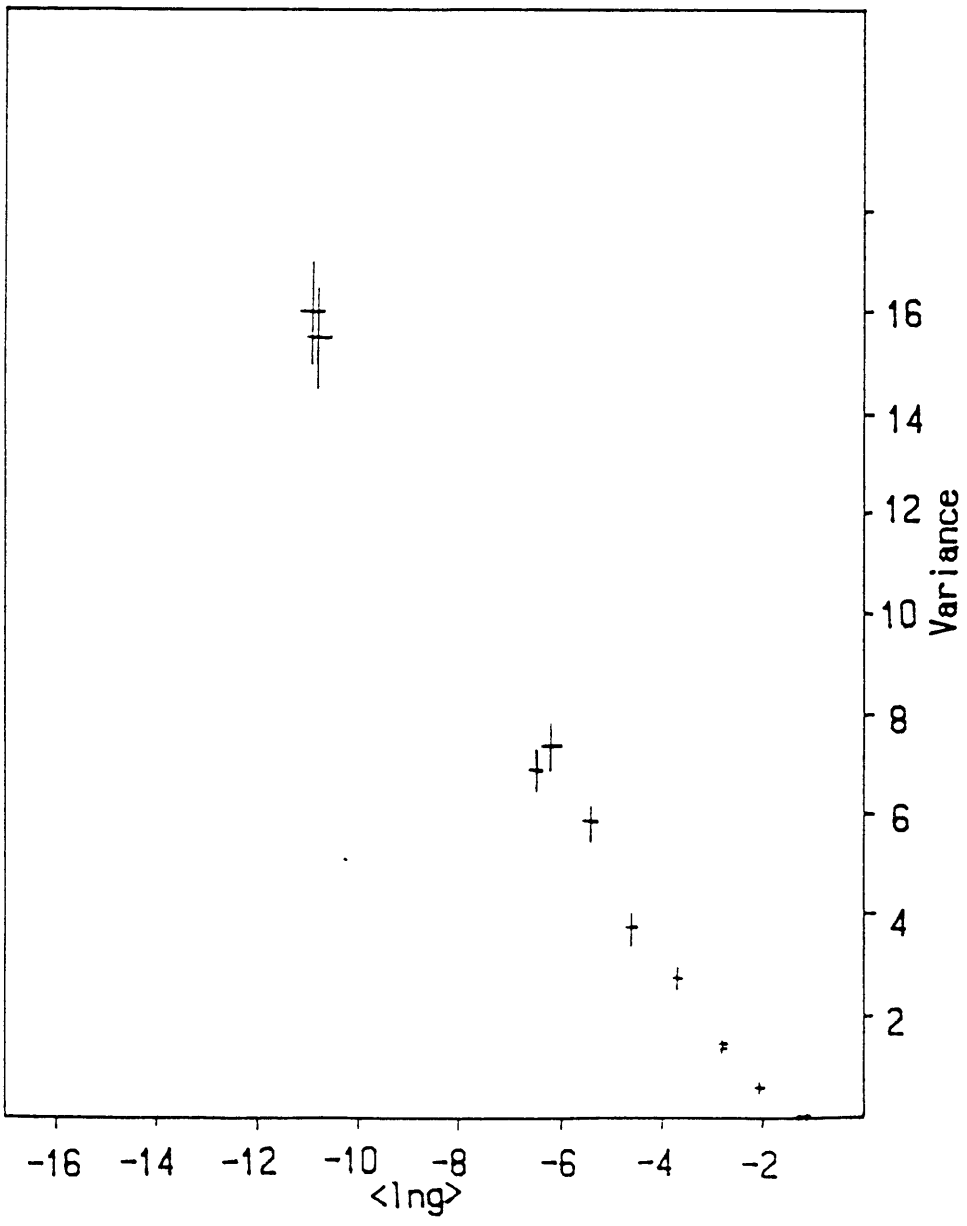


Fig 4.5 The variance V of Lng plotted against the average of Lng, in one dimension.

4.3.3 One dimension

Fig[4.5] shows a plot of the variance of lng vs the mean <lng> in one dimension for systems of various sizes and disorders. We have not calculated many points as the limiting forms of the probability distributions have been calculated by several authors, see for example Pendry and Kirkman(1984). At small conductances the variance increases linearly with <lng>

$$V \sim A - B\langle \ln g \rangle \quad \text{with} \quad A \sim -4, \; B \sim 2 \qquad \{4.11\}$$

It is interesting to note that the slope of the linear portion B is now ~ -2, compared with ~ -1 in two and three dimensions. The slope of -2 agrees with the results of Pendry. See section 4.5.

4.4 Self-averaging properties

To examine the self-averaging properties of the conductance from our data we have to determine the relative error in the conductance as a function of system size. If the conductance is to self-average its relative error must vanish in the thermodynamic limit. A relative error of order r induces an r.m.s error of Ln(1±r) in the logarithm of g, for small r

$$\mathrm{Ln}(g[1\pm r]) = \mathrm{Ln}\,g + \mathrm{Ln}(1\pm r)$$

Hence

$$1\pm r = \exp(V^{1/2})$$

where V is the variance of lng. Thus for small V the relative error in the conductance is the true error or variance of the logarithm of the conductance.

$$r \sim V^{1/2} \qquad \{4.12\}$$

The results of the preceding section show that in one and two dimensions and on the localized side in three

dimensions the variance of Lng increases with system size and therefore, by the above argument, the relative error in the conductance itself, does so as well. Thus the conductance does not self-average. Note that a linear increase in V implies an exponential increase in r. This is one of the reasons why we chose to examine lng instead of g.

4.5 Scaling of the variance

Fig[4.1] to [4.5] show that the variance of Lng scales with the mean, for the range of disorder and system size we have considered. This implies that the scaling hypothesis extends beyond averages, and may even apply to the whole distribution. ie every moment scales with the mean.

$$dP[\ln g]/d\ln L = f(\langle \ln g \rangle) \qquad \{4.13\}$$

This would certainly explain why past work on several different types of averages in one dimension, Sak and Kramer(1981), led to the same scaling behaviour and exponential increase of the resistance with system size. However exponents can be different, perturbative methods which average the conductance give a critical exponent of 1 in three dimensions, whilst numerical work which averages Lng, MacKinnon and Kramer(1983), indicates that the exponent is 3/2, so one has to be careful.

The scaling of the distribution can be demonstrated in, the weak disorder limit, in one dimension where Pendry and Kirkman (1984) have calculated the asymptotic form of the probability distributions. From their work one obtains for the probability distribution of Lng

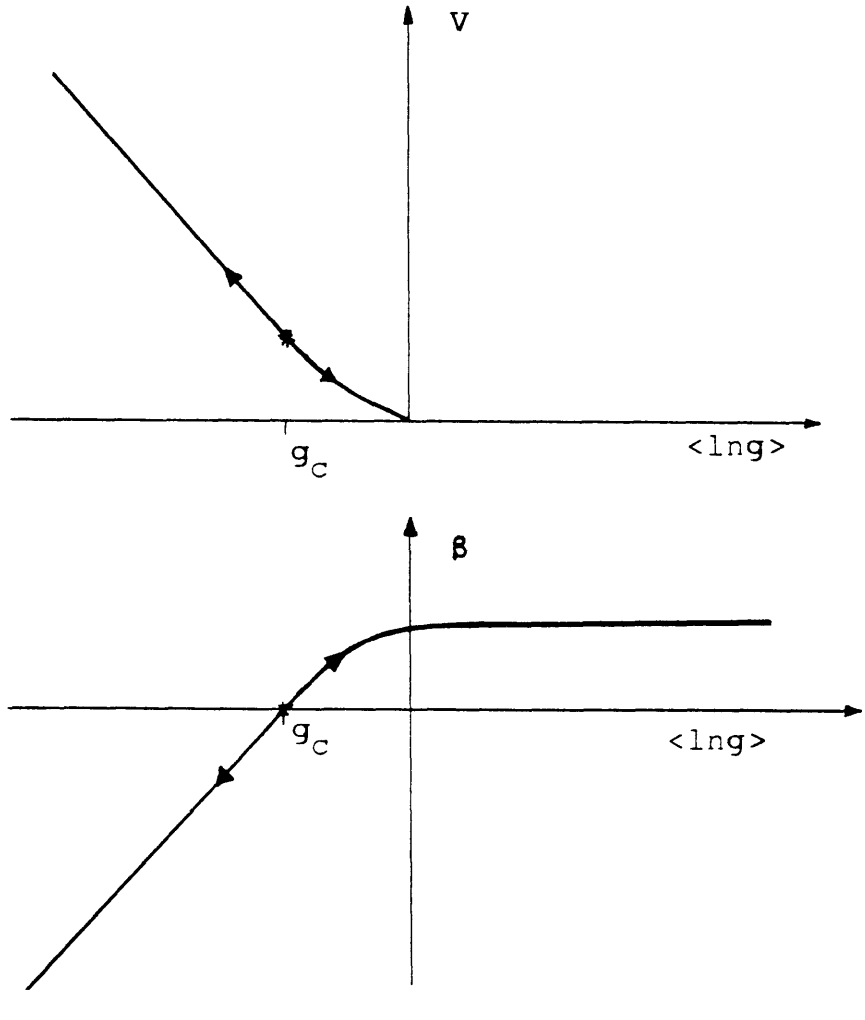
$$P(\ln g) = 1/\sqrt{(4\pi\langle \ln g \rangle)}\ \exp[\ -\ (\ln g + \langle \ln g \rangle)^2/4\langle \ln g \rangle]$$

where

$$\langle \ln g \rangle = -\alpha L$$

the whole distribution is characterized by <Lng>, hence one parameter scaling. At large disorder the distributions are still asymptotically log normal but no longer characterized by only one parameter, because we are presumably beyond the range of validity of scaling at this point.

From a scaling point of view the variance behaves rather like the conductance, it exhibits a repulsive fixed point in three dimensions at a value of the conductance g_c which we estimate to be approximately e^{-3}. This is roughly the conductance at which quantum corrections become important.



For $g>g_c$ one scales towards extended states and self-averaging, whilst for $g<g_c$ one scales towards exponential localization and non self-averaging. We can define a critical exponent for the variance by linearising about the fixed point g_c. Near the fixed point

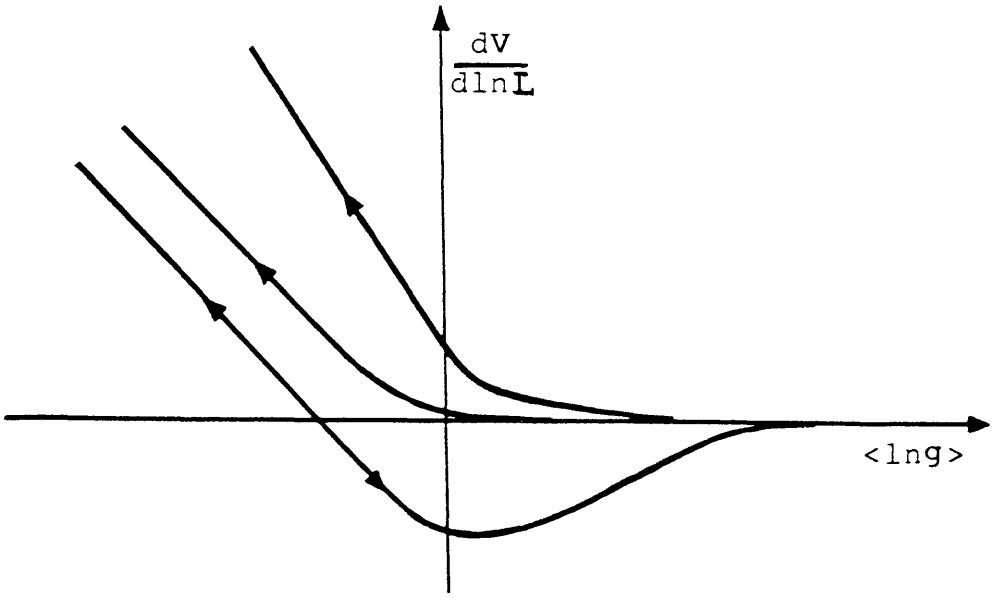
$$<Lng> \sim \mu Ln(E-E_c)$$

let $$V \sim \delta Ln(E-E_c)$$

then $$V \sim \mu/\delta <Lng> \qquad \{4.14\}$$

From fig[4.3] we estimate the gradient around g_c to be about unity. Hence the exponents for the conductivity and variance are equal. This is however only a rough estimate and it is possible that the exponents are anomalous such as those for the moments of the, square of the modulus, of the wavefunctions, Wegner (1979).

Just as the renomalization group beta function, describes the scale dependence of the conductance we can define dV/dLnL which describes the scale dependence of the fluctuations. Using fig[4.3] and the behaviour of the beta function we expect the behaviour of dV/dLnL to be that shown below.



4.6 Universal conductance fluctuations

Recently there has been much interest in systems in the mesoscopic size range,where Altshuler(1985) and Lee and Stone(1985) have extended the impurity diagram technique to calculate the r.m.s fluctuations of the conductance. Mesoscopic systems are those which are smaller then both the localization length and the inelastic scattering length L_T, but larger then the mean free path. Their calculations predict that the r.m.s fluctuations are independent of system size and disorder, but their estimates of the magnitude of these fluctuations are different ,though still of order unity. We have examined our data in the appropriate regime, and find that the variance is approximately scale invariant, in two dimensions at very low disorder and in three dimensions near the mobility edge.

4.6.1 Two dimensions

In section 4.3.1 we found that in the low disorder or large conductance limit the variance of the logarithm of the conductance behaves as

$$V = e^{\alpha}/g_o^2 + 2e^{\alpha}g_o^{-3}ALn(L/L_o) \qquad \{4.15\}$$

In this regime our system sizes are much shorter then the localization length, which is about 100 lattice spacings at W = 5, so we are well into the mesoscopic regime. For sufficiently short systems the first term dominates and thus the variance is scale independent

$$V \sim e^{\alpha}/g_o^2 \qquad \{4.16\}$$

From section 4.5, for small V, this is roughly the relative error in g. Hence

$$g_{r.m.s}/g \sim (e^{\alpha/2})/g_o \qquad \{4.17\}$$

g_o is the classical value of the conductance, which is of order unity. Furthermore in this regime $g \sim g_o$, so the root mean square fluctuations are given

$$g_{r.m.s} \sim e^{\alpha/2} \qquad \{4.18\}$$

α is equal to -4 which leads to $g_{r.m.s} \sim 0.13$. We have checked this number by direct computation of the fluctuations in g, which gave $g_{r.m.s} \sim 0.15$. These numbers agree with the estimate of Altshuler, who obtains $g_{r.m.s} \sim 0.11$, in contrast to the the estimate of Lee and Stone who obtain $g_{r.m.s} \sim 0.862$.

4.6.2 Three dimensions

Fig[4.4] shows that the variance of lng is scale independent near the mobility edge, which is approximately in the region W=14 $\longrightarrow$ 16, and has a value of about unity.

Therefore $g_{r.m.s} \sim g_o$ $\qquad \{4.19\}$

and g_o lies between e^{-2} and e^{-3}. This leads to

$$g_{r.m.s} \sim 0.13 \longrightarrow 0.05$$

Altshuler obtains a value of 0.12 whilst Lee and stone obtain a value of 1.088.

4.6.3 One dimension

We have examined the variance of g for systems which are typically 1/10 of the localization length and find no evidence for any universal fluctuations. The reason for this lies in the fact that in one dimension the mean free path is always of the order of the localization length, so that the mesoscopic regime is not accessible. However as Lee and Stone note, quasi one dimensional systems can exhibit universal fluctuations.

4.7 Possible reasons for non self-averaging

Localization is essentially a manifestation of quantum interference over macroscopic length scales. The conductance of a system is determined by the phase relationships between the many Feynman paths that connect two points at opposite ends of the sample. This was been demonstrated first by the experiments of Sharvin and Sharvin (1984), and then by the many experiments on small metal rings, which showed that the conductance oscillated with a period e^2/h, with an applied transverse magnetic field. A magnetic field changes the phase relationship between various Feynman paths, which results in changes in the conductance. We can expect that changing the sample will have a similar effect in that it will lead to a different set of phase relationships and thus lead to a completely different conductance. Thus the classical argument for self-averaging will fail because of the dependence of the conductance on long range correlations.

Another, perhaps not totally unrelated, way of looking at the problem, is from the Landauer picture in which one considers the problem as one of tunneling through a potential barrier. In one dimension it is believed, Azbel(1983), that the transmission coefficient is large when the Fermi level coincides with an eigenenergy of the system, and is exponentially small otherwise. The width in energy of an eigenstate is determined by how strongly it couples with the continuum of states in the leads. If the coupling is small as should be for localized states the spectrum of the system will be discrete, and since states are randomly distributed in energy the chances of the Fermi-level coinciding with an eigenstate depend upon the particular sample being considered. Thus we expect exponentially different conductances between different samples. This point will be considered in greater detail in chapter 6.

Kramer et al(1983) have suggested non self-averaging may be related to the non ergodic nature of localized

states. Localized states in contrast to extended states do not access all of phase space available to them, and thus do not average themselves out.

4.8 Finite temperature effects

All our results so far are valid only at T = 0, where the inelastic scattering length is infinite, and the Fermi level sharply defined. At finite temperatures the inelastic scattering length becomes finite and the Fermi is blurred into a region of width ~ kT. Inelastic scattering destroys phase coherence and suppresses localization, so that if the system is larger then L_i the inelastic scattering length the relevant upper cutoff becomes L_i. Thus the system is effectively partitioned into systems of dimension L_i which are uncorrelated. Within each region of dimension L_i the fluctuations will still be severe, but the observed conductance will be averaged over typically L/L_i independent units. Thus the magnitude of the fluctuations will be reduced by a factor $(L/L_i)^{1/2}$, and the system self averages. The blurring of the Fermi level is also expected to reduce the fluctuations, as one now has to average over $kT/\delta E$ independent conduction paths, where δE is the separation in energy of neighbouring peaks in the conductance.

Finite temperature effects can be simulated by applying an imaginary part to the energy. This gives states a lifetime, and broadens the spectrum so we expect the distributions to self average. That this is so has been shown by Mackinnon(1981) and Thouless and Kirkpatrick(1980).

Conclusions

We have demonstrated that in two and three dimensions, in the regime where states are expected to be exponentially localized, the conductance does not self-average. Indeed as in one dimension the variance of the conductance increases exponentially with system size. This shows that non self-averaging is an intrinsic property of localized states and not a peculiarity of one dimensional systems. We have further demonstrated that the variance of lng scales with the mean, which suggests that the scaling concept applies to the whole distribution rather the the mean alone.

Chapter 5

Scaling of the conductance in two dimensions

5.1 Introduction

The scaling theory of localization is now the most widely accepted explanation for the metal-insulator transition for non-interacting electrons in disordered systems. Initially a hypothesis of Anderson et al(1979) the theory has since received much support from both analytical and numerical work. Much of the analytical work is limited to the weak disorder regime and is either based on perturbation theory or mappings onto models of continuum field theories. Within these approaches we essentially assume that the motion of the electrons is diffusive, the density of states is featureless and the length scales are such that the details of the underlying lattice are irrelevant. Such assumptions are reasonable in the light of the success of the theory of phase transitions upon which scaling theory is based. However the localization problem differs from the theory of phase transitions, in certain respects in that the order parameter does not change over the transition and the symmetry is spontaneously broken for localized and extended states.

Numerical simulations have been instrumental in providing justification for the assumptions of the scaling hypothesis, MacKinnon and Kramer (1981, 1983). These have generally relied on using finite size scaling on long strips, and usually study the behaviour of the smallest Lyaponov exponent or largest localization length. The behaviour of the other exponents has not as far as we are aware been examined in detail, and they may well be relevant in real two or three dimensional systems. Indeed there is much evidence, Economou and Soukoulis(1984), Schreiber(1985), that on short length scales the wavefunctions have a fractal behaviour so that there could be several important length scales over small distances.

In the light of these complications, and the results of the last chapter concerning divergent fluctuations of the conductance for localized states, it would be desirable to check the predictions of scaling using a method which does not make any assumptions, regarding the number of relevant length scales, and does not disregard the lattice as the continuum field theories do, especially in two dimensions where the existence or not of a mobility edge has been a subject of constant debate, Mott (1978).

The algorithm of chapter 3 allows us to calculate the conductance exactly for finite systems. In this chapter we shall use this algorithm, to calculate the form of the beta function, dlng/dlnL, explicitly to check the predictions of the scaling theory in two dimensions.

Other objections to validity of a one parameter scaling theory, which have appeared recently include those of Efetov(1985) who has examined a system comprised of weakly coupled metallic granules separated by insulating interfaces, and has presented results which are incompatible with the scaling hypothesis although this system is supposed to be a prime candidate for the scaling theory, Imry (1980). His objections follows from the fact that in two dimensions corrections to the conductivity, contain terms with integrals which diverge in both the low and high momentum limits.

$$\int \frac{dq}{q}$$

The small q cutoff is the system size, but the large q cutoff which probes the short distance behaviour is problematic, and normally taken to be the shortest diffusion step or mean free path. For the first few orders in perturbation theory the cutoff turns out to be irrelevant, as far as scaling is concerned but this may not be generally true as is normally assumed. Higher order proofs of scaling, Hikami(1983), rely on mappings onto continuum field theories and the use of dimensional

regularization which ab-initio assumes the irrelevance of short range behaviour. This is an assumption of the scaling theory which is not rigorously proven. In short, the continuum field theory may not describe the lattice theory from which it is derived. This is a common problem when constructing field theories from lattice theories, and even for the Ising model there is a small discrepancy between exponents calculated from continuum approximations and series expansions, which is not fully understood.

Efetov has shown that his model can be mapped onto a lattice sigma model in which the lower cutoff is well defined, and is simply the inverse grain size, but he does not find a behaviour consistent with scaling. Instead his renormalization group equation for the conductance depends upon the structure of the lattice.

Efetov (1984) has also recently presented an exact calculation, for the conductance on a Cayley tree and finds a minimum metallic conductivity, on the basis of which he concludes that the scaling theory is wrong. However we believe his conclusion is not generally applicable because the mechanism for weak localization, closed loops, are specifically excluded from the Cayley tree.

5.2 Method

The predictions of the scaling theory of localization are most easily expressed in terms of the renormalization group beta function dLng/dLnL, which if scaling is correct should be a function of the conductance only and be strictly negative in two dimensions. The results we require in order to calculate the beta function have already been calculated in the last chapter, where we evaluated the conductance and its first few moments for two dimensional systems of various disorders and sizes. All we have to do to obtain dLng/dLnL is to numerically differentiate the data with respect to system size, and we have chosen to

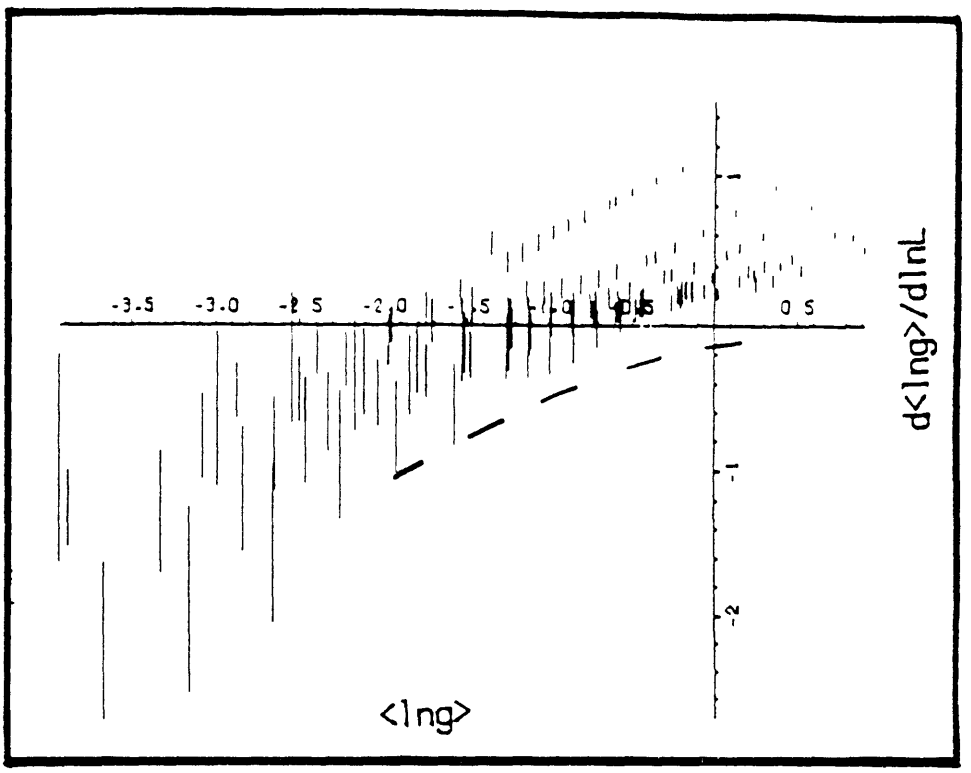


Fig 5.1 The beta function, defined as d<lng>/dlnL ,plotted against the average of lng. The dashed line is the perturbative prediction $\beta(g) = -1/g$. The points that deviate most from this line, correspond to small systems at low disorders.

work with <Lng> because unlike g it is representative of the ensemble.

5.3 Results

Fig[5.1] shows a plot of d<Lng>/dLnL, the dashed curve is the scaling prediction. The data is rather scattered because numerical differentiation is a noisy process but the important features are still distinguishable, and the data is quite systematic. The beta functions are seen to have an explicit system size dependence, which decreases with increasing system size. The points which lie furthest away from the dashed line, which is the scaling prediction, eqn{6.2}, correspond to small systems at low disorders. For small disorder the points become positive which would appear to indicate the existence of a fixed point. There are two reasons for this apparent departure from scaling :-

a) At very low disorder where the discrepancy with scaling is most obvious, the system sizes are smaller then the mean free path l. Scaling is only expected to be valid when the system size is much greater then l, so we can expect deviations.

b) As discussed in chapter 2 the algorithm we use, is expected to give incorrect conductances at very low disorder or a small number of channels, ie small system size, as a result of embedding the system in a perfect medium and evaluating the Kubo formula only over the disordered region.

The presence of a mobility edge and explicit system size dependence in our data can be understood by examining the effect on the beta function of the Economou-Soukoulis procedure, sec 3.5, which we use in our algorithm, in one dimension. Here the Economou-Soukoulis procedure gives the conductance as

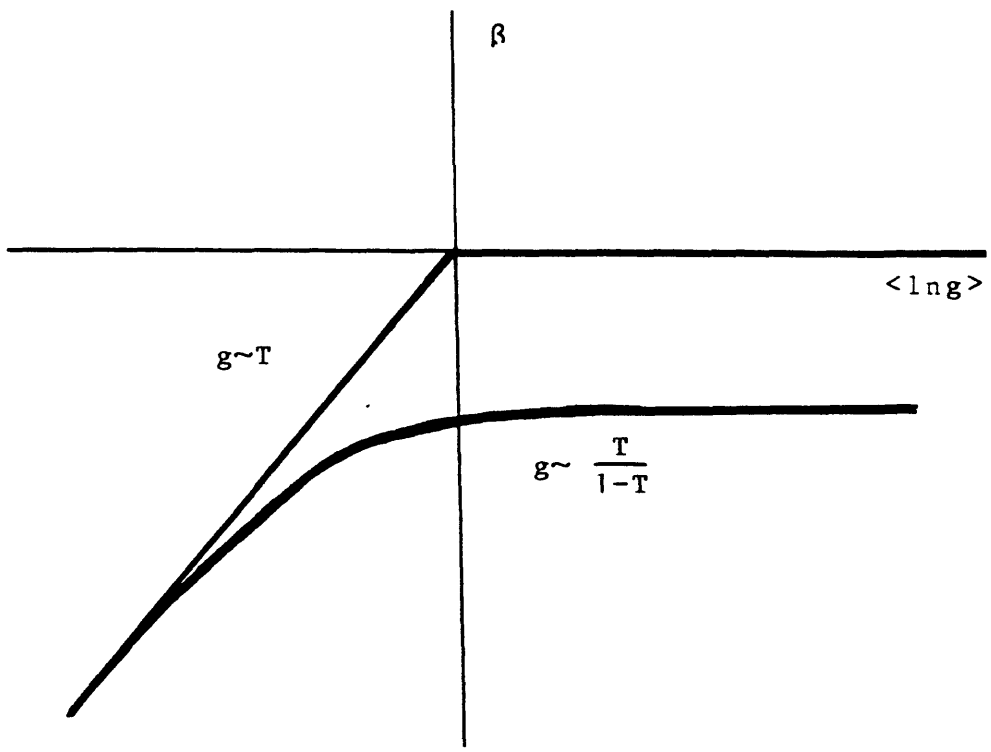


Fig 5.2 The two different beta functions obtained from eqn{1.5} and eqn{2.5} respectively.

$$g \sim T \qquad \{1.5\}$$

Where T is the transmission coefficient. The Landauer formula on the other hand gives

$$g \sim T/1-T \qquad \{2.5\}$$

the beta functions obtained using these two expressions are shown in fig[5.2]. We can expect a similar behaviour in two dimensions, as discussed in chapter 3, where in the limit of a large number of channels or large disorder

$g \sim Tr(t^{+}t)$ t is the transmission matrix

We showed at the end of chapter 3 that in one dimension the difference between {1.5} and {2.5} was simply a zero disorder resistance, and that {1.5} could be corrected to give {2.5} by subtracting from it, its zero disorder value. ie unity. We do not know whether the same procedure is valid in higher dimensions but fig[5.3] shows that it improves the data considerably, the corrected beta functions are much closer to the scaling result $\beta \sim -1/g$ at weak disorder, and much of the explicit system size dependence has also disappeared.

5.4 Conclusions

Despite the expected shortcomings of our method, at weak disorder for small systems, and the noise in the data which is probably a result of numerical differentiation, our results indicate that the beta function obtained by evaluating <lng> for systems of finite size in two dimensions, is close to that predicted by the scaling theory. We do not see any clear evidence of a minimum metallic conductivity or a mobility edge in two dimensions. Moreover we have evaluated the beta funtion using a method which deals with real two dimensional systems, and does not make any assumptions about the number of relevant length scales. Our results seem to agree with the scaling theory of localization.

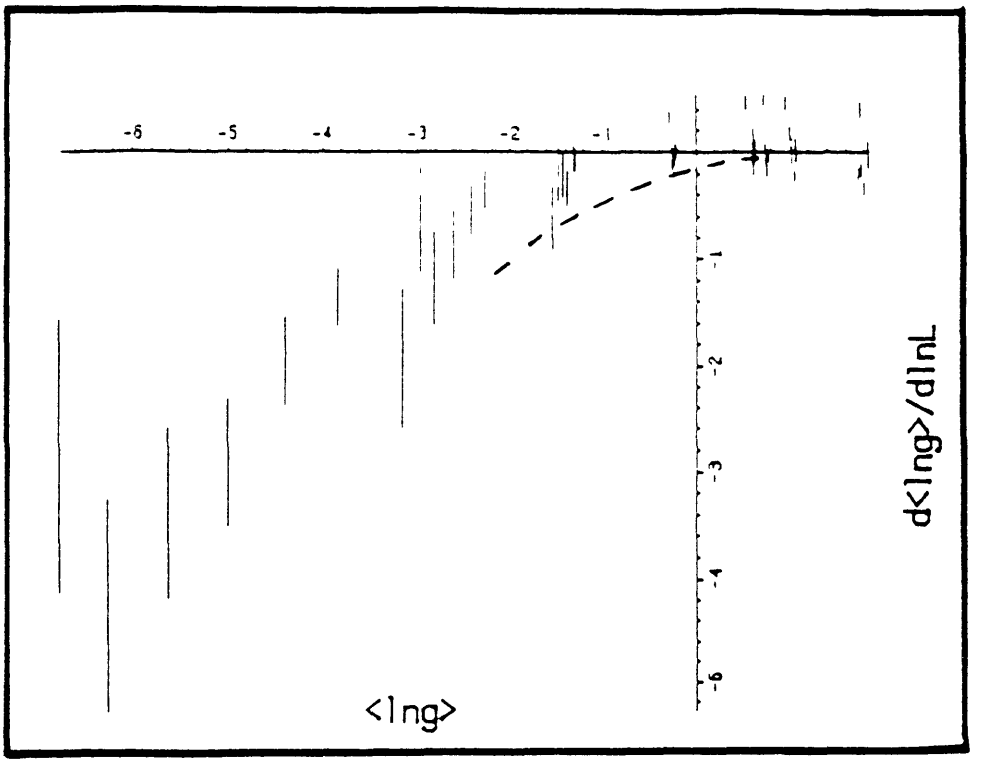


Fig 5.3 The beta function of fig[5.1] after the approximate correction outlined in the text. The agreement with the scaling prediction is now much better.

Chapter 6

A study of the measure of the spectrum, and its connection to the statistics of the conductance

6.1 Introduction

It has recently become clear, from extensive work in one dimension, Anderson et al(1980), and the results of chapter 4 concerning two and three dimensional systems, that the behaviour of the transport coefficients of disordered systems is more complicated then was at first thought. Quantum interference leads to localization of eigenstates and divergent sample to sample fluctuations in the conductance and resistance.

In this chapter we investigate the possibility that fluctuations in the conductance are correlated with fluctuations in the density of states. The density of states is generally believed to be smooth and featureless. Whilst this may be true on average it certainly is not for any individual system when the eigenstates are localized, as can be seen from fig[3.2]and fig[3.3], where the density of states of a finite disordered system, coupled to infinite ordered leads, becomes more structured as we increase the size of the system.

Extrapolating to the thermodynamic limit, it seems that the density of states will eventually consist of a set of very sharp δ-functions, and its support will be of measure zero, rather like the measure of the rationals in the field of real numbers.

Consequently the conductance will vanish almost everywhere, except when the Fermi-level coincides with a state. As the peaks get sharper with increasing system size, the probability of hitting a state decreases and thus the average conductance vanishes and its statistics become more extreme.

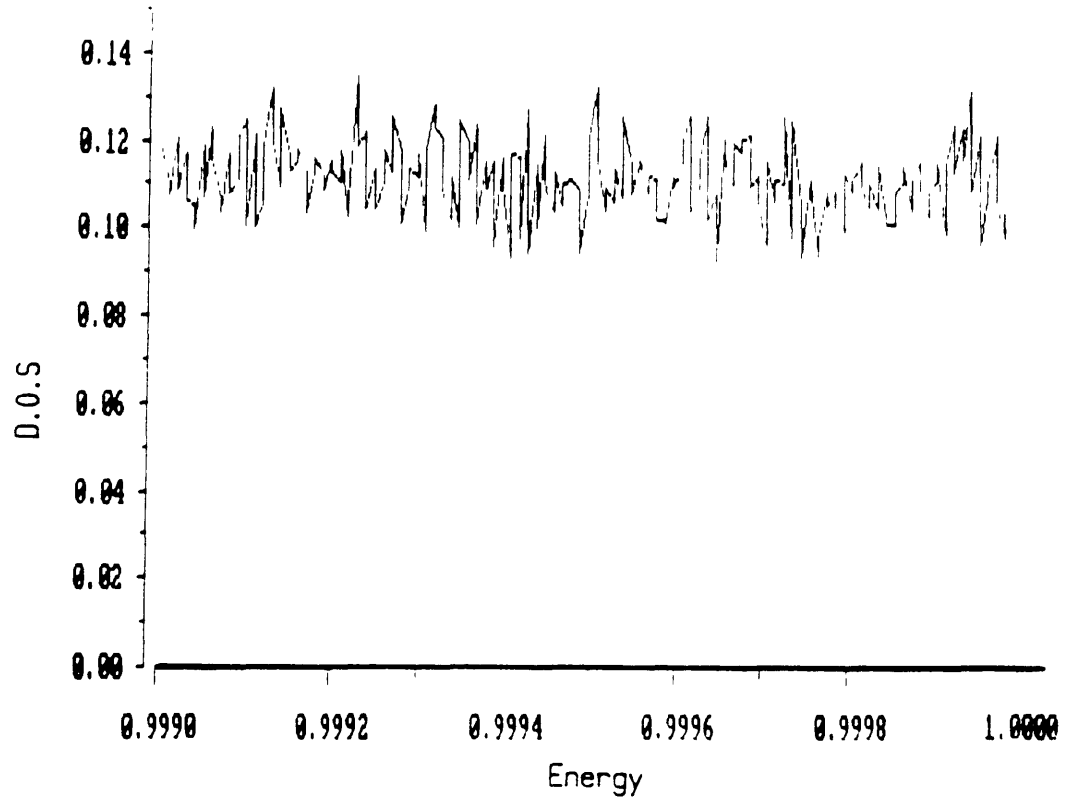


Fig 6.1a The density of states of a three dimensional cube of dimension 4^3, at a disorder W = 5.

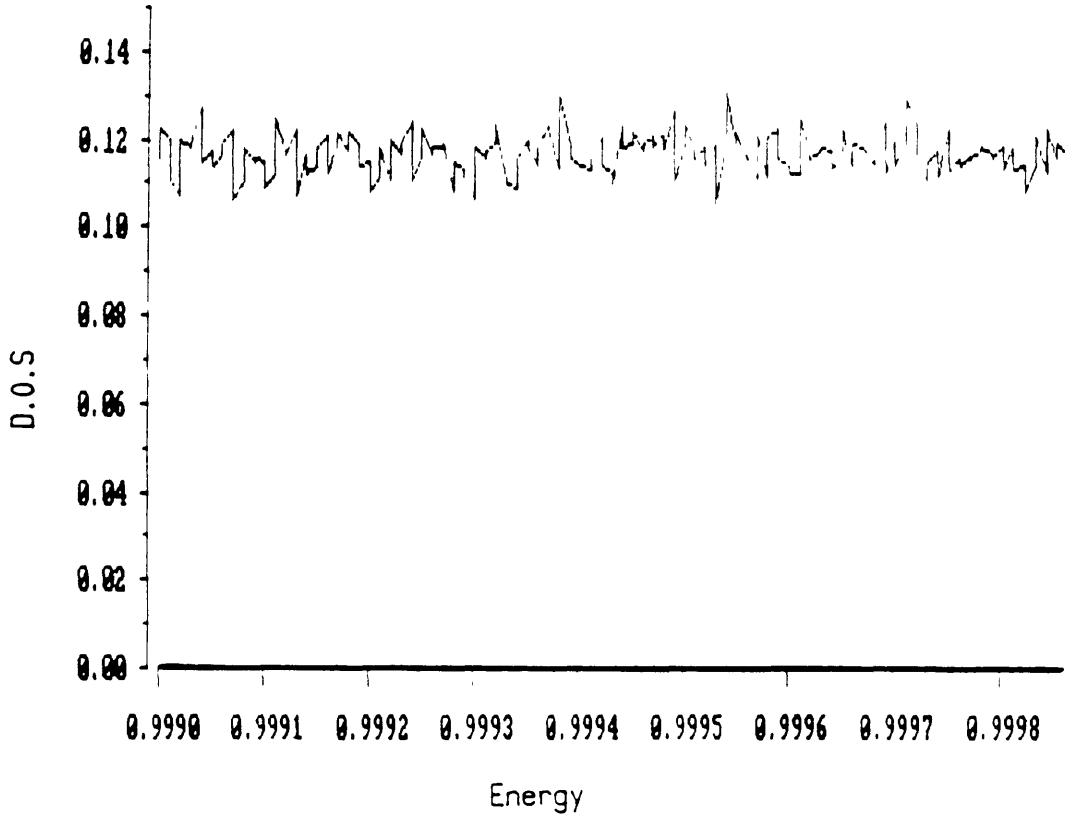


Fig 6.1b Same as in fig[6.1a] but now for a cube of dimension 8^3. Notice that density of states is getting smoother.

On the other hand, for extended states the results of chapter 4 show that the conductance self-averages, and so we expect that if there exists a correlation between the conductance and density of states, the density of states should become smooth in the thermodynamic limit.

Using the method of chapter 3 we have calculated the density of states of a three dimensional cube embedded in a perfect medium, in the regime where the eigenstates are expected to be extended. The results are shown in fig[6.1] and clearly show a tendency for the state density to smoothen out with increasing system size.

The physical model consists of a disordered system connected to perfect leads. Coupling of the states in the system to the continuum of states in the leads broadens the discrete states of the system and the extent to which this occurs depends upon the strength of the coupling between them. The exact form of this coupling is difficult to ascertain but we might expect it to be related to the conductance of the state, which is a measure of how sensitive it is to boundary conditions, Edwards and Thouless(1972). Indeed the scaling arguments of Thouless, for the average properties of the system imply that this is so, but in reality each state is quite different and Azbel(1983) has suggested that the most important features of the conductance may in fact be governed by resonant tunneling. We recall that for a large resonant transmission coefficient the width of a state in energy, should be small so that its lifetime is large. Thus those states that are most weakly coupled to the leads will have the largest resonant conductance. In this work we shall not distinguish between the different resonant or normal transmission contributions from different states, but will try to determine the importance of gaps in the spectrum.

Thus we shall consider a simplified picture in which all states for which the density of states is appreciable have equal conductance, and will show that this can

account for much of the extreme behaviour of the conductance observed in chapter 4. In reality each state will have a different transmission coefficient, and only those with the largest transmission relative to the gap will be important. Thus the probability of the Fermi-level coinciding with a state which has a transmission coefficient close to unity will be smaller then in our model, and so we expect the fluctuations to be even worse in reality. In some sense we obtain a lower bound on the severity of the fluctuations.

6.2 Our model

Although the algorithm of chapter 3 allows us to examine the density of states, the regions of the spectrum over which the state density is appreciable are hard to quantify. In order to investigate the behaviour of the density of states in a systematic way we shall consider the following model. Instead of attaching infinite metals we treat the disordered sample as a unit cell and periodically continue it to infinity in one direction. The discrete levels of a finite cell are broadened into bands, which may or may not overlap. If the coupling between cells is weak the bands will be narrow. The measure of the spectrum of this model is easier to study as bands and gaps are always well defined, and we expect that the band width is a good estimate of the amount by which the corresponding level in the disordered system will be broadened, when coupled to ordered leads. Anderson and Lee(1980), have shown that this is true on average in one dimension.

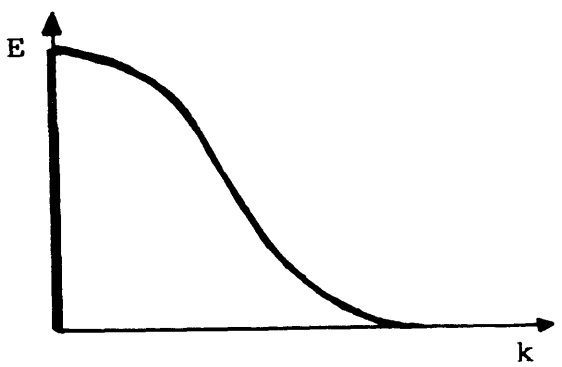
One way of looking at this is the following picture due to Thouless(1974). Consider a disordered sample connected to perfect leads. If an electron of energy E_α takes a time τ to diffuse across the sample then its energy is uncertain by an amount $\delta E_\alpha = h/\tau$, using the uncertainty principle. In terms of the diffusion coefficient D we may write

$$\delta E_\alpha \sim hD/L^2$$

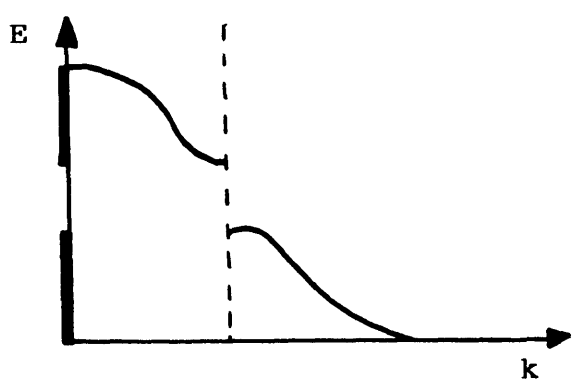
This is an estimate of the width of the energy level E_α. Now consider repeating the disordered system so that it forms a periodic system. The discrete levels of a finite sample are broadened into bands and Thouless has shown, that if the levels are uncorrelated, the band width of the state α, has a Cauchy distribution of half width δE. The independence of levels for localized states has recently been proved by Gorkov et al(1983).

Thus we expect that the measure of the spectrum of the physical system, and that of the periodically continued system are similar. The properties of the spectrum can then be examined as a function of cell size and disorder, and limiting behaviours deduced.

The behaviour of this model is easy to deduce in one dimension. Consider first a unit cell with one atom, its spectrum consists of one energy band



A unit cell with two atoms per unit cell has a Brillouin zone of half the size and if the atoms are different a gap opens up at the zone boundary. The spectrum now consists of two bands separated by a gap.



Continuing this procedure it is plausible that each band carries on splitting until at infinity the bands are flat and of infinitesimal width. The measure of the spectrum vanishes.

In higher dimensions the behaviour is not as obvious, because the bands may overlap due to the increased degeneracy caused by the enlargement of k space. With a view to examining the statistics the important question to be asked is, How does the ratio of band to gap depend upon cell size and cell disorder ?

6.2.1 The average conductance

The model of a periodically continued unit cell, is very similar to that of Edwards and Thouless (1972) who formulated the early ideas on scaling. They proposed that localized and extended states of, a finite block, could be distinguished by comparing the shift in energy of a state to changes in boundary conditions. Localized states are exponentially small at the boundary so their response will be small, whilst extended states will show a relatively large shift. They were able to give heuristic arguments which related the ratio of the average energy shift on changing boundary conditions from periodic to antiperiodic to the average level spacing, to the conductance. Essentially the perturbation involved in changing from periodic to antiperiodic boundary conditions, is simply the momentum operator, the matrix elements of which appear in the Kubo formula. Under certain conditions equivalent to large disorder, the average level shift δE and the average level spacing w can be related to g by

$$g \sim (\delta E/w) \qquad \{6.1\}$$

Anderson and Lee(1980) have shown that at least in one dimension this is not quite correct and that the conductance is in fact related to the square of the ratio.

$$g \sim (\delta E/w)^2 \qquad \{6.2\}$$

However as far as scaling is concerned, what is important is not the exact form but the functional dependence.

From our point of view, the level shifts are simply the width of the energy bands that would be formed if the cell were periodically continued as pointed out by Licciardello and Thouless (1975). If P is the proportion of band in the spectrum then

$$\delta E \sim P/N_b \qquad \{6.3\}$$

$$w \sim 1/N_b \qquad \{6.4\}$$

where N_b is the number of bands per unit energy interval.

hence $$g \sim P \qquad \{6.5\}$$

Thus the proportion of band in our model can be related to the average conductance of a real system.

6.2.2 Fluctuations

Fluctuation of the conductance in our model are a result of the extreme changes in the density of states. From Bloch's theorem, if the Fermi-level lies in a band there is must be perfect transmission t=1. If it lies in a gap t = 0.

Since the probability of hitting a band is P the relative fluctuations are given by

$$r = \sqrt{(1-P)/P} \qquad \{6.6\}$$

The measure of the spectrum thus determines the mean and all moments because we have a very simple distribution. The lack of self-averaging is manifested by a decrease in the proportion of band P, as can be seen from eqn{6.6}.

In this chapter we shall examine the behaviour of the measure of the spectrum of a periodically continued unit cell, as a function of cell size and disorder, using a numerical procedure which we derive in section 6.3. It is shown that in the presence of localized states the measure of the spectrum is a vanishing quantity in any dimension. Moreover for localized states it vanishes exponentially with system size, which in our model leads to exponentially increasing fluctuations, in agreement with the results of chapter 4. Towards the end of the chapter we discuss the results of some preliminary investigations, on the nature of the fluctuations in a more realistic model.

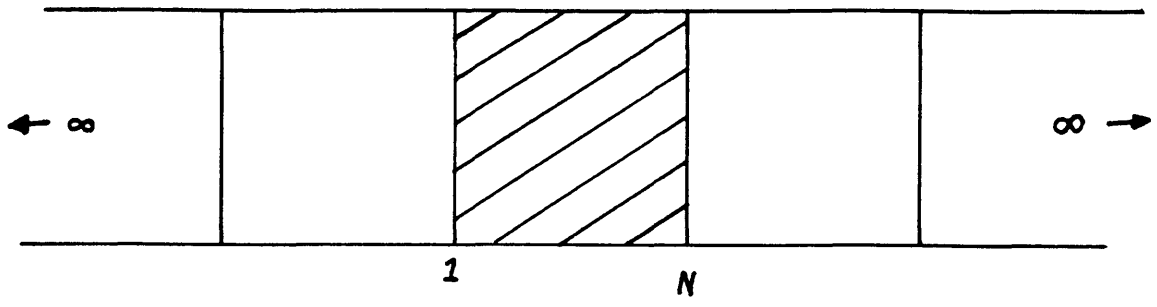
6.3 The Density of States of a disordered periodically continued unit cell

In this section we describe the procedure used to calculate the density of states of an arbitrary unit cell which has been periodically continued to infinity in one direction. The boundary conditions in the other directions can either be free or periodic.

Much of this is based on the algorithm described in chapter 3 and like that algorithm computational restrictions limit us to systems of fairly small cross section. The length of the unit cell is however arbitrary. We shall study the behaviour of the density of states as a function of the cross section so that its limited size is not a serious limitation.

6.3.1 The Algorithm

We consider constructing the system by attaching semi-infinite periodically continued strips to both ends of a unit cell.



The Hamiltonian of the system can be written as

$$H = H^{+}(\infty)+H^{-}(\infty)+H_u+V \qquad \{6.7\}$$

Where $H^{+}(\infty)$ is the Hamiltonian of a 0 to ∞ semi-infinite strip, H_u is the Hamiltonian of a isolated unit cell and V is the coupling between the unit cell and the semi-infinite strips.

$$V = |0><1|+|1><0|+|N><N+1|+|N+1><N| \qquad \{6.8\}$$

The $|N>$'s are vectors in the subspace of a slice. For simplicity we take the hopping elements to be equal to unity.

The Greens function operator for the uncoupled system separates into three subspaces.

$$G^0 = G^{+}(\infty)+G^{-}(\infty)+G^u \qquad \{6.9\}$$

G^u acts in the subspace of the unit cell and $G^{+}(\infty)$ acts in subspace of the 0 to ∞ strip.

To calculate the density of states we need the diagonal elements of the Greens function for the coupled system. These may be obtained by treating the coupling as a perturbation and using Dyson's equation as follows.

Dyson's equation $\qquad G = G^0+G^0VG \qquad \{6.10\}$

Taking matrix elements

$$G_{ii} = G^0_{ii} + G^0_{i1} G_{0i} + G^0_{iN} G_{N+1i} \qquad \{6.11\}$$

It is sufficient to restrict i to lie in one unit cell $0<i<n+1$. Then $G^0_{ij} = G^u_{ij}$ for $0<j<N+1$.

Hence $$G_{ii} = G^u_{ii} + G^u_{i1} G_{0i} + G^u_{iN} G_{N+1i} \qquad \{6.12\}$$

But from {6.10} $$G_{0i} = g_0 G_{1i} \qquad \{6.13\}$$

and $$G_{N+1\ i} = g_{N+1} G_{Ni}$$

Where we have defined $G^0_{00} = g_0$ and $G^0_{N+1\ N+1} = g_{N+1}$.

Thus $$G_{ii} = G^u_{ii} + G^u_{i1} g_0 G_{1i} + G^u_{iN} g_{N+1} G_{Ni} \qquad \{6.14\}$$

We can eliminate G_{Ni} and G_{1i} in favor of G^u_{Ni} and G^u_{1i} by again using Dyson's equation.

$$\begin{aligned} G_{Ni} &= G^u_{Ni} + G^u_{NN} G_{N+1\ i} + G^u_{N1} G_{0i} \\ G_{1i} &= G^u_{1i} + G^u_{11} G_{0i} + G^u_{1N} G_{N+1i} \end{aligned} \qquad \{6.15\}$$

using {6.12} these become

$$\begin{aligned} G_{Ni} &= G^u_{Ni} + G^u_{NN} g_{N+1} G_{Ni} + G^u_{Ni} g_0 G_{1i} \\ G_{1i} &= G^u_{1i} + G^u_{11} g_0 G_{1i} + G^u_{1N} g_{N+1} G_{Ni} \end{aligned} \qquad \{6.16\}$$

or in matrix form

$$\begin{bmatrix} 1-G^u_{NN} g_{N+1} & -G^u_{N1} g_0 \\ -G^u_{1N} g_{N+1} & 1-G^u_{11} g_0 \end{bmatrix} \begin{bmatrix} G_{Ni} \\ G_{1i} \end{bmatrix} = \begin{bmatrix} G^u_{Ni} \\ G^u_{1i} \end{bmatrix} \qquad \{6.17\}$$

This can be inverted to get G_{Ni} and G_{1i} in terms of G^u_{Ni} and G^u_{1i}.

Let $$\begin{aligned} G_{Ni} &= A G^u_{Ni} + B G^u_{1i} \\ G_{1i} &= C G^u_{Ni} + D G^u_{1i} \end{aligned} \qquad \{6.18\}$$

Then {6.14} becomes

$$G_{ii} = G^u_{ii}+G^u_{i1}g_0BG^u_{1i}+G^u_{iN}g_{N+1}CG^u_{Ni}+G^u_{i1}g_0AG^u_{Ni}+G^u_{iN}g_{N+1}DG^u_{1i}$$

Taking the trace over a unit cell

$$\Sigma\, G_{ii} = \Sigma\, G^u_{ii} +R^N_{N1}g_0A+R^N_{11}g_0B+R^N_{NN}g_{N+1}C+R^N_{1N}g_{N+1}D \qquad \{6.19\}$$

Where we have defined

$$R^N_{ab} = \Sigma\, G^u_{ai}G^u_{ib} \qquad \{6.20\}$$

Thus the problem of calculating the density of states is essentially solved if we can calculate:-

a) The elements of the Greens function at the ends of a semi-infinite strip g_o and g_{N+1}.

b) The quantities G^u_{NN}, G^u_{N1}, G^u_{1N}, G^u_{11} which appear in equation {6.17}.

c) The quantities R^N_{ab}.

We now show how these can be obtained.

6.3.2 <u>The elements of the Greens function at the ends of a semi-infinite strip</u>

Consider the set of equations {6.15} relating G_{Ni} and G_{1i} to G_{0i} and G_{N+1i}. They can be written in the form

$$\begin{bmatrix} -G^u_{11} & 1 \\ -G^u_{N1} & 0 \end{bmatrix} \begin{bmatrix} G_{0j} \\ G_{1j} \end{bmatrix} = \begin{bmatrix} 0 & G^u_{1N} \\ -1 & G^u_{NN} \end{bmatrix} \begin{bmatrix} G_{Nj} \\ G_{N+1j} \end{bmatrix} + \begin{bmatrix} G^u_{1j} \\ G^u_{Nj} \end{bmatrix} \qquad \{6.21\}$$

To solve this consider first the homogeneous problem

$$\begin{bmatrix} -G^u_{11} & 1 \\ -G^u_{N1} & 0 \end{bmatrix} \begin{bmatrix} G_{0j} \\ G_{1j} \end{bmatrix} = \begin{bmatrix} 0 & G^u_{1N} \\ -1 & G^u_{NN} \end{bmatrix} \begin{bmatrix} G_{Nj} \\ G_{N+1j} \end{bmatrix} \qquad \{6.22\}$$

Bloch's theorem tells us that on shifting by a lattice vector the Greens functions only differ by a phase factor.

$$\text{ie} \quad G_{N+1j} = \alpha G_{1j}$$
$$\text{and} \quad G_{Nj} = \alpha G_{0j} \qquad \{6.23\}$$

Hence we have to solve the generalized eigenvalue problem

$$\begin{bmatrix} -G^u_{11} & 1 \\ -G^u_{N1} & 0 \end{bmatrix} \begin{bmatrix} U_a \\ U_b \end{bmatrix} = \alpha \begin{bmatrix} 0 & G^u_{1N} \\ -1 & G^u_{NN} \end{bmatrix} \begin{bmatrix} U_a \\ U_b \end{bmatrix} \qquad \{6.24\}$$

Since the problem is time reversal invariant the eigenvalues of eqn{6.24} come in pairs which are inverses of each other.

The eigenvalues and eigenvectors may be obtained numerically by using standard library routines such as the NAG library.

The solution to the full inhomogeneous problem are linear combinations of the solutions of the homogeneous problem.

For a 1 to ∞ strip we may write

$$G_{N+11} = U_b \alpha B$$
$$\text{and} \qquad \{6.25\}$$
$$G_{N1} = U_a \alpha A$$

Where $|\alpha|<1$ because physically we cannot have exponentially increasing solutions into the strip, and U_a and U_b are submatrices of the matrix of eigenvectors corresponding to those eigenvectors whose eigenvalues are of modulus less then unity. α is the matrix of

eigenvalues such that $|\alpha| < 1$ and A and B are matrices containing the coefficients of the linear combinations.

The matrices A and B can be determined by demanding that the solutions satisfy the inhomogeneous equation .

For a 1 to ∞ strip all G_{1j} and G_{Nj} vanish for $j<1$

Thus {6.21} reduce to

$$G_{11} = G^u_{1N} G_{N+11} + G^u_{11}$$

and $$G_{N1} = G^u_{NN} G_{N+11} + G^u_{11} \qquad \text{on setting } j=1$$

Substituting for the G_{ab} from eqn{6.25} we obtain A and B

$$B = [U_b - G^u_{1n} U_b \alpha]^{-1} G^u_{11} \qquad \{6.26\}$$

and $$A = [U_a \alpha]^{-1} \{G^u_{nn} U_b \alpha B + G^u_{n1}\}$$

The Greens function at the end of 1 to ∞ strip is then given by

$$g_{N+1} = G_{11} = U_b B \qquad \{6.27\}$$

Similarly we can find g_0 by considering those eigenvectors with eigenvalues $|\alpha| > 1$.

6.3.3 Calculation of $R_{\alpha\beta}$ and $G^u_{\alpha\beta}$

The quantities $R_{\alpha\beta}$ and $G^u_{\alpha\beta}$ depend only on an isolated unit cell and can all be obtained using a set of recursion relations which we derive below.

Consider constructing the unit cell by adding together slices as in chapter 3. We showed that the elements of the Green's function of a N+1 slice cell could be related to those of an N slice cell by the following relationship

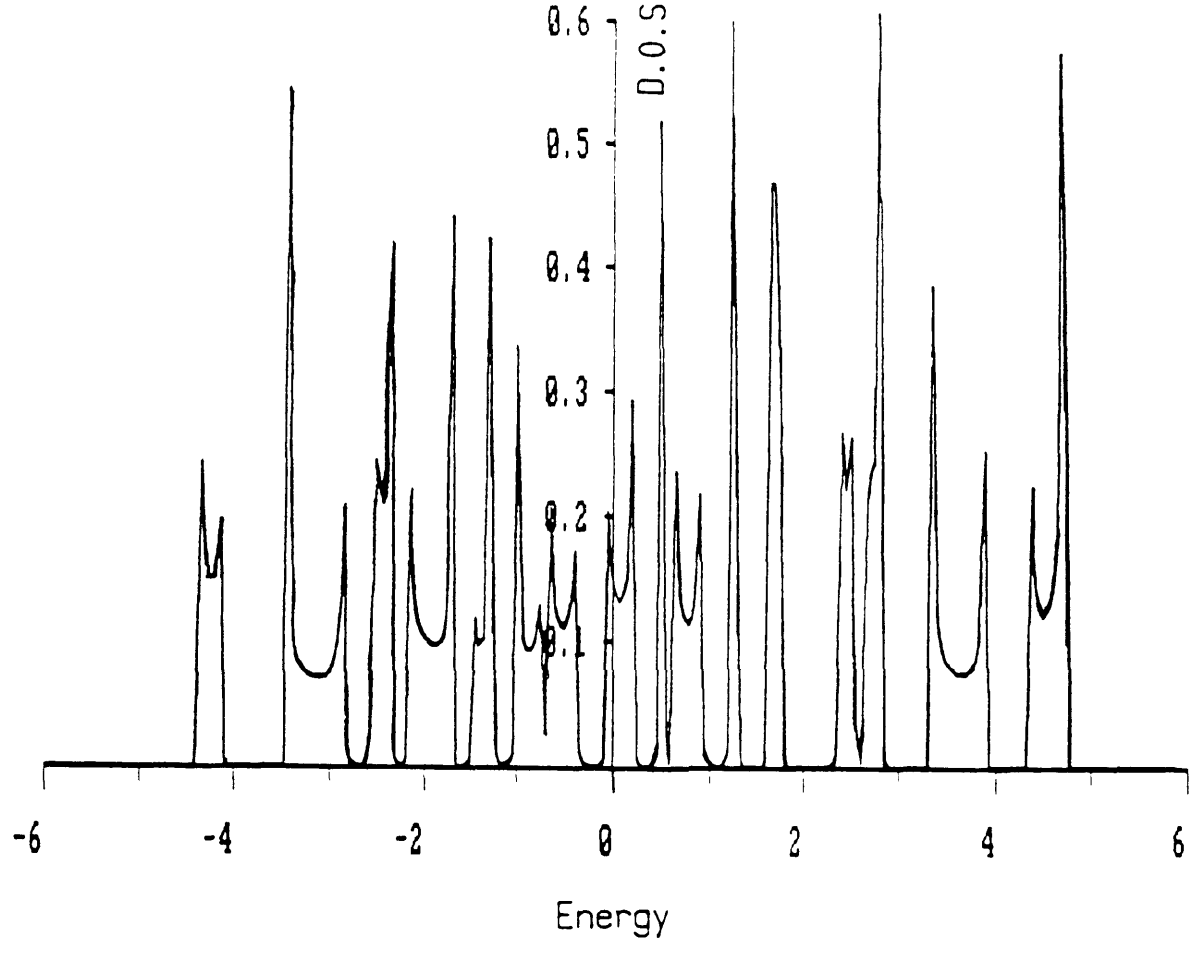


Fig 6.2 The density of states of a system consisting of a disordered unit cell periodically continued to infinity in one direction, calculated using the algorithm of section 6.3.

$$G^{N+1}_{ij} = G^{o}_{ij} + G^{o}_{iN} G^{N+1}_{N+1\ j} + G^{o}_{i\ N+1} G^{N+1}_{Nj} \qquad \{6.28\}$$

Using this it is easily shown that

$$\begin{aligned} G^{N+1}_{N+1\ N+1} &= [(G^{o}_{N+1\ N+1})^{-1} - G^{N}_{NN}]^{-1} \\ G^{N+1}_{1\ N+1} &= G^{N}_{1N} G^{N+1}_{N+1\ N+1} \\ G^{N+1}_{11} &= G^{N}_{11} + G^{N}_{1N} G^{N+1}_{N+1\ 1} \end{aligned} \qquad \{6.29\}$$

with initial conditions $G^{o}_{oo} = G^{o}_{11} = 0$ and $G^{o}_{10} = 1$.

and

$$\begin{aligned} R^{N+1}_{N+1\ N+1} &= G^{N+1}_{N+1\ N+1} \ [\ 1 + R^{N}_{NN}\ ]\ G^{N+1}_{N+1\ N+1} \\ R^{N+1}_{N+1\ 1} &= G^{N+1}_{N+1\ N+1} \ [\ R^{N}_{N1} + R^{N}_{NN} G^{N+1}_{N+1\ 1} + G^{N+1}_{N+1\ 1}\ ] \\ R^{N+1}_{1\ N+1} &= [\ R^{N}_{1N} + G^{N+1}_{1\ N+1}\ R^{N}_{NN} + G^{N+1}_{1\ N+1}\ ] G^{N+1}_{N+1\ N+1} \\ R^{N+1}_{1\ 1} &= R^{N}_{11} + G^{N+1}_{1\ N+1}\ R^{N}_{N1} + R^{N}_{1N} G^{N+1}_{N+1\ 1} + \\ &\qquad G^{N+1}_{1\ N+1} [\ 1 + R^{N}_{NN}\ ] G^{N+1}_{N+1\ 1} \end{aligned} \qquad \{6.29\}$$

with initial conditions $R^{o}_{\alpha\beta} = 0$

This completes the derivation for the density of states. A typical density of states is shown in fig[6.2].

To examine the measure of the density of states it is not necessary to go through the whole procedure. If we pick an energy which lies in energy band then at least one of the eigenvalues of equation {6.24} must be of modulus unity. Thus to determine whether there is a state at any

given energy all we have to do is search through the eigenvalues and see if there are any of modulus unity.

6.4 Calculation of the measure of the spectrum

We have used the method described above to calculate the proportion of band, near the band centre for ensembles of systems of differing disorders and unit cell dimension L, in one, two and three dimensions. The disorder, represented by differing site energies in a unit cell, is random and selected from a normalized top hat distribution. The proportion of band was calculated by fixing the Fermi-level close to the centre of the band, and checking what pecentage of systems, chosen from an ensemble, had a state at that point.

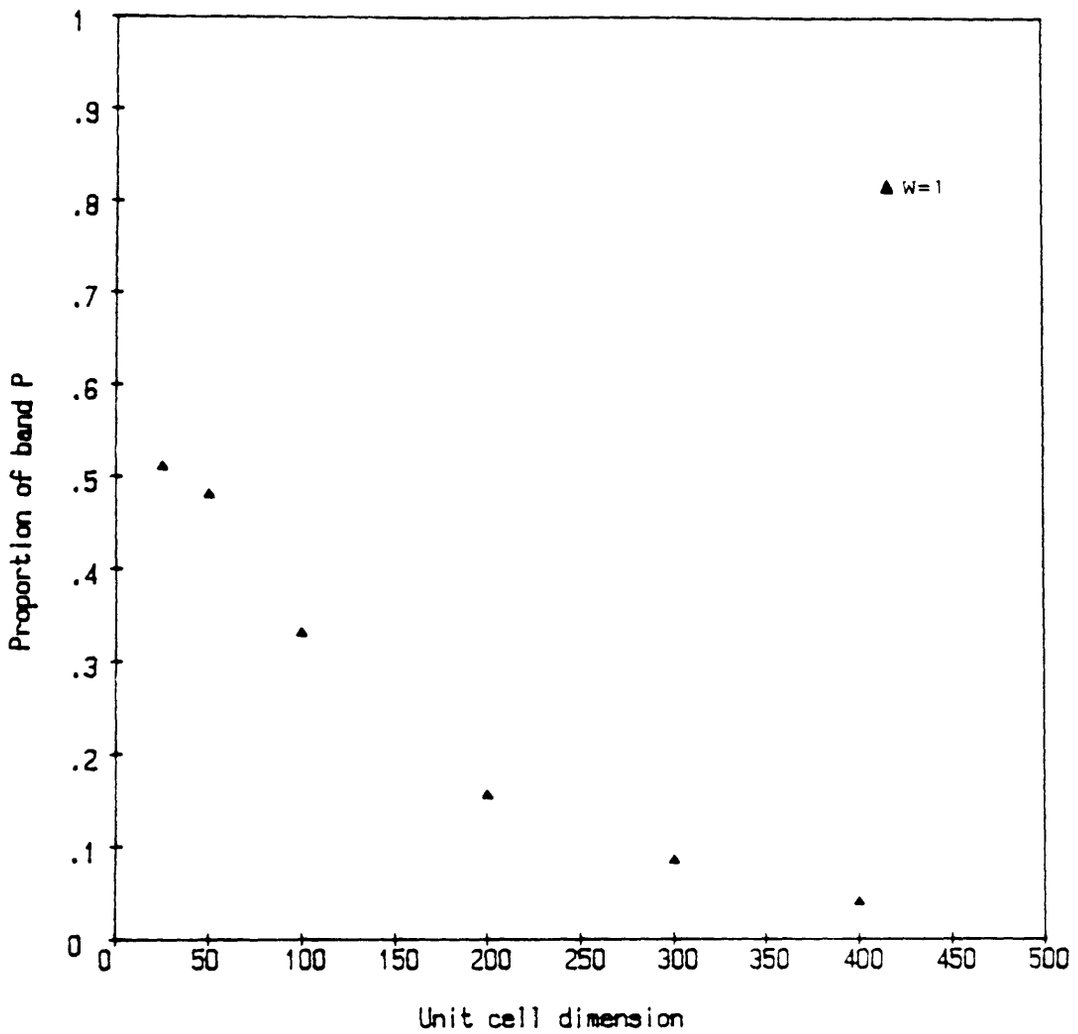


Fig 6.3 The proportion of band P plotted against the size of the unit cell, for a one dimensional system at disorder W = 1. The error bars are not significant.

Results

6.4.1 One dimension

Fig[6.3] shows a plot of P vs L at disorder unity. The behaviour of P for short systems is rather random, but settles down when the system size approaches the localization length, after which P starts to drop exponentially. Thus the measure of the spectrum is vanishing with system size. This is found to occur at all disorders up to the smallest we studied which was W = 0.1, and the rate at which it drops depends upon disorder, according to

$$P \sim \exp(-L/L_o) \qquad \{6.30\}$$

Fig[6.4] shows a plot of Log P against L, for disorders W=1 and W=2. The slopes of the curve determine the length scale over which P drops, and are found to be

$$L_o \sim 150 \quad \text{at} \quad W=1$$

and

$$L_o \sim 40 \quad \text{at} \quad W=2$$

Anderson and Lee(1980) have shown that in one dimension the conductance is in fact related to P^2, so that $L_o/2$ should be the localization length. Thus we obtain for the localization length $\xi = 75$ at $W = 1$, and $\xi = 20$ at $W = 2$. The accepted values for these quantities are 100 and 25 respectively. Our values seem to differ by a factor of about a quarter, though they are of the right order of magnitude.

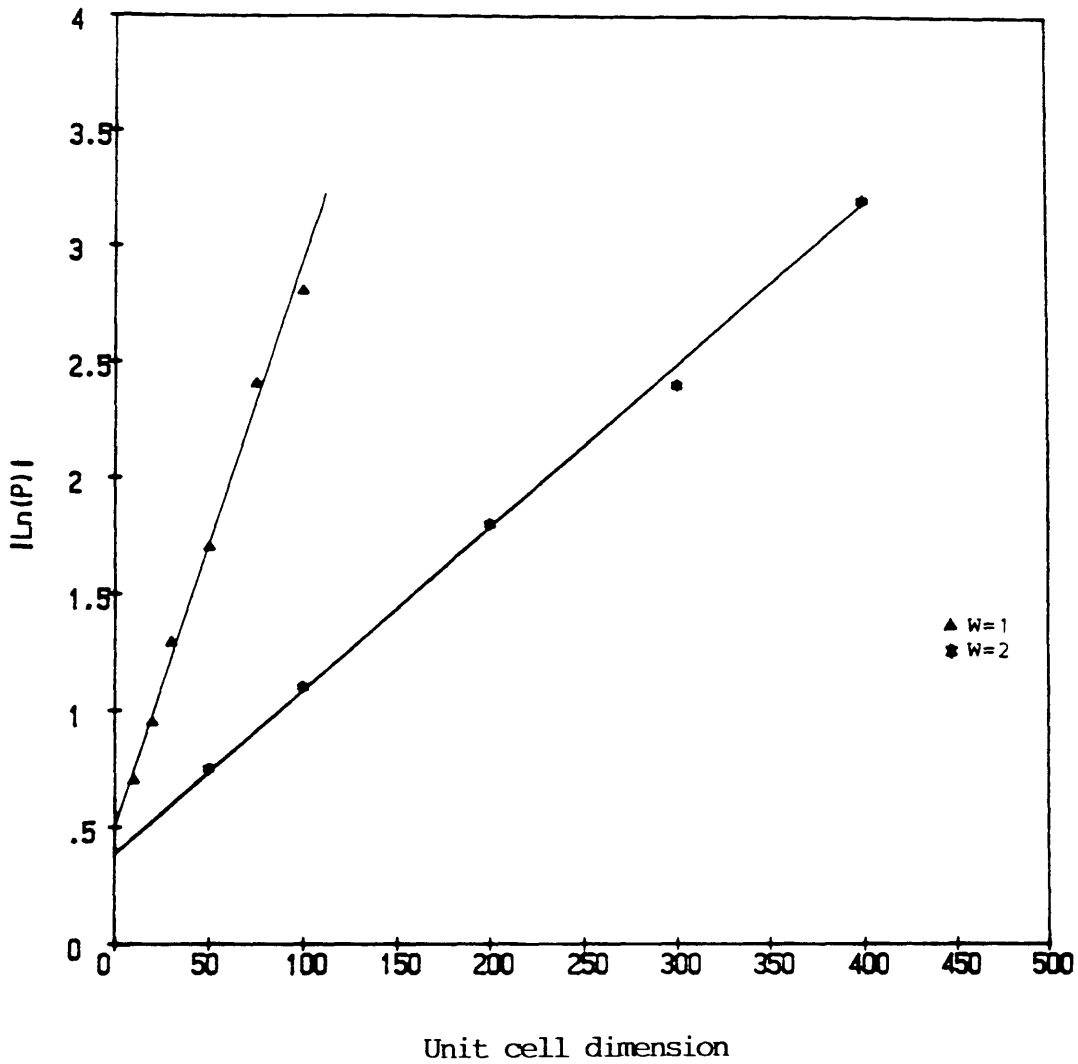


Fig 6.4 The modulus of the logarithm of P plotted against the unit cell dimension for one dimensional systems at disorders W = 1 and W = 2.

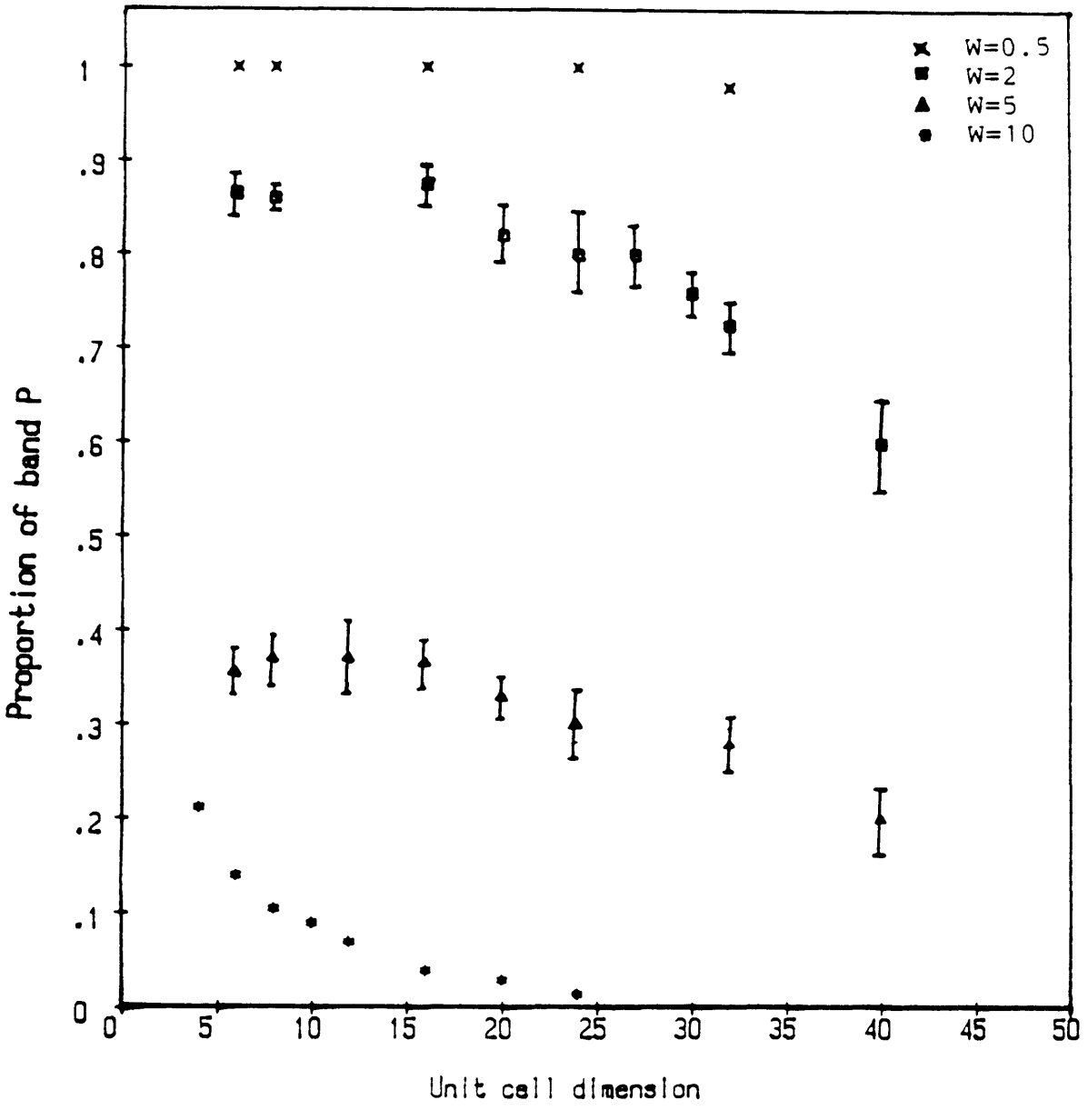


Fig 6.5 The proportion of band P plotted against unit cell dimension, for a two dimensional system at various values of the disorder parameter W.

6.4.2 Two dimensions

Fig[6.5] shows a plot of P against the unit cell dimension L for a variety of disorders ranging from W = 0.5 to W = 8. The system sizes ranged from 4^2 to 40^2. This range was found to be sufficient to determine the main features of the behaviour of P with L. At the lowest disorder, W = 0.5 the proportion of band is approximately constant over the range of systems considered. As the disorder is increased P remains constant for a while and then starts to drop until at about W = 10, which is fairly strong disorder in two dimensions, it drops exponentially from the smallest systems, as can be seen from fig[6.6] where we have plotted the log of P vs L for this disorder

Thus it seems that P will eventually drop for large enough systems even for the lowest disorders, and thus there is no evidence for an Anderson transition. All states appear to be localized. We can compare our results with those of Licciardello and Thouless (1975), who calculated the ratio of the average level shift on changing boundary conditions from periodic to antiperiodic, to the average spacing between levels. As we discussed in section 6.1.1 this is equivalent to P. Their results appear to indicate that an Anderson transition takes place at W = 5. However the largest systems they considered were of dimension 14^2 which as our data shows is too small to be able to see the imminent drop in P. Up to systems of dimension 20^2 P remains approximately constant which could have been taken as a sign for a transition.

At large disorder P drops exponentially over a length L_o, which we estimate to be about 9 at W = 10. The localization length at this disorder is about 10. Notice that the proportion of band initially remains steady over a significant change in scale, before starting to fall, for disorders W = 1/2, 2 and 5. The fact that P is scale invariant implies that the fluctuations are constant over

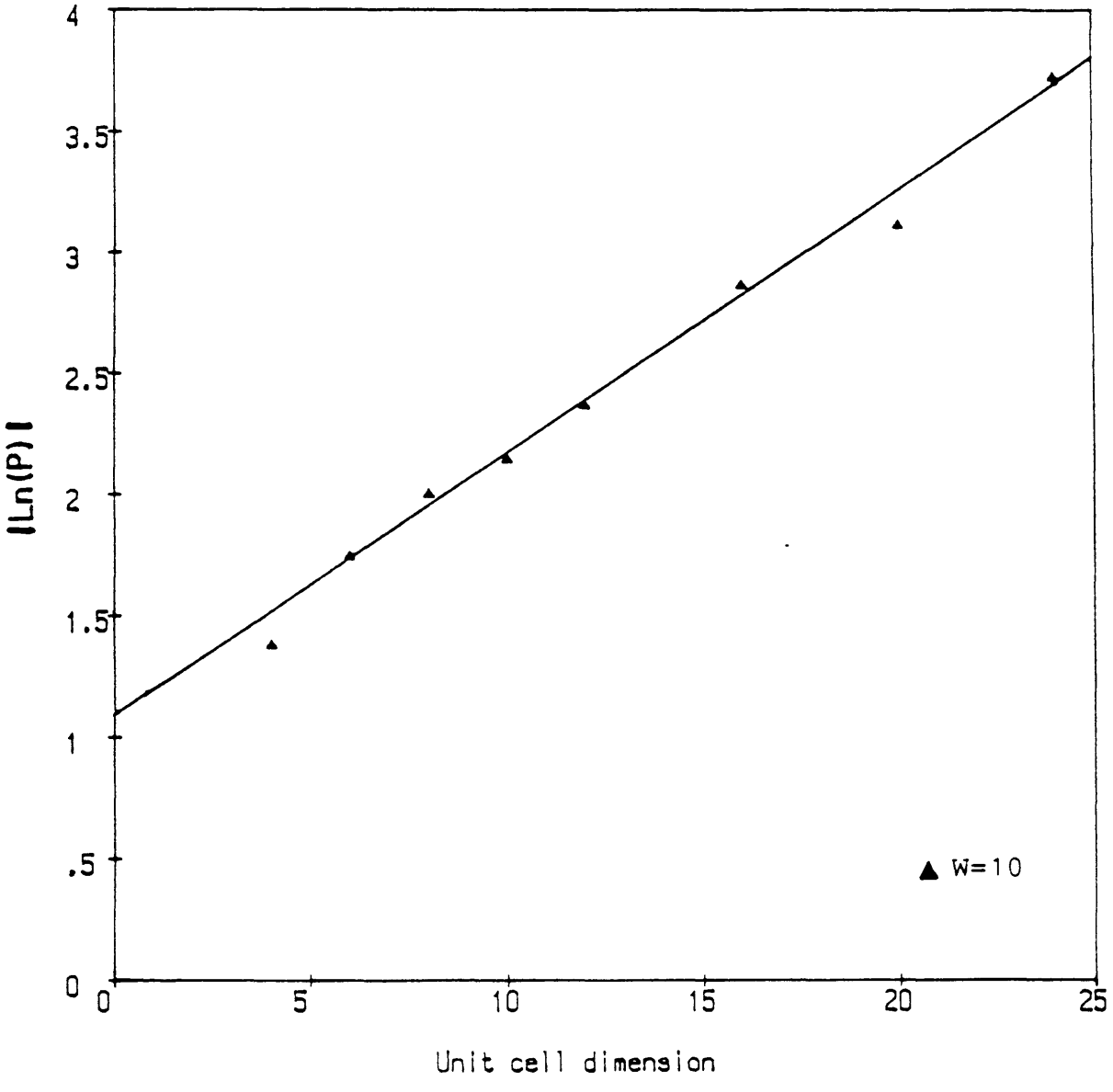


Fig 6.6 The modulus of the logarithm of P plotted against the unit cell dimension for a two dimensional systems at disorder W = 10.

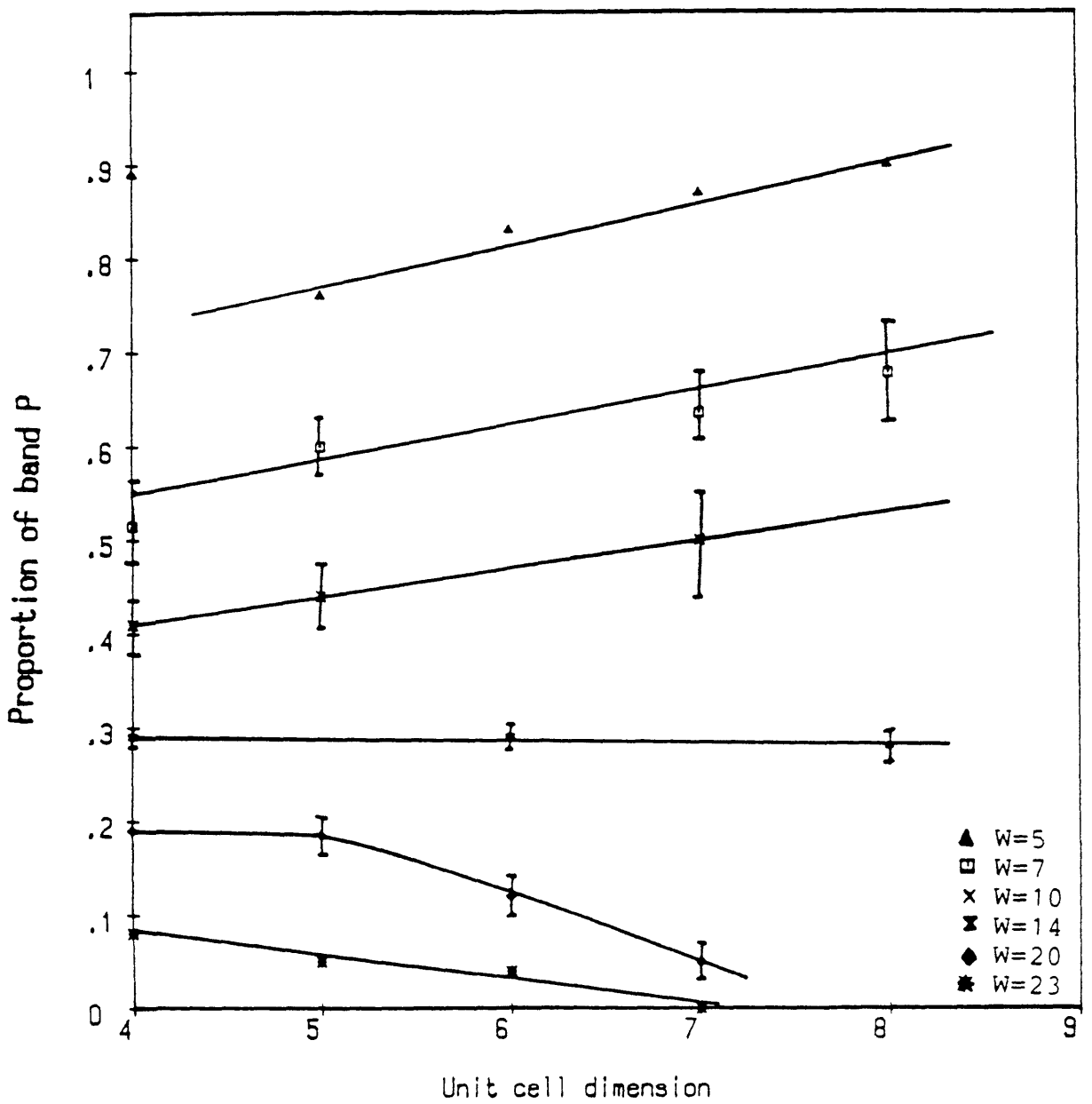


Fig 6.7 The proportion of band P plotted against unit cell dimension, for a three dimensional system at various values of the disorder parameter W.

this range, which may be related to the universal conductance fluctuations.

6.4.3 Three dimensions

Fig[6.7] shows a plot of P vs unit cell dimension L, for a range of disorders, W = 5 to W = 23. The maximum size of the unit cell we could study was limited to 8^3 atoms, by limitations on computer time, but the trends in the behaviour of P are clear. At and around W = 14, P stays approximately constant as would be expected at the Anderson transition. Below W = 14 the proportion of band increases with system size, reflecting the extended nature of the eigenstates. Above W = 14 P drops slowly at first and then in an exponential manner as in one and two dimensions. It is interesting to note that even at the Anderson transition the fluctuations are of the order of the mean. That fact that P remains constant at about 0.3 around the Anderson transition implies that the fluctuations are scale invariant, which is in agreement with the current ideas about universal conductance fluctuations.

6.5 Non self-averaging

We have seen above that the measure of the spectrum P is a vanishing quantity, when the eigenstates are expected to be localized. This means that the relative error increases with system size, and so the conductance as defined in this model cannot self average. For strong disorder the measure P drops exponentially with system size over a length scale of the order of the localization length.

$$P \sim \exp(-L/L_0) \qquad \{6.31\}$$

Hence the relative error $r = \sqrt{(1-P)/P}$ behaves as

$$r \sim [\exp(L/L_0) - 1]^{1/2}$$

for large L $r \sim \exp(L/2L_0)$ {6.32}

which agrees qualitatively with the behaviour we observed in chapter 4.

On the extended side of the transition, in three dimensions, the proportion of band increases in an approximately linear fashion with system size before tailing off to unity, as can be seen from fig[6.7]. Here it is reasonable to assume that the conductance g defined as P/(1-P), will increase linearly with system size which is the accepted result in three dimensions. Using this we obtain a relative error

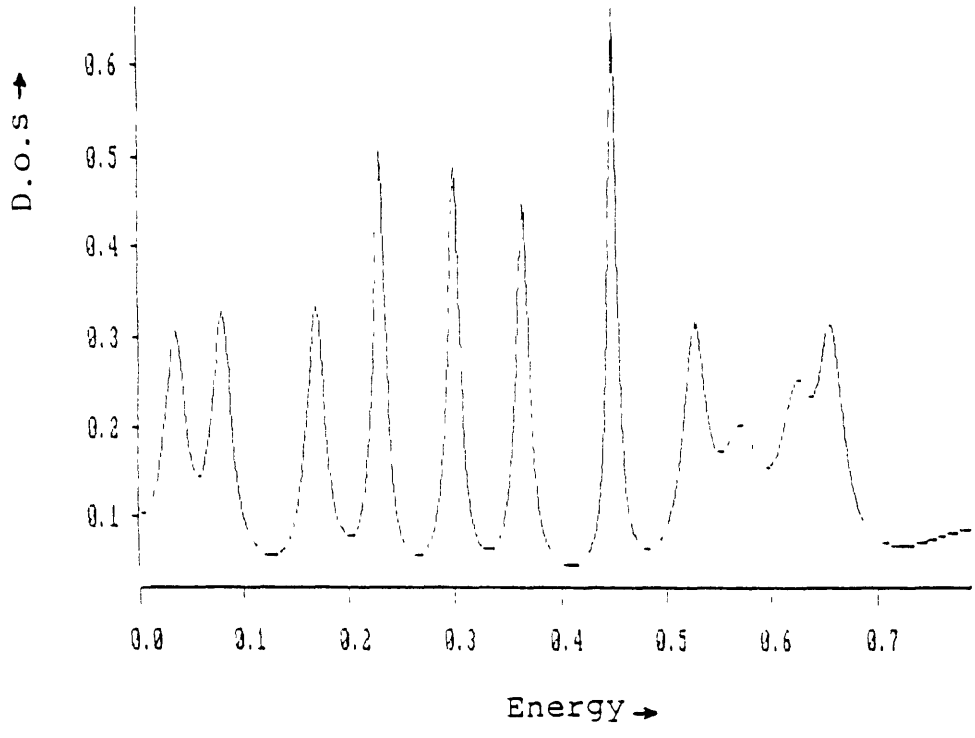
$$r \sim (1/L)^{1/2} \qquad \{6.33\}$$

which is the analagous to the self-averaging behaviour of normal thermodynamic quantities.

6.6 Conclusions

We have shown that the measure of the spectrum of a system consisting of disordered unit cell periodically continued to infinity in one direction, decreases with increasing system size in the region of the spectrum where we would expect to find localized states. Since we expect the properties of this system to approach those of a real system, ie one consisting of a unit cell embedded in a perfect medium, we conclude that the measure of the density of states of a random systems is a decreasing function of system size, when its eigenstates are localized.

Furthermore in the region where states are expected to be strongly localized, the measure of the spectrum decreases exponentially with system size, over a length scale of the order of the localization length. By contrast on the extended side the measure of the spectrum increases. Thus in the thermodynamic limit the density of



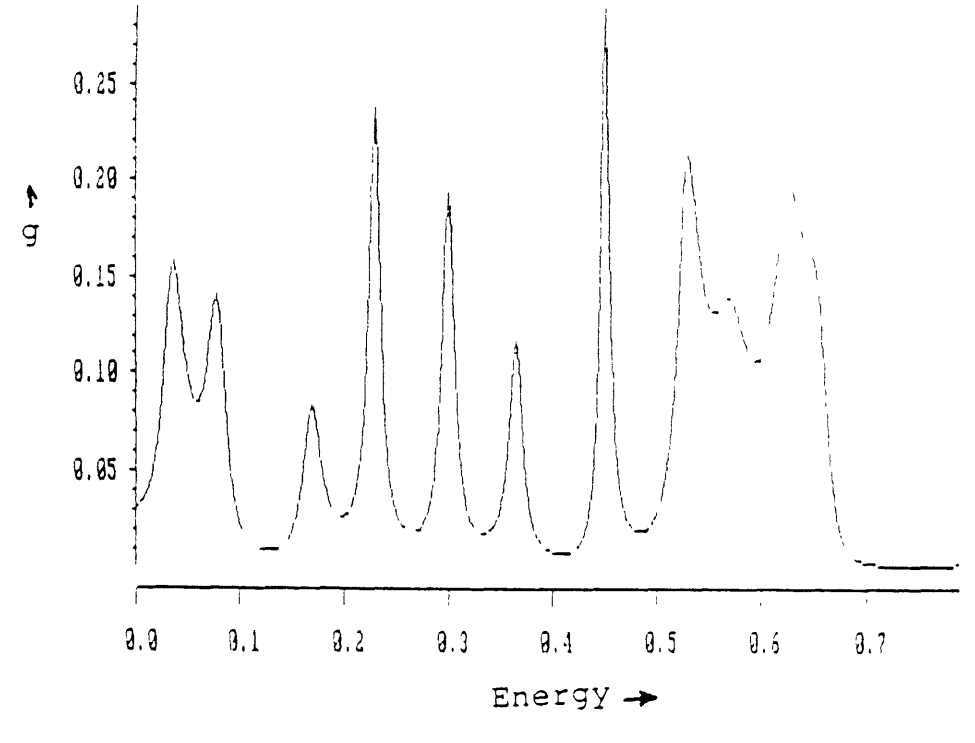


Fig 6.8 Plots of the density of states and conductance vs the position of the Fermi-level, for a one dimensional system consisting of one hundred atoms at disorder W = 1.

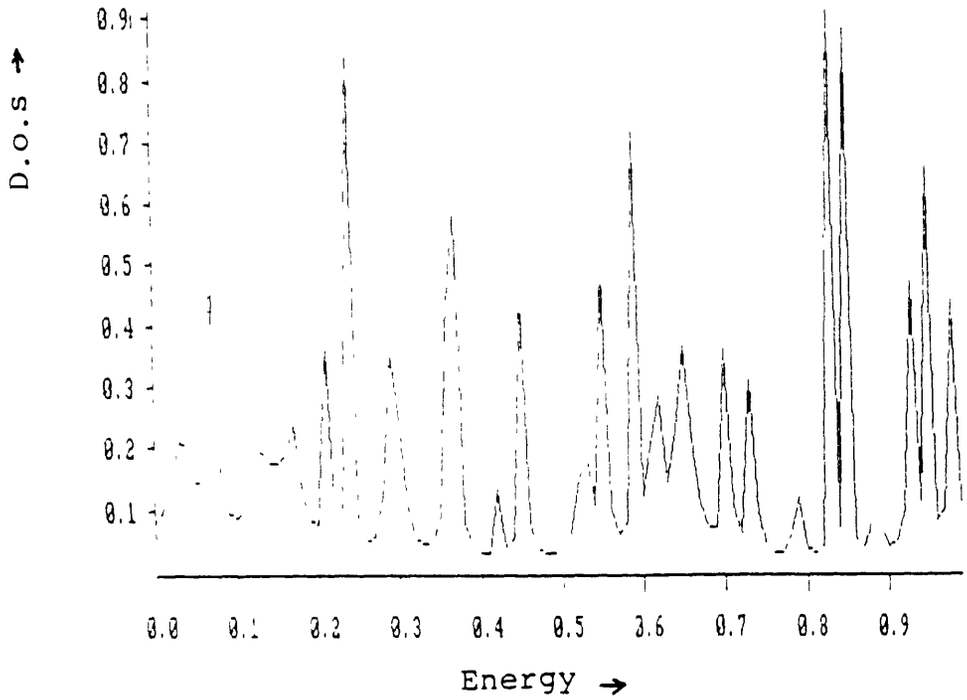
states is expected to be highly singular on the localized side, and smooth and relatively featureless on the extended side of the Anderson transition.

If we assume that the transmission coefficient has a value of unity every time the Fermi level coincides with a band, we can obtain a lower limit on the expected fluctuations in the conductance. Section 6.5 shows that the form of the fluctuations is qualitatively the same as that observed in chapter 4. The relative error increases exponentially with system size, in the region of localized states, so that the conductance is non self-averaging.

We note that this only a lower bound, and in general we expect the fluctuations to be worse, because not every peak in the density of states is expected to have a transmission coefficient of unity. To check this we have computed using the algorithm of chapter 3 the density of states, conductivity correlation function $\langle Q\, g \rangle$ in two dimensions, and find that it decreases with system size. This clearly indicates that not every peak in the density of states corresponds to an appreciable peak in the conductance. Further it indicates that the number of cases where the density of states and conductance are well correlated decreases with system size.

This is clearly illustrated in fig[6.8] which shows a plot of the conductance and density of states for a chain of one hundred atoms at a disorder of unity. For this system each peak in the density of states corresponds to a significant peak in the conductance. However for a chain of two hundred and fifty atoms, fig[6.9], the correlation has all but disappeared.

Different transmission contributions apart, the vanishing measure of the spectrum means that most direct calculations of the conductance, localization length etc, do in fact calculate properties of the gap. The only way to examine the properties of the eigenstates is to calculate them by direct diagonalization of the Hamiltonian. Even then it is not possible to calculate



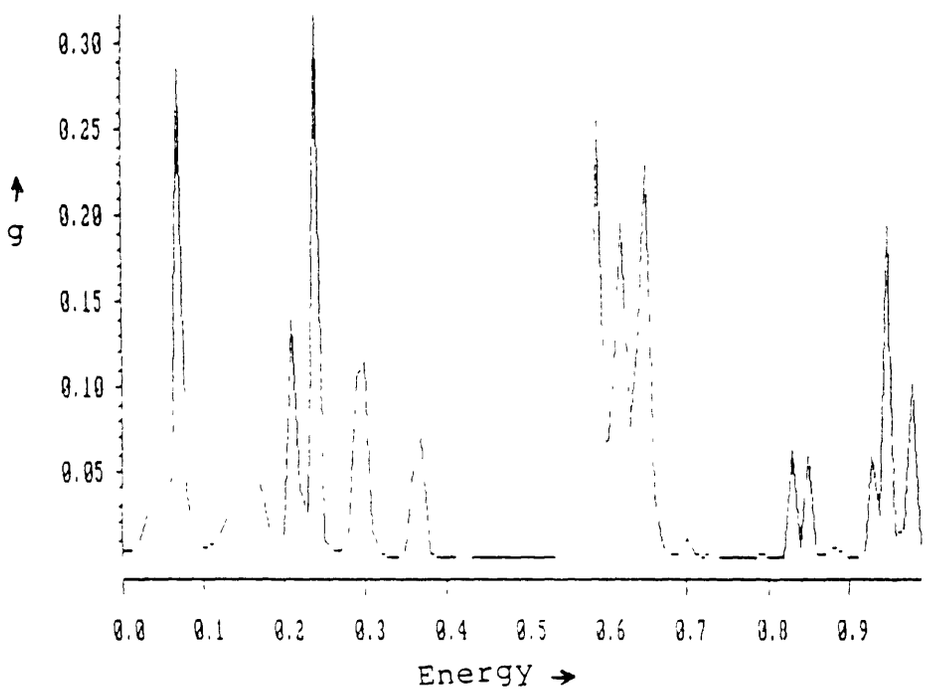


Fig 6.9 Plots of the density of states and conductance vs the position of the Fermi-level, for a one dimensional system consisting of two hundred and fifty atoms at disorder W = 1.

the conductance and the best we can do is calculate participation ratios, which give us a rough guide as to the number of sites over which an eigenstate is localized.

Schreiber(1985) has carried out extensive calculations of the participation ratio and seems to find that the eigenstates have a powerlaw like behaviour at short distances. However the sizes of systems he could investigate were small, since direct diagonalization is a costly procedure, so he concludes that the powerlaw behaviour may be swamped by the expected exponential behaviour at large enough distances.

6.7 Fluctuations in the transmission of individual states

We have shown above that the presence of gaps in the spectrum can account for some features of the extreme behaviour of the conductance observed in chapter 4. We have also shown that our model needs to be modified because, not every state has a transmission coefficient of unity in a real system, and that the number of states with such a transmission, decreases with system size. The next thing to be investigated is, what mechanism causes the transmission of individual states to fluctuate so wildly.

Azbel(1983) has investigated conductance fluctuations extensively in one dimension, and has developed a theory based on resonant conduction. In his theory as explained in the introduction the dominant peaks in the conductance come from eigenstates localized near the centre of the sample which as a consequence have the narrowest width in energy because they couple least strongly to the metals. The width of these states decreases exponentially with system size in agreement with the results of this chapter.

As a preliminary study to check whether resonant conduction is indeed the dominant mechanism we have examined the density of states and conductance, of a chain of one thousand atoms for which the localization length is

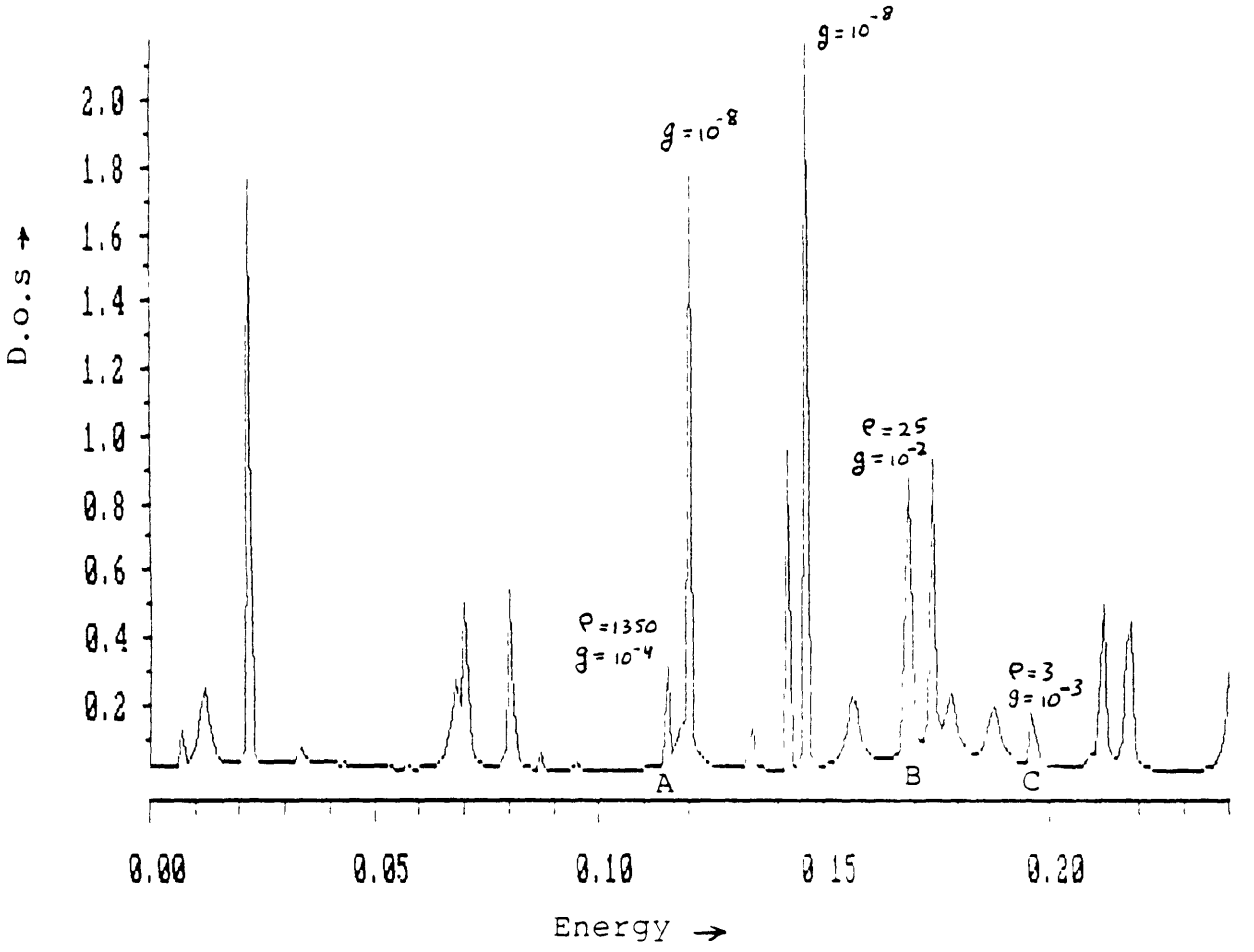


Fig 6.10 The density of states of a one dimensional system whose length is ten times the localization length. Some peak values of the density of states and conductance, obtained by increasing resolution, until no more change was detected are labeled.

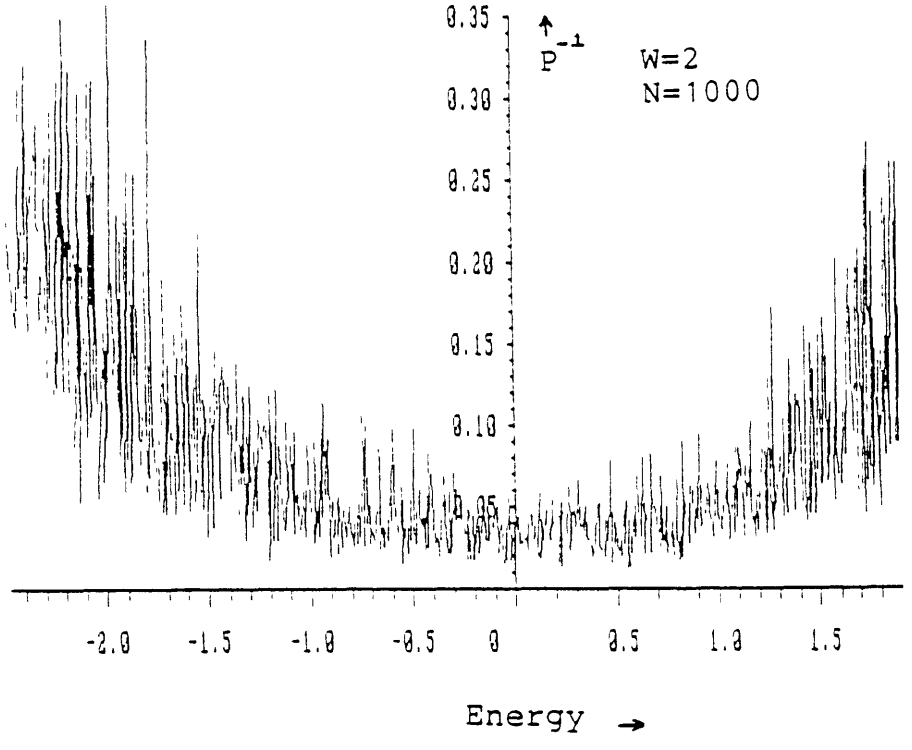
a tenth of the system size, as a function of the Fermi energy. This puts us in the strongly localized regime, and also in the regime in which the Azbel picture is supposed to be valid. Fowler et al(1986).

Our results, fig[6.10], indicate that this picture may not be correct as we do not find that the narrowest peaks necessarily have the largest conductance. As fig[6.10] shows the peak labeled A has a maximum density of states of 1350 and a conductance of 10^{-4}, but the peak labeled B which has a maximum density of states of only 25 and is therefore much wider, since the integrated density of states under a peak must be at least unity, has a conductance two orders of magnitude greater.

The Azbel picture assumes that the localization length is the same for each state. In reality we expect that the localization length like everything else will also fluctuate as we change the position of the Fermi-level, so that peaks with relatively large widths and conductances could be due to states that have an anomalously large localization length. We have no way of calculating this quantity for individual eigenstates, but we can calculate participation numbers which give us an idea of how many sites have an appreciable amplitude, for any given eigenstate. The inverse participation number scales as 1/N for extended states and is constant for localized states.

Fig[6.11] shows plots of the inverse participation number P^{-1} against energy for typical samples of a thousand atoms, at disorder W=2 and W=4 respectively. These were evaluated by calculating the eigenvectors by direct diagonalization of the Hamiltonian.

The inverse participation number increases slowly as we move away from the centre of the band and then rises sharply towards the edges, because the states are more strongly localized in the tails. There are as expected large fluctuations in P^{-1}, the relative error in which does not decrease



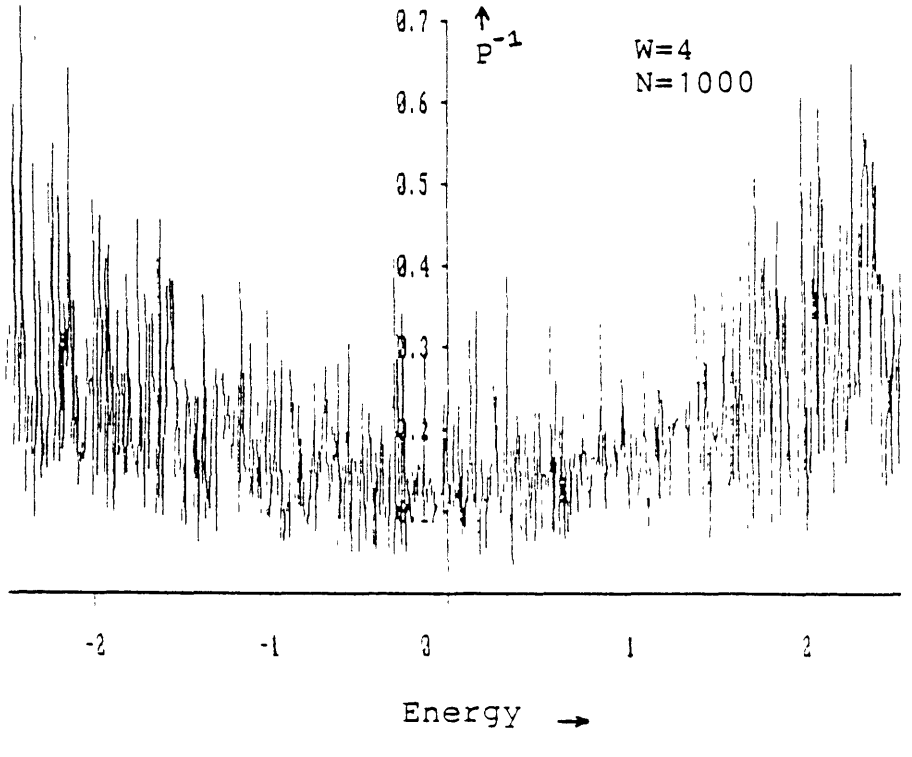


Fig 6.11 The inverse participation number P^{-1} as a function of energy, for one dimensional chains of 1000 atoms at disorders W = 1 and W = 4.

with increasing disorder. The fluctuations are typically about fifty percent of the mean, but there are individual states with fluctuations of about three or four times the mean. If we assume that the states have an exponential form

$$\Phi_j(x) \sim \exp[-|x-x_j|/\xi_j]$$

with individual localization lengths ξ_j, then the inverse participation number is given by

$$P_j^{-1} \sim \frac{\int_0^L e^{-|x-x_j| \times 4/\xi_j}}{\left(\int_0^L e^{-2|x-x_j|/\xi_j}\right)^2} \qquad \{6.34\}$$

$$P_j^{-1} \sim 1/\xi_j \qquad \{6.35\}$$

Thus under this assumption the localization length is proportional to the participation numbers. If the conductance of an individual state is given by

$$g_j \sim \exp(-L/\xi_j) \qquad \{6.36\}$$

Then it is easily seen that fluctuations in the localization length can lead to exponentially different conductances.

These have only been preliminary investigations and much more investigation is required before any definite statements can be made. It is not yet clear which mechanism is responsible for states which have large conductances, but it seems likely that the true situation involves some aspects of both resonant tunneling and normal conduction due to fluctuations in the localization length of individual states. It should be mentioned that the discreteness of the spectrum is not merely an academic

question. Sophisticated experimental techniques are now able to examine the conductance of individual peaks. Fowler, Timp, Wainer and Webb(1986), and seem to observe a wide variation in the conductance of individual peaks.

Chapter 7

The electronic properties of the one dimensional Quasicrystal

7.1 Introduction

Since the discovery by Shechtman et al(1984) of an alloy of manganese and alumimium with icosahedral symmetry there has been much interest in Quasicrystalline lattices. An icosahedral symmetry is not compatible with any of the crystalline point groups, but quasiperiodic lattices with a five fold symmetry can be constructed. Quasicrystals have no translational order but possess long range bond orientational order, and are constructed by the infinite repetition in space of two or more distinct unit cells.

They differ from the much studied incommensurate structures, Sokoloff(1985), in that there is a minimal separation between lattice sites, and from fractal lattices in that there is more than one length scale.

From an electronic point of view these structures are interesting as they are intermediate between ordered and disordered structures, because the disorder is deterministic and also because they are topologically disordered rather than the normally studied substitutionally disordered systems. Thus a study of their electronic properties may reveal something about the conditions necessary for a metal-insulator transition. In addition wavefunctions in quasiperiodic structures are thought to be characteristic of those at the mobility edge of real disordered systems, in that they are generally fractal in nature, Economou and Soukoulis(1984).

In this chapter we shall examine the band structure and wavefunctions of one dimensional quasicrystals. We shall deal only with the simplest case consisting of two units arranged in a quasiperiodic manner. These may exist at grain boundaries in defective crystals. See Rivier

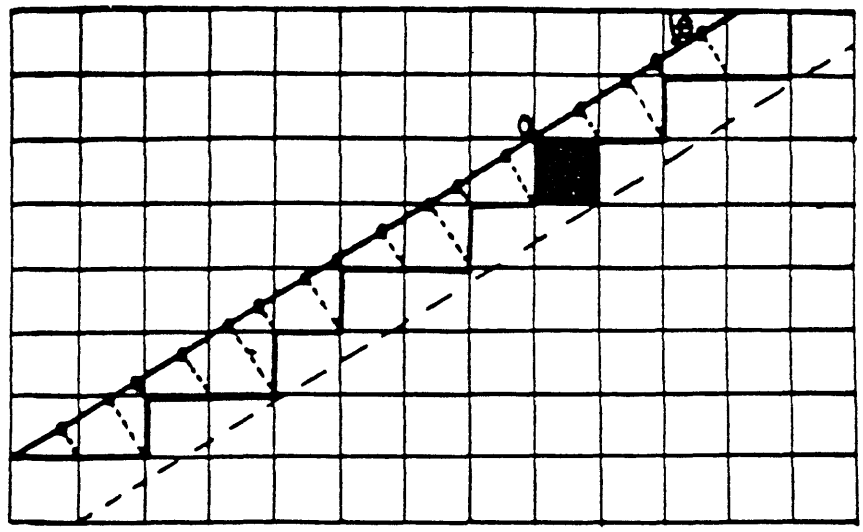


Fig 7.1 The grid projection method. All points within the window formed by the solid and dashed parallel lines are projected perpendicularly onto the solid line.

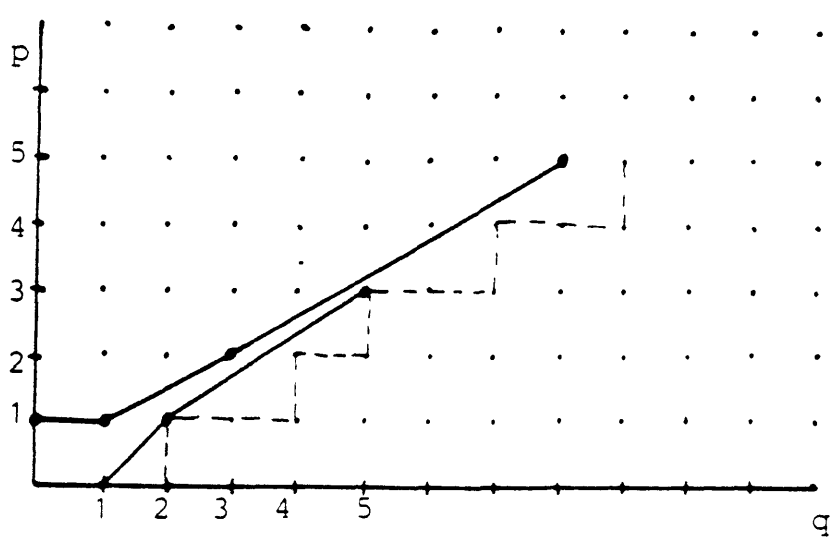


Fig 7.2 The rational approximants to the irrational golden mean.

(1986) for a botanical example. Superlattices with a quasiperiodic structure in one dimension have recently been constructed, Merlin et al(1985), so it should be possible to examine their bandstructure and other electronic properties in the near future.

The layout of this chapter is as follows, Section 7.2 contains a brief discussion of the general properties of one dimensional quasicrystals. In 7.4 we study the spectrum of a one dimensional tight binding model with bonds arranged in a quasicrystalline manner. The properties of the wavefunctions are examined in 7.5, and a study of the renormalized perturbation expansion for the self-energy, which shows that the band centre eigenstates are extended is contained in 7.6. Finally in section 7.7 we show that the Schrödinger equation can be decimated, in a way that preserves the quasicrystalline nature of the lattice. An iterative map for the site energies and hopping elements is derived and some of its expected properties discussed.

7.2 Definition

There are many equivalent ways of generating one dimensional quasicrystals, of which the projection method is perhaps the most useful for illustrating the almost periodic nature, and is also generalizable to higher dimensions. In one dimension one starts with a periodic two dimensional lattice and constructs a line with an irrational slope w passing through the origin. The irrational chosen is not important as it only determines the length of the units, so we shall choose it to be the golden ratio $\tau = \frac{1}{2}(1+\sqrt{5})$. A window is defined by translating the unit square along the line, and the quasicrystal obtained by projecting all points within the window onto the line. Fig[7.1]. Clearly as the line has an irrational slope it cannot pass through any other lattice point, and is divided by the projections into segments of length $\cos\Theta$ and $\sin\Theta$. We shall call these long bonds L and short bonds S.

The almost periodic nature can be understood by considering rational approximants to the irrational w. We recall that any irrational number has an infinite continued fraction expansion, and its rational approximants are obtained by terminating the continued fraction at some point. τ has an expansion

$$\tau = 1 + \cfrac{1}{1 + \cfrac{1}{1 + \cfrac{1}{1 + \cfrac{1}{\ddots}}}} \qquad \{1.7\}$$

and its rational approximants $r_n = p_n/q_n$ obey the simple recursion relations

$$r_n = (p_{n-1} + p_{n-2})/p_{n-1} \qquad \{2.7\}$$

where $p_{n+1} = p_n + p_{n-1}$

and $p_1 = 1 , \quad p_0 = 0$

If the slope of the line is chosen to be equal to r_n instead of τ we obtain a periodic system with period q_n. The unit cell consists of a sequence of long and short bonds LSLLS.....LS which we call a word W_n . Fig[7.2] shows that the rational approximants form two polygonal lines which collimate the line with slope τ, and there are no lattice points within these lines. Thus the beginning of the word W_n is the same as the word W_{n-1} and the rest is the word W_{n-2}. The words obey the relation

$$W_n = W_{n-1}W_{n-2} \qquad \{3.7\}$$

with W_1 = L and W_2 = LS

Hence the sequence can be obtained algebraically and is identical to the Fibonacci sequence obtained by the inflation rule L -> LS and S -> L. The first few words are

L
LS
LSL
LSLLS
LSLLSLSL
LSLLSLSLLSLLS

A major feature of the one dimensional quasicrystal is that no more then one S or two L's can appear in succession. The ratio of L's to S's at any stage is r_n and equals τ in the limit $n = \infty$.

From a computational point of view a useful formula, which can be deduced from the projection method and gives the coordinates of the points, Levine and Steinhardt(1985) ,is

$$X_n = n + \frac{1}{\tau}\left\lfloor \frac{n}{\tau} \right\rfloor \qquad \{4.7\}$$

where $\lfloor\ \rfloor$ is the greatest integer function. This allows us to deduce the n^{th} item in the sequence without having to know all the preceding ones.

7.3 Model

We study the following one dimensional tight binding model which describes electrons on a lattice with variable hopping elements.

$$H = \Sigma\ |n\rangle\varepsilon_n\langle n| + |n\rangle V_{n\ n+1}\langle n+1| + |n+1\rangle V_{n+1\ n}\langle n| \qquad \{5.7\}$$

The site energies are taken to be zero and the hopping elements $V_j \equiv V_{jj+1}$ take one of two values V_L or V_S depending upon whether the j^{th} element of the Fibonacci sequence is long or short. We take $V_S > V_L$.

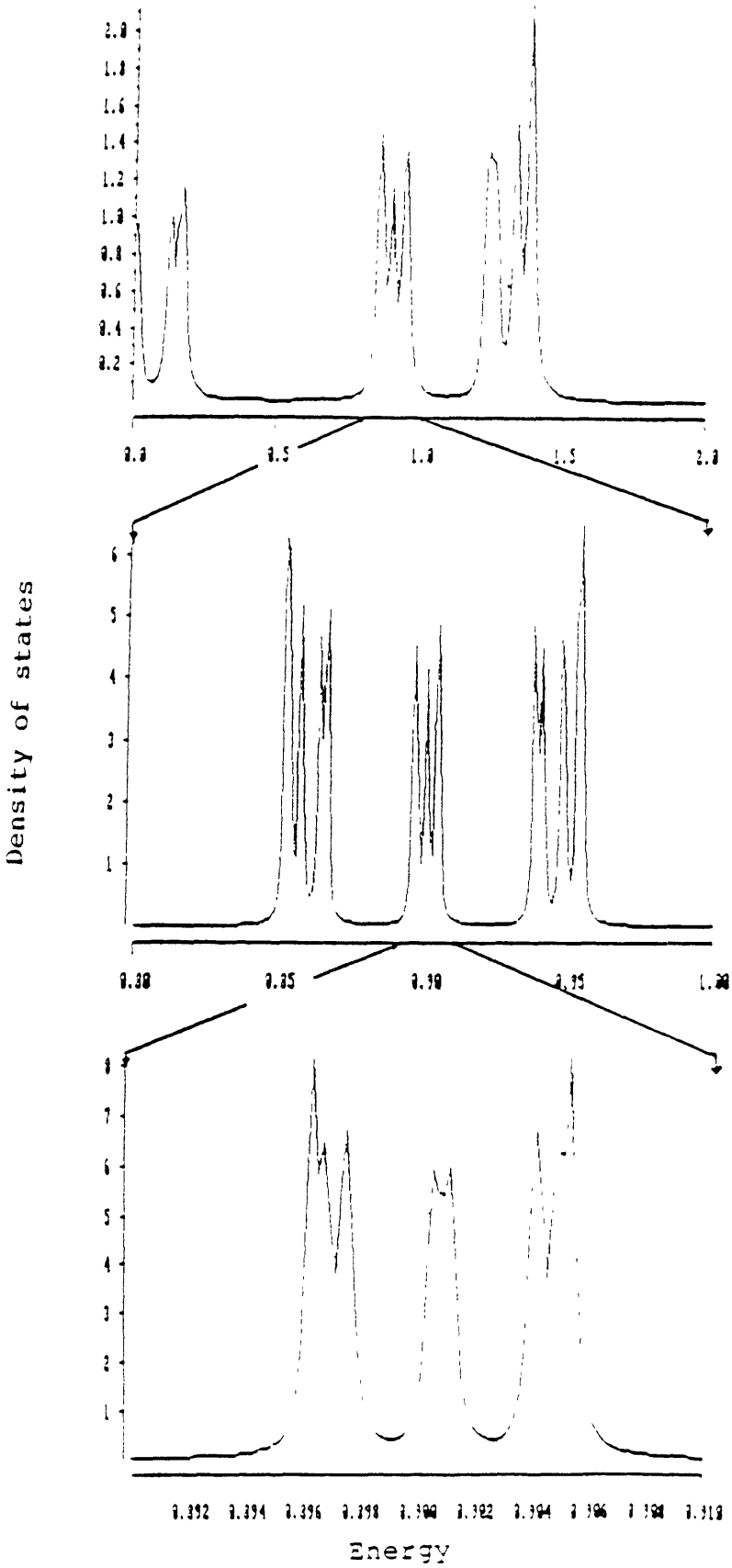


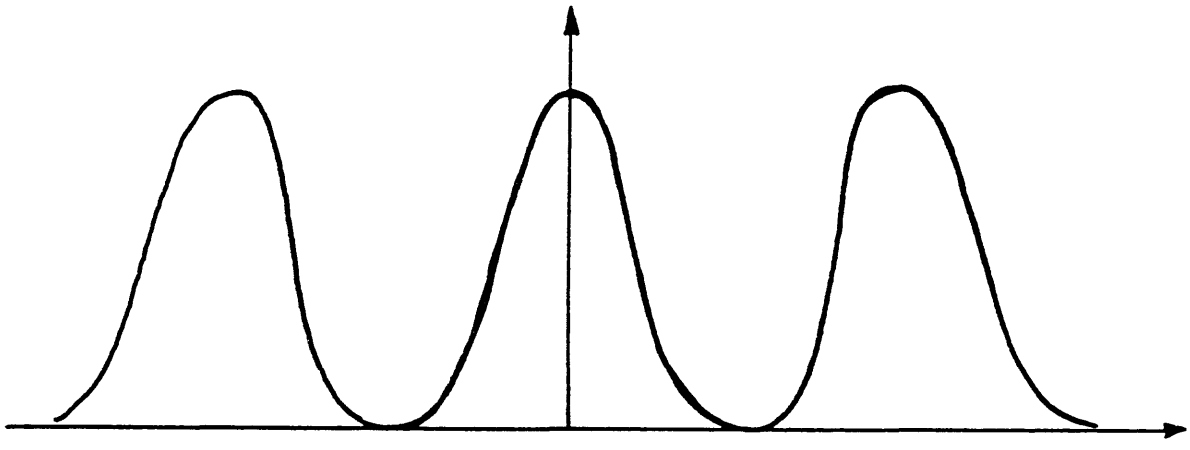
Fig 7.3 The density of states of a one dimensional quasicrystal, under increasing energy resolution.

7.4 The spectrum

We have numerically evaluated the density of states of the model defined above, using the algorithm of chapter 3, for a very long chain of about 10,000 atoms. The results are shown in fig[7.3] as a function of increasing resolution. Only half the spectrum is shown as off diagonal models have a density of states which is symmetric about the origin.

There are two features to note:-

a) The density of states at low resolution consists of three main features one at the origin and two symmetrically placed about it.



This can be understood by setting V_L , the smaller hopping element, to zero, whereby the chain disconnects into single atoms and pairs connected by short bonds.



Each single atom gives a state at E = 0, whilst the other states are due to the two vibrational modes of the pair. Increasing V_L allows these units to interact and broadens these features.

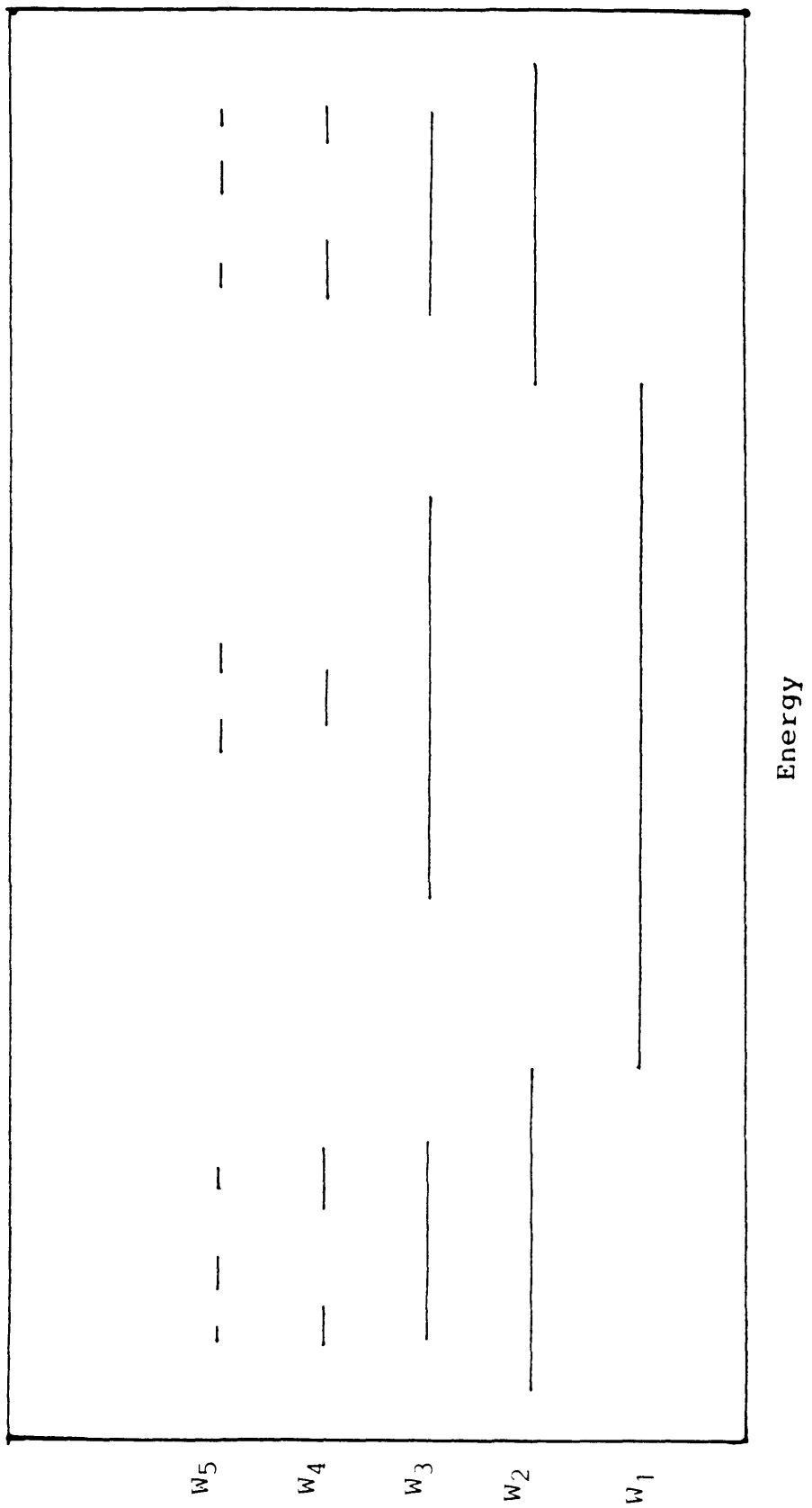


Fig 7.4 The spectrum of succesive periodic approximations to the quasicrystal.

b) On increasing the energy resolution each peak subdivides into three and this continues ad infinitum.

In order to understand the way this subdivision occurs we have evaluated the density of states of periodic systems, with unit cells corrosponding to the 1^{st}, 2^{nd}, 3^{rd}, etc approximants to the Fibonacci sequence. The support of the density of states is plotted in fig[7.4] against W_n the n^{th} approximant. The main features of the spectrum observed above can now be clearly seen. At W_3, which corresponds to the unit cell LSL, the spectrum shows the three main features because the unit cell now contains the two units necessary to get this. As the size of the unit cell is increased the major features start to subdivide. It is interesting to notice that the central feature at W_1 and the one off centre at W_3 subdivide in the same way.



This is found to happen at other points as well and indicates that the spectrum as a function of n has a nested hierarchical structure. The structure is similar to that of a Cantor set.

We also find that the states at the edge of the spectrum occur at twice the average of the hopping element in a unit cell, so that for the final system the band edges are at

$$E = \pm 2(\tau V_L + V_S)/(1 + \tau) \qquad \{6.7\}$$

since $N_L/N_S = \tau$ the golden ratio.

The Cantor set nature of the spectrum can be understood in terms of a dynamical map discovered by Kohmoto et al (1984). They studied the equation

$$a_{n+1} + a_{n-1} + V(nw)a_n = \epsilon a_n$$

with $$V(t) = V(t+1) \qquad \{7.7\}$$

and $$V(t) = V_1 \quad \text{for} \quad -w < t < -w^3$$

$$= V2 \quad \text{for} \quad -w^3 < t < w^2$$

and were able to demonstrate the hierarchical nature of the spectrum. We have found that this choice of potential generates a quasicrystal, so they had essentially solved the model with constant hopping elements and variable site energies. Their potential can be related to the projection method, for generating a quasicrystal Aubry(1986). Our model of variable hopping elements and constant masses can be mapped onto their model with a few modifications and their conclusions carry over, so we leave the derivation to Appendix 7.2.

The essence of their method lies in showing that the trace of the transfer matrices for periodic approximations to the quasicrystal obey a three parameter dynamical map, namely

$$X_{l+1} = 2X_lX_{l-1} - X_{l-2} \quad \text{where } X_l = 1/2\text{tr } T_l$$

and T_l are transfer matrices for words of length F_l. If a particular energy, specified by the initial conditions is to be an allowed state of the final system then the trace must remain less than modulus unity, under the iteration of the map. They show that the map has an embedded Smale horseshoe structure, which accounts for the hierarchical splitting of bands, and were able to derive a scaling relation for the bandwidths. For our model we find that the centre of the band E=0 is always in the spectrum of the infinite quasicrystal. This will turn out to be useful when we consider the transport properties of the system.

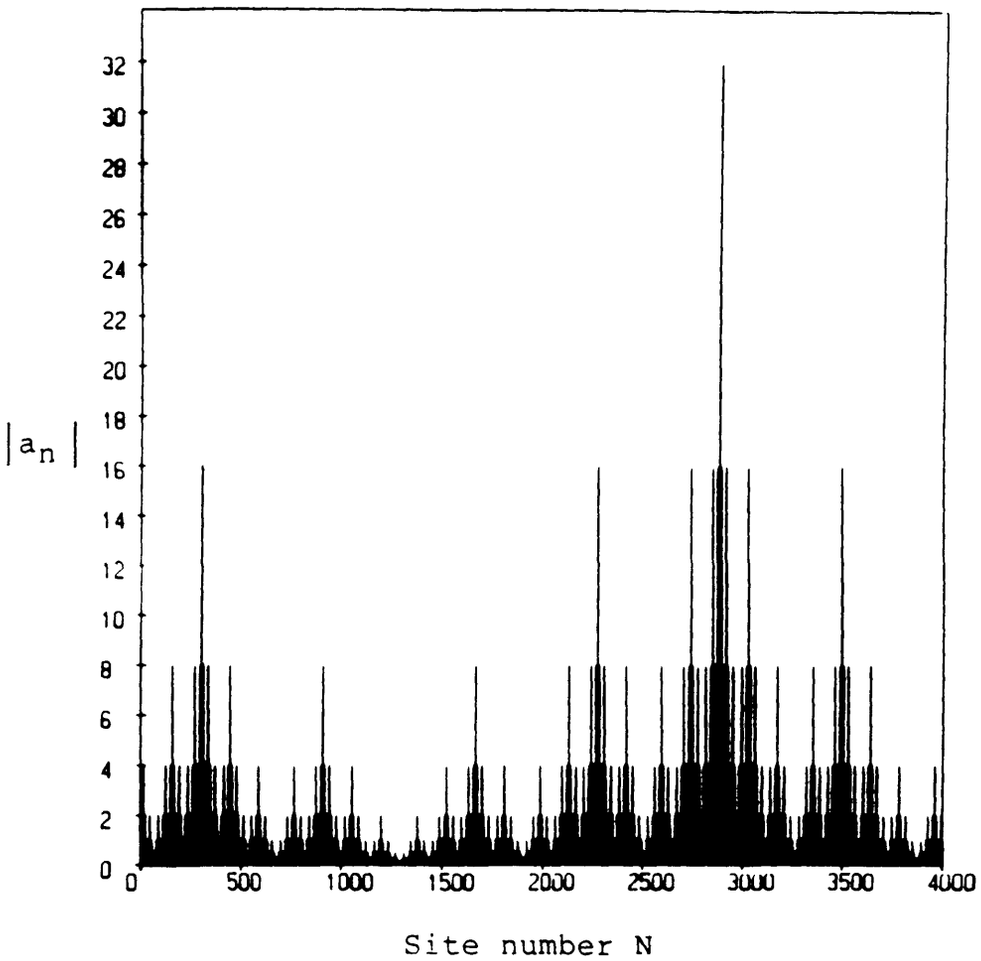


Fig 7.5a

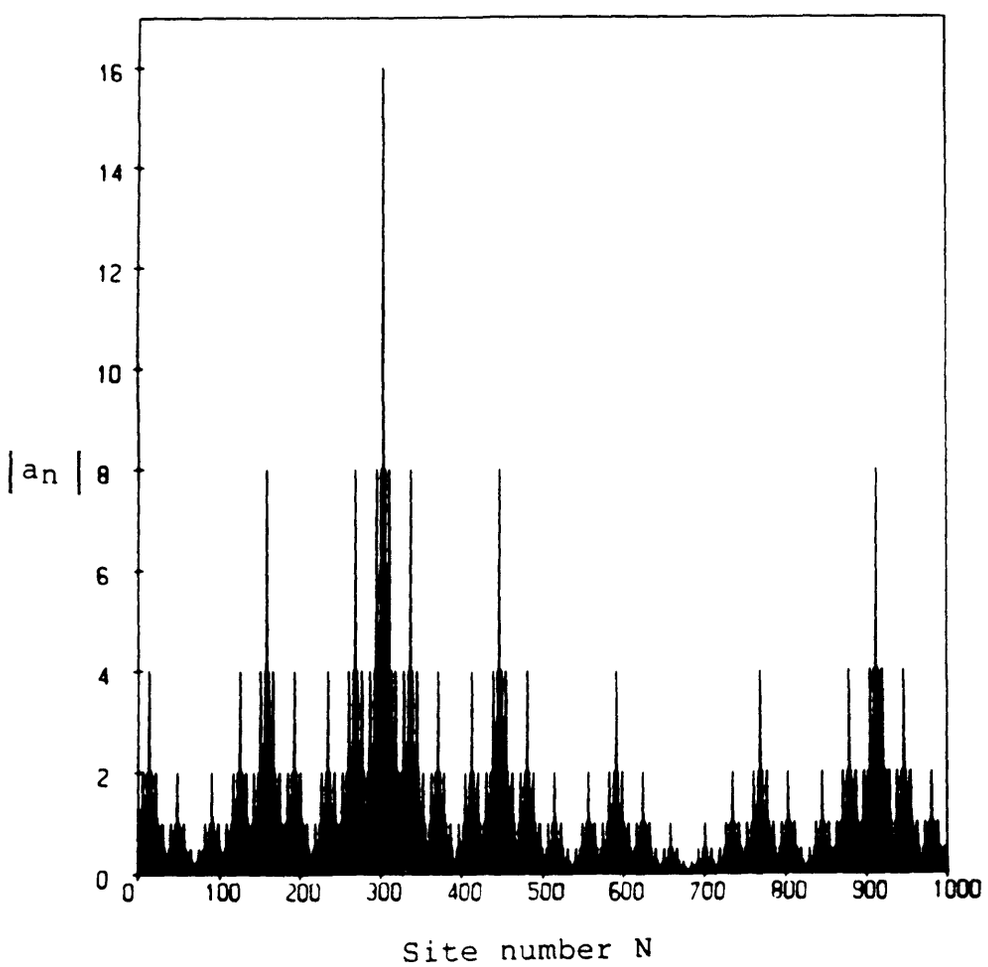


Fig 7.5b

7.5 Properties of the eigenstates

Introduction

There is not much universality in the transport properties of systems with exotic spectra, such as that found above and which exist in most incommensurate structures. Some models such as the Aubry model, Aubry and Andre(1980), exhibit Anderson transitions, whilst others have properties which are borderline between localized and extended. In this section we examine the properties of the wavefunctions at several points in the spectrum of a one dimensional quasicrystal, and demonstrate that wavefunctions with a range of transport properties, from localized to extended can exist. These do not appear to be separated by a single mobility edge as in disordered systems.

7.5.1 Band centre

At E=0 the Schrödinger equation in its transfer matrix representation takes a very simple form.

$$\begin{bmatrix} a_{n+1} \\ a_n \end{bmatrix} = \begin{bmatrix} 0 & -V_{n-1}/V_n \\ 1 & 0 \end{bmatrix} \begin{bmatrix} a_n \\ a_{n-1} \end{bmatrix} \qquad \{8.7\}$$

If we start with initial conditions $a_1 = 1$ and $a_0 = 0$, which corresponds to free boundary conditions then the wavefunction must vanish at all the even sites, and its amplitude at any odd site is given by {8.7}, which can be written as

$$| a_n | = \frac{V_{n-1}}{V_n} \cdot \frac{V_{n-3}}{V_{n-2}} \cdot \cdots \qquad \{9.7\}$$

We have used this relation to study the wavefunctions at the band centre, and the type of bond at site n was determined using {4.7}. Fig[7.5] shows a plot of $|a_n|$ for systems of various sizes. The wavefunctions are highly self-similar down to the smallest length scales and the

7.5c

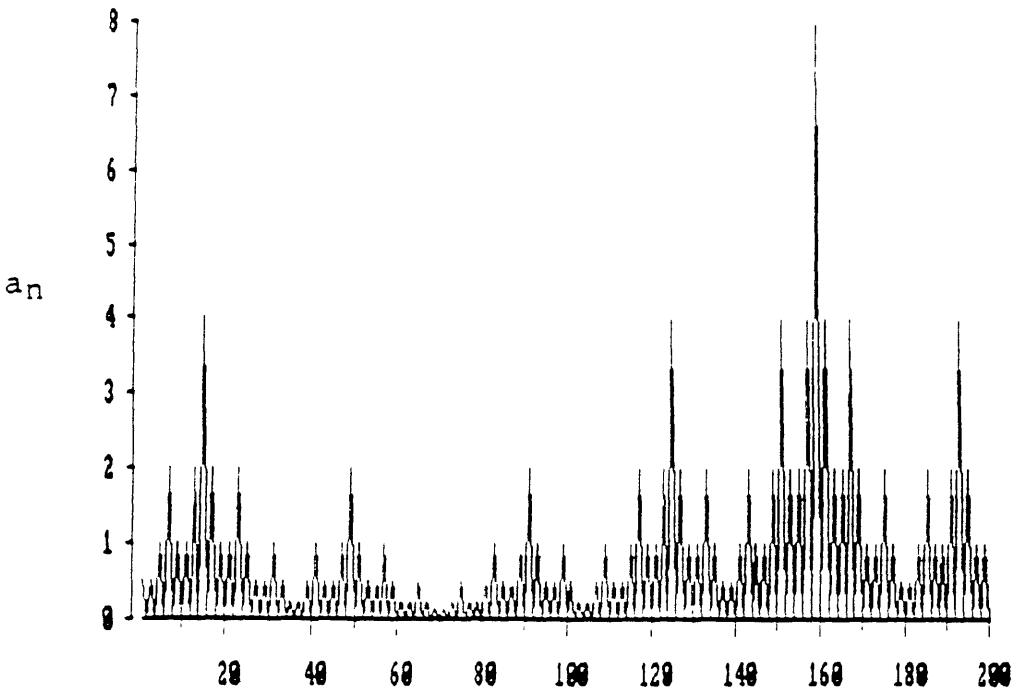


Fig 7.5 a, b and c. The modulus of the wavefunction as a function of position at the band centre, for V_S/V_L = 2 and several different system sizes.

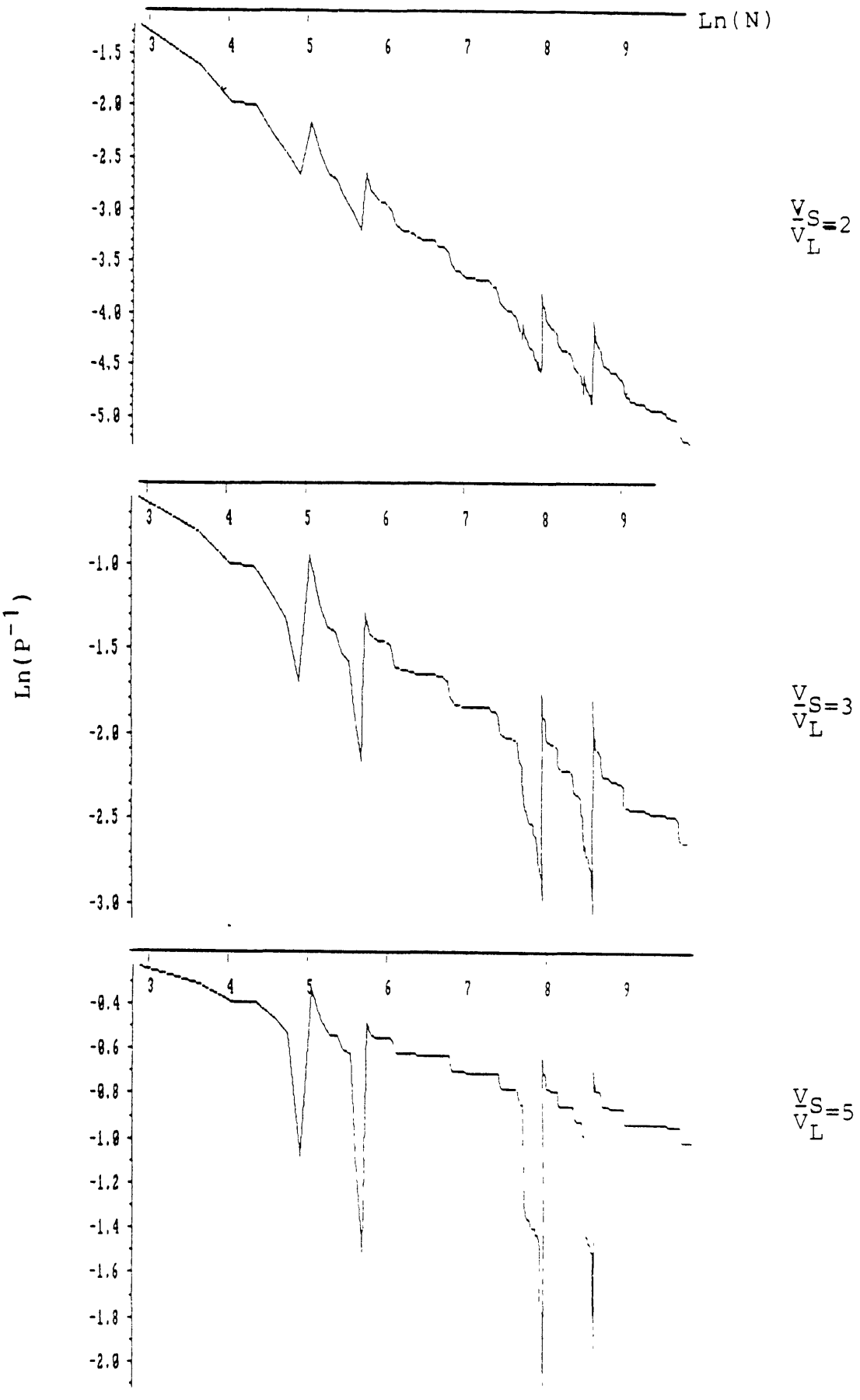
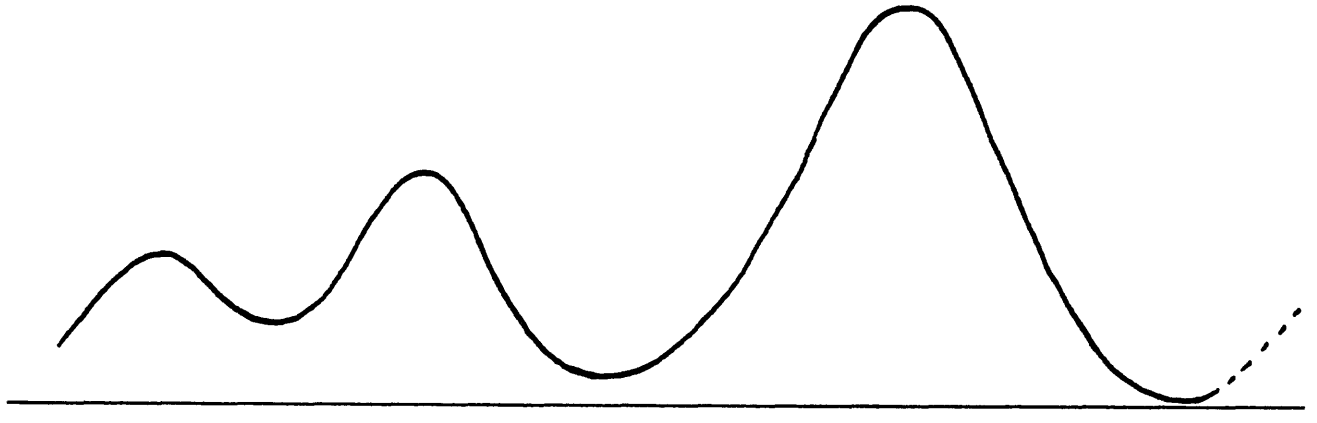


Fig 7.6 The Logarithm of the inverse participation number plotted against the logarithm of the number of sites, at the band centre, for different values of V_S/V_L.

various peaks and dips seem to scale as $(V_S/V_L)^{\alpha}$ where α = $\pm 1, \pm 2, \pm 3.....$ It can be seen that successively larger peaks and dips appear with increasing system size and the spacing between these increases with the order of the peak or dip. Thus the distance between the 1^{st} peak of amplitude 4 and amplitude 8 is about 140 lattice spacings whilst the distance between the 1^{st} peaks of amplitudes 16 and 32 is about 2500 lattice spacings. The envelope of the wavefunction looks like



Whether these states are localized or extended is not clear because although the peaks appear with increasing amplitude, the dips get smaller and thus the peaks may effectively be connected by exponential tails.

To check whether these states are localized or not we have evaluated the participation number P as a function of system size fig[7.6]. As was mentioned in 2.2 of chapter 2 the inverse participation number is expected to drop as 1/N for extended states and scale towards a constant value for localized states. In fig[7.6] we have plotted $\ln(P^{-1})$ against lnN and it can be seen that P^{-1} drops with increasing system size as it should for extended states. The drop is however not uniform but rather like a staircase. The spikes occur at the positions of the first peak of order $(V_S/V_L)^{\alpha}$ which as we noticed get increasingly further apart. Between these drops P^{-1} remains approximately constant and the states appear to be localized. We can define a fractal dimension d which effectively measures the volume of a wavefunction by

$$P^{-1} \approx L^{-d} \qquad \{10.7\}$$

for extended Bloch like states d is equal to unity, whilst for exponentially localized states d=0. For the quasi-crystal our results show that $d = (V_S/V_L)^{-1}$ so that the states are not extended in the Bloch sense but are somewhere in between extended and localized, depending upon the ratio (V_S/V_L).

7.5.2 Scaling behaviour of the wavefunction

Recently Kohmoto and Banaver(1986) have noticed that the transfer matrices T_l which describe transfer across cells corrosponding to the words W_l, exhibit a six cycle at the band centre

$$T_{l+6} = T_l \qquad \{11.7\}$$

and have used it to explain the scaling behaviour of the wavefunctions. However our results seem to differ slightly from theirs, which is probably due to the form of the matrices T_l. The form of these matrices T_l is rather subtle for a model in which the disorder is in the bonds and is explained in detail in appendix 7.1. From appendix 7.1 the matrices T_l for the six approximants are

$$T_1 = \begin{bmatrix} 0 & 1 \\ -1 & 0 \end{bmatrix} \qquad T_2 = \begin{bmatrix} -1/r & 0 \\ 0 & -r \end{bmatrix}$$

$$T_3 = \begin{bmatrix} 0 & -r \\ 1/r & 0 \end{bmatrix} \qquad T_4 = \begin{bmatrix} 0 & 1 \\ -1 & 0 \end{bmatrix} \qquad \{12.7\}$$

$$T_5 = \begin{bmatrix} r & 0 \\ 0 & 1/r \end{bmatrix} \qquad T_6 = \begin{bmatrix} 0 & 1/r \\ -r & 0 \end{bmatrix}$$

where $r = V_S/V_L$

and they satisfy the recursion relation

$$T_n = T_{n-2}T_{n-1}$$

If we operate with any T_n on the initial vector (1,0) we only get a non zero amplitude if $(T_n)_{11}$ is finite. To obtain the major peaks which scale as r^α we require that $(T_n)_{11}$ equals r^α. T_n's which have this property can be constructed out of combinations of the first six T_1's. For example

$$T_3T_6 = \begin{bmatrix} r^2 & 0 \\ 0 & 1/r^2 \end{bmatrix} \qquad \{13.7\}$$

and

$$T_5^2 = T_5T_{11} = \begin{bmatrix} r^2 & 0 \\ 0 & 1/r^2 \end{bmatrix} \qquad \{14.7\}$$

Hence $(T_n)_{11}$ which scale as $r^{2(n+1)}$ can be constructed out of forms like

$$(T_3T_6)(T_9T_{12})\cdots\cdots T_{3(n+1)}T_{3(n+1)+6}$$

and $\qquad \{15.7\}$

$$(T_5T_{11})(T_{17}T_{23})\cdots\cdots T_{5(n+1)}T_{5(n+1)+6}$$

$$n = 1, 2, \ldots.$$

$(T_n)_{11}$ which scale as $r^{2(n+1)+1}$ can be constructed out of forms like

$$(T_3T_4)(T_5T_{11})(T_{17}T_{23})\cdots\cdots \qquad \{16.7\}$$

note that these forms can be constructed by taking a particular T_1 and successively reducing it using the relation {A9.7.1}.

$$T_{l+1} = T_{l-1}T_l$$

Thus $T_7 = T_5T_6 = T_3T_4T_6 = T_3T_2T_3T_6$

now transfer matrices act to the right so we are free to remove sequences from the left

hence $T_2^{-1}T_3^{-1}T_7 = T_3T_6$

and this corresponds to a chain of length $F_3 + F_6$

Thus there are peaks of height $r^{2(n+1)}$ at lengths

$$n = (F_3 + F_6) + (F_9 + F_{12})+.....(F_{3(n+1)} + F_{3(n+1)+6})$$

and

$$n = (F_5 + F_{11}) + (F_{17} + F_{23})+.....(F_{5(n+1)} + F_{5(n+1)+6})$$

and there are peaks of height $r^{2(n+1)+1}$ at

$$n = F_3 + F_4 + (F_5 + F_{11}) + (F_{17} + F_{23})+.....$$

The major dips in the wavefunction can be explained in a similar manner.

A scaling relation for the wavefunction can be deduced by considering successive peaks of order $r^{2(n+1)}$ and $r^{2(n+2)}$ generated by the sequences

$$(T_3T_6)(T_9T_{12}).....T_{3(n+1)}T_{3(n+1)+6}$$

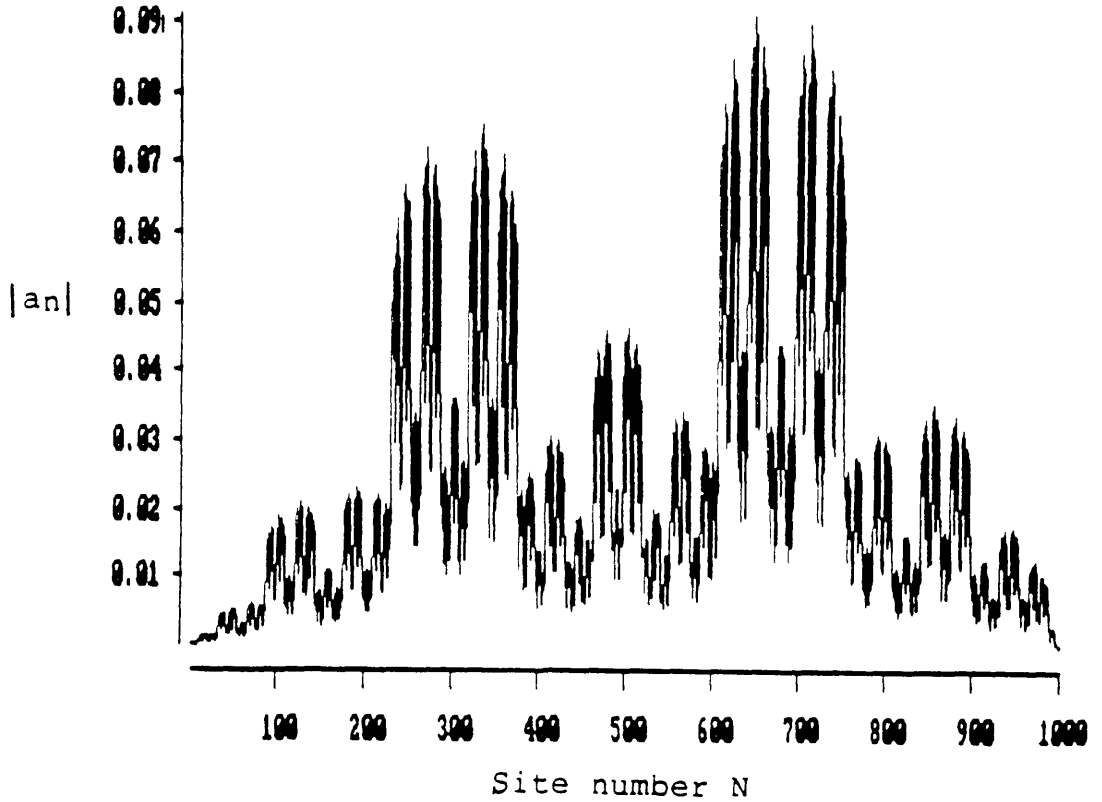
and

$$(T_3T_6)(T_9T_{12}).....T_{3(n+2)}T_{3(n+2)+6}$$

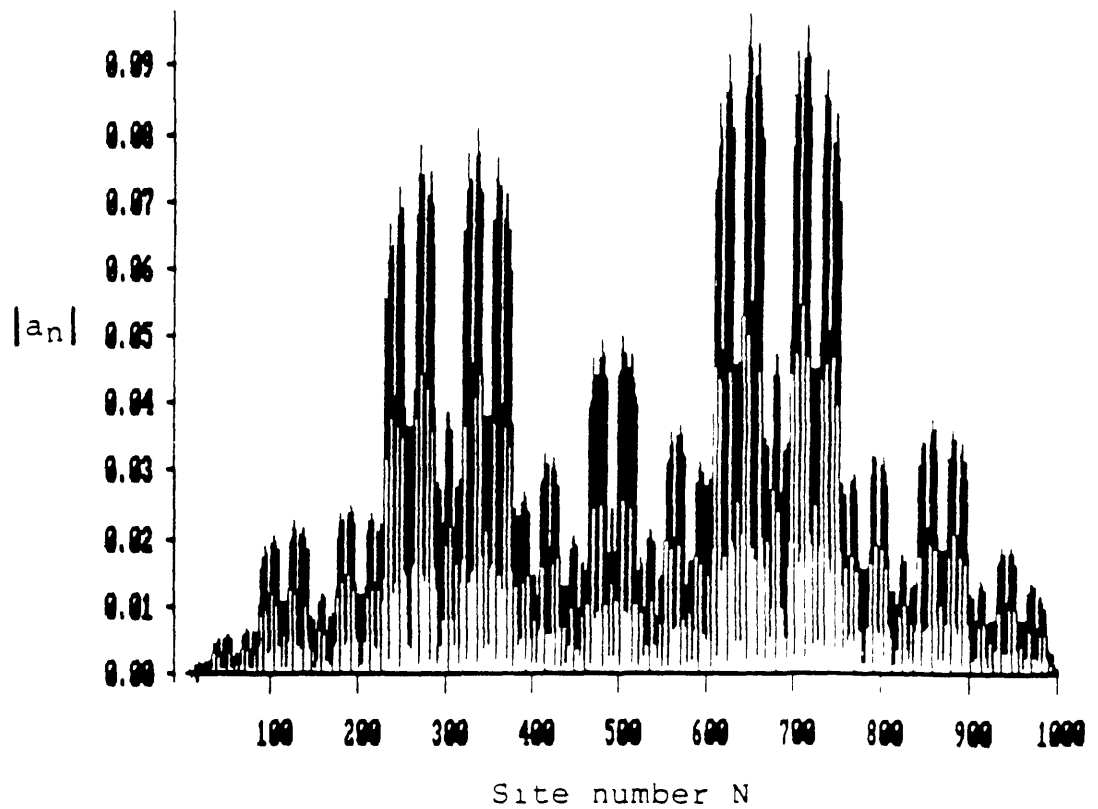
for sufficiently large n the number of atoms in the chain are well approximated by

$$F_{3(n+1)+6} \text{ and } F_{3(n+2)+6}$$

since these numbers will swamp the rest in the sequence. For large n the Fibonacci numbers obey



7.7a



7.7b

Fig 7.7a The modulus of the wavefunction as a function of position, at the edge of the spectrum. $V_S/V_L = 2$.

Fig 7.7b The modulus of the wavefunction as a function of position, at the inner edge of the outermost sub-band of W_3. Notice that fig[7.7a] is at the outer edge of this sub-band.

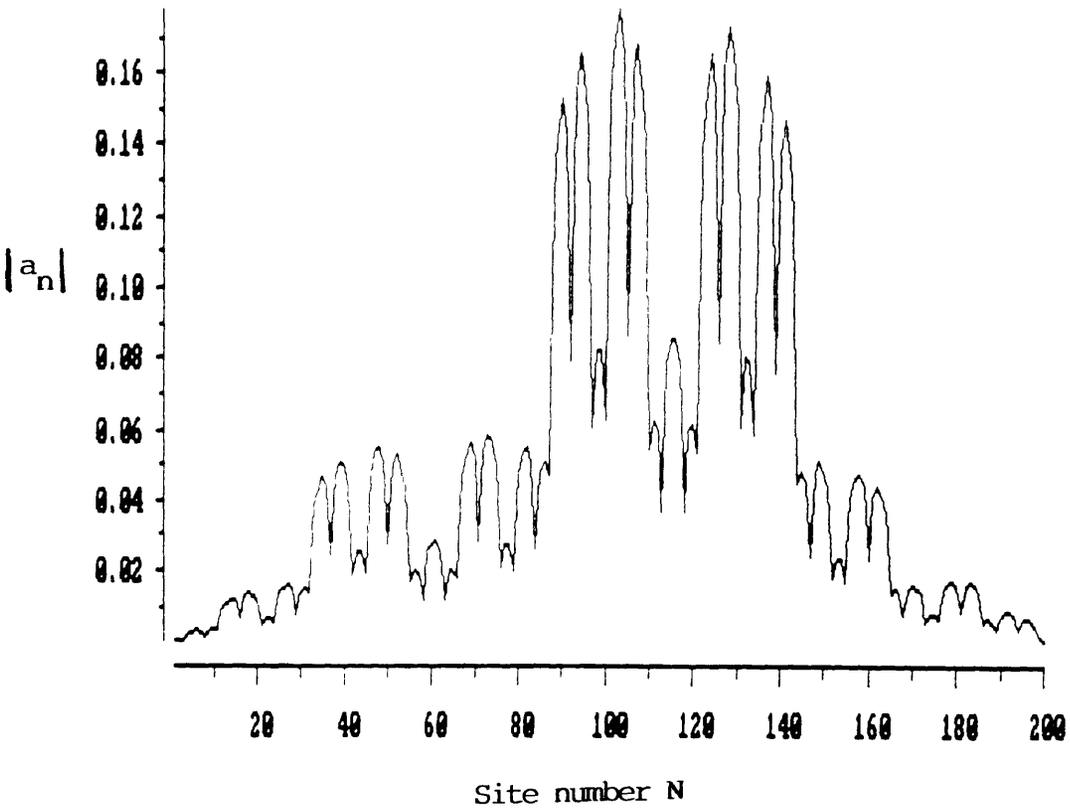


Fig 7.7c Same as Fig 7.7a but on an expanded scale to show that the self-similarity, holds to the smallest length scales.

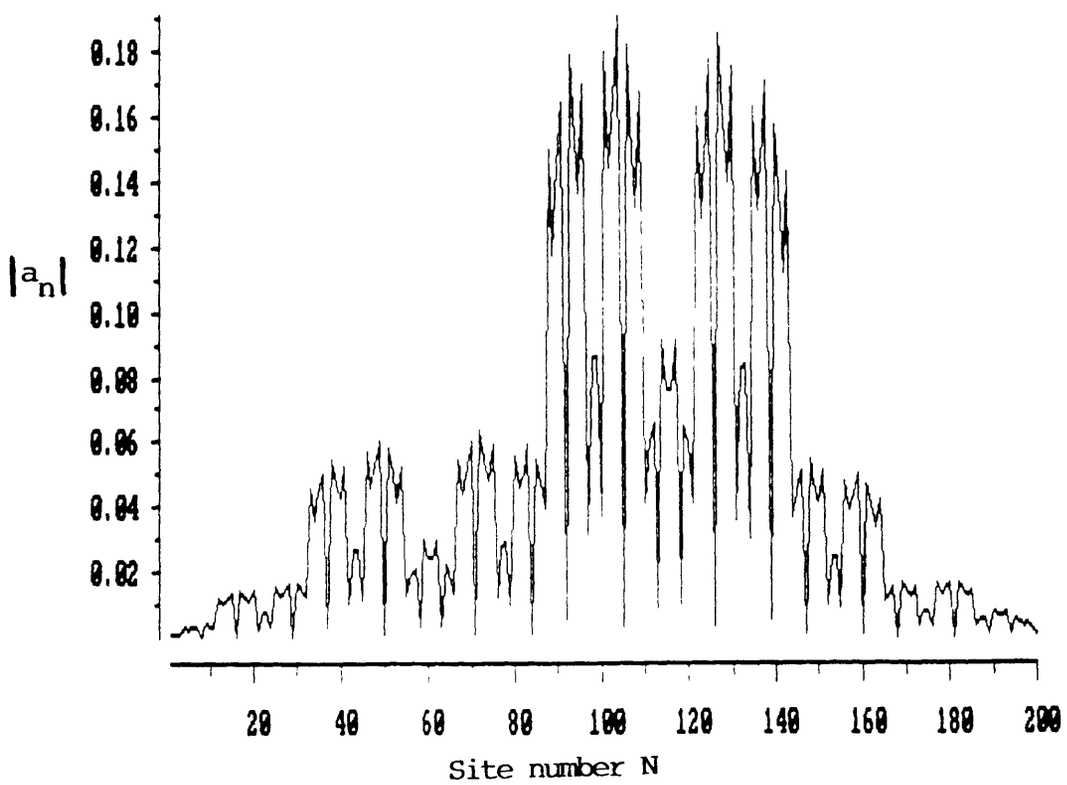


Fig 7.7d Same as 7.7b but at the edge of the middle sub-band of W_3.

$$F_n \approx \tau F_{n-1}$$

Hence $$F_{3(n+2)+6} \approx \tau^6 F_{3(n+1)+6}$$

The wavefunction is invariant under the transformation

$$n \rightarrow n\tau^6 \quad \text{and} \quad a_n \rightarrow r^2 a_n \qquad \{17.7\}$$

Thus the envelope of the wavefunction goes as

$$a \approx n^{\beta} \quad \text{where } \beta = \ln r / \ln \tau^3 \qquad \{18.7\}$$

notice that rescaling by a factor τ^6 is equivalent to going back six iterations in the deflation algorithm, so that the wavefunction is qualitatively self similar under an inflation or deflation of the lattice six times.

7.5.3 Wavefunctions at other points in the spectrum

Much of the self-similarity in the wavefunctions appears to be retained at other points in the spectrum. We have evaluated these by direct diagonalization of the Hamiltonian. Fig[7.7a] and fig[7.7c] show plots of the wavefunction at the edge of the spectrum, at different resolutions. As at the centre of the spectrum the wavefunction is highly self similar and it appears that successively larger peaks will continue to appear as we increase the size of the system, so these states are probably 'extended' as well. Fig[7.8] shows the behaviour of the participation number at the band edge as a function of system size, for $V_S/V_L = 2$. This leads to a fractal dimension, as defined in 7.5.1, of approximately 0.75, compared with 0.5 at the band centre, so it appears that the band edge states are 'more' extended then those at the centre. This is rather surprising as off diagonal disordered models in one dimension are known to be rather pathological at the band centre, where they exhibit a much larger conductance than at other points in the band.

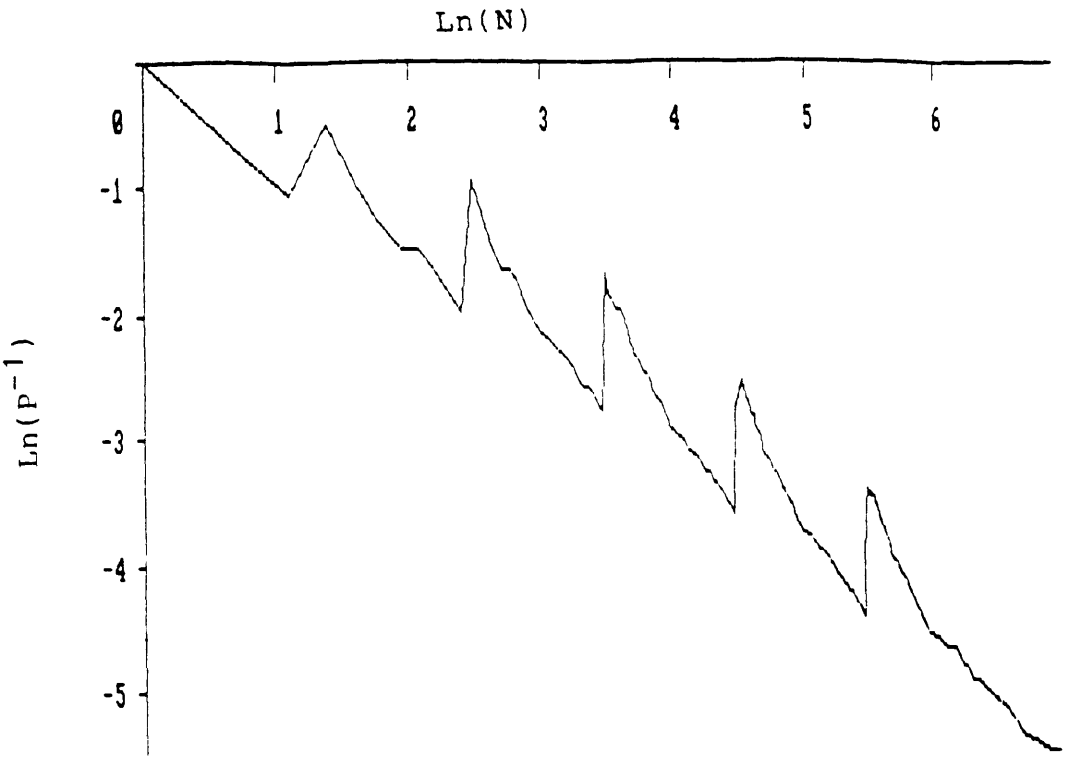


Fig 7.8 The Logarithm of the inverse participation number plotted against the logarithm of the number of sites, at the edge of the spectrum, V_S/V_L. = 2.

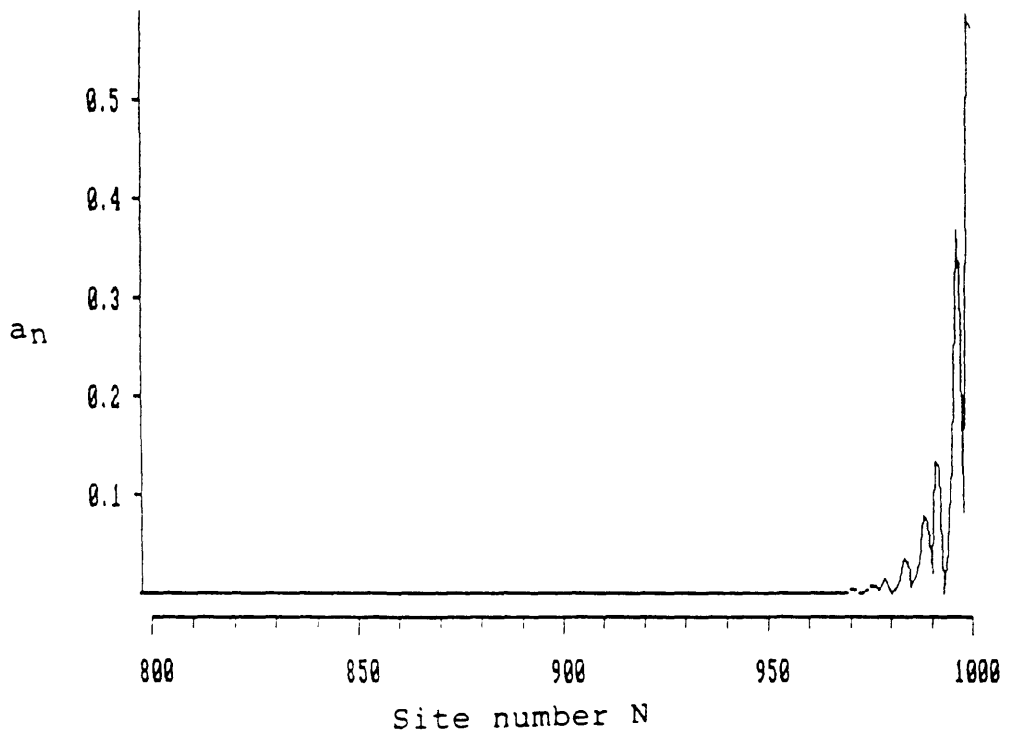


Fig 7.9 A Localized wavefunction, in the spectrum of the quasicrystal.

However not all wavefunctions of the quasicrystal are of the extended kind. Wavefunctions which are clearly localized, Fig[7.9], are found at some points in the spectrum.

7.5.4 Hierarchical symmetry of wavefunctions

We found in section 7.4 that the spectrum had a hierarchical structure in that certain sub-bands tend to split in the same way under an increasing resolution. Fig[7.*]. We have noticed that the modulus of the wavefunctions, at the edges of the sub-bands, are identical as far as their large scale features are concerned. This is shown in fig[7.7a] and fig[7.7b] which depict the moduli of the wavefunctions at the edges of the outermost sub-band at W_3, and fig[7.7d] which depicts the wavefunction at the edge of the middle sub-band at W_3, see fig[7.4]. This means that many of the states in the main band must have similar transport properties, as these are governed only by the large scale features of the wavefunction.

7.6 R.P.E for the self energy

The transport properties of the eigenstates of a system can be deduced by examining the convergence of the self energy, as in the original work of Anderson. The self energy Σ is defined by

$$G_{oo} = [(G^{o}_{oo})^{-1} - \Sigma]^{-1} \qquad \{19.7\}$$

and is known to be convergent on the real axis for localized states and oscillatory for extended states, because of the existence of a branch cut, Licciardello and Economou(1974). The self energy is essentially the shift in energy of a state when it is coupled to the rest of the system. The diagonal element of the Green's function at the end of one dimensional chain is given by eqn{A1.3} of chapter 3, ie

$$g_{n+1} = [Z - H^{o}_{n} - V^{2}_{n} g_{n}]^{-1} \qquad \{20.7\}$$

so for this element the self energy can be identified as

$$\Sigma(n+1) = V^{2}_{n} g_{n} \qquad \{21.7\}$$

Using {19.7} this can be expressed as a continued fraction

$$\Sigma(n) = \cfrac{V_n^2}{Z - \cfrac{V_{n-1}^2}{Z - \cfrac{V_{n-2}^2}{Z - \cfrac{V_{n-3}^2}{\ddots}}}} \qquad \{22.7\}$$

Now at the band centre of our model this takes a very simple form

$$\Sigma(n) = \frac{V_n^2}{V_{n-1}^2} \cdot \frac{V_{n-2}^2}{V_{n-3}^2} \cdots \qquad \{23.7\}$$

This product of ratios of V_n's is exactly that, which determines the amplitude of the wavefunction at site n, so

$$\Sigma(n) = | a_n |^2$$

We know from section 7.5.2 that as n increases successively larger peaks appear in the wavefunction so that asymptotically the self energy is not bounded. Hence this state cannot be localized. However the oscillations are not uniform, so that these states are probably not extended in the normal sense either. What these results, and those from the participation number indicate is that whether a state appears to be localized or extended depends to a great extent upon its length. As one approaches a peak in the wavefunction the self-energy appears to diverge, but on passing the peak it appears to converge, until it comes into the vicinity of another peak. Thus one has to be rather careful when calculating the transport properties of these states, as there is a very non uniform system size dependence.

7.7 Decimation of the quasicrystal

We saw in section 7.2 that the quasicrystal possesses inflation and deflation symmetry, in that the structure of the lattice is unchanged under the transformation

$$L \leftrightarrow LS \text{ and } S \leftrightarrow L$$

This suggests that it should be possible to implement a real space renormalization group scheme to investigate the critical properties of the system, such as the existence of the mobility edge. For the electronic problem it is convenient to decimate the Schrödinger equation rather than the partition function in order to obtain an effective Hamiltonian.

The basic idea consists of writing the Schrödinger equation in a tight binding form, and eliminating chosen sites. One then obtains a new effective Hamiltonian with

renormalized site energies and hopping elements. The important quantity as far as the transport properties of the chain are concerned is $(E-\varepsilon)/V$ the ratio of site energies to hopping elements. If $(E-\varepsilon)/V \rightarrow \infty$ as we decimate the system then the renormalized coupling tends to vanish, whilst the site energies remain finite. This means the system effectively decouples into isolated sites, which means that states at energy E must be localized, or we have an energy which lies in a gap. If $(E-\varepsilon)/V \rightarrow$ constant, then the site energies and hopping elements scale in the same way and the state at E must be extended. It is possible to show that this criterion is essentially Anderson's criterion concerning the convergence of the renormalized perturbation expansion for the self energy, José(1983).

We first illustrate the procedure for a perfect system, and then show how it extends to the quasicrystal.

The perfect system

The Schrödinger equation at site n has the form

$$(E-\varepsilon)a_n = Va_{n+1} + Va_{n-1} \qquad \{24.7\}$$

where a_n is the amplitude of the wavefunction at site n. Similarly at sites n-1 and n+1 we have

$$(E-\varepsilon)a_{n-1} = Va_{n-2} + Va_n$$

and $\qquad \{25.7\}$

$$(E-\varepsilon)a_{n+1} = Va_{n+2} + Va_n$$

eliminating a_{n-1} and a_{n+1} between eqn{24.7} and {25.7} we obtain

$$[(E-\varepsilon)^2 - 2V^2]a_n = V^2a_{n+2} + V^2a_n \qquad \{26.7\}$$

This has exactly the same form as our original equation, but with redefined couplings

$$E - \varepsilon \rightarrow [(E-\varepsilon)^2 - 2V^2] \qquad \{27.7\}$$

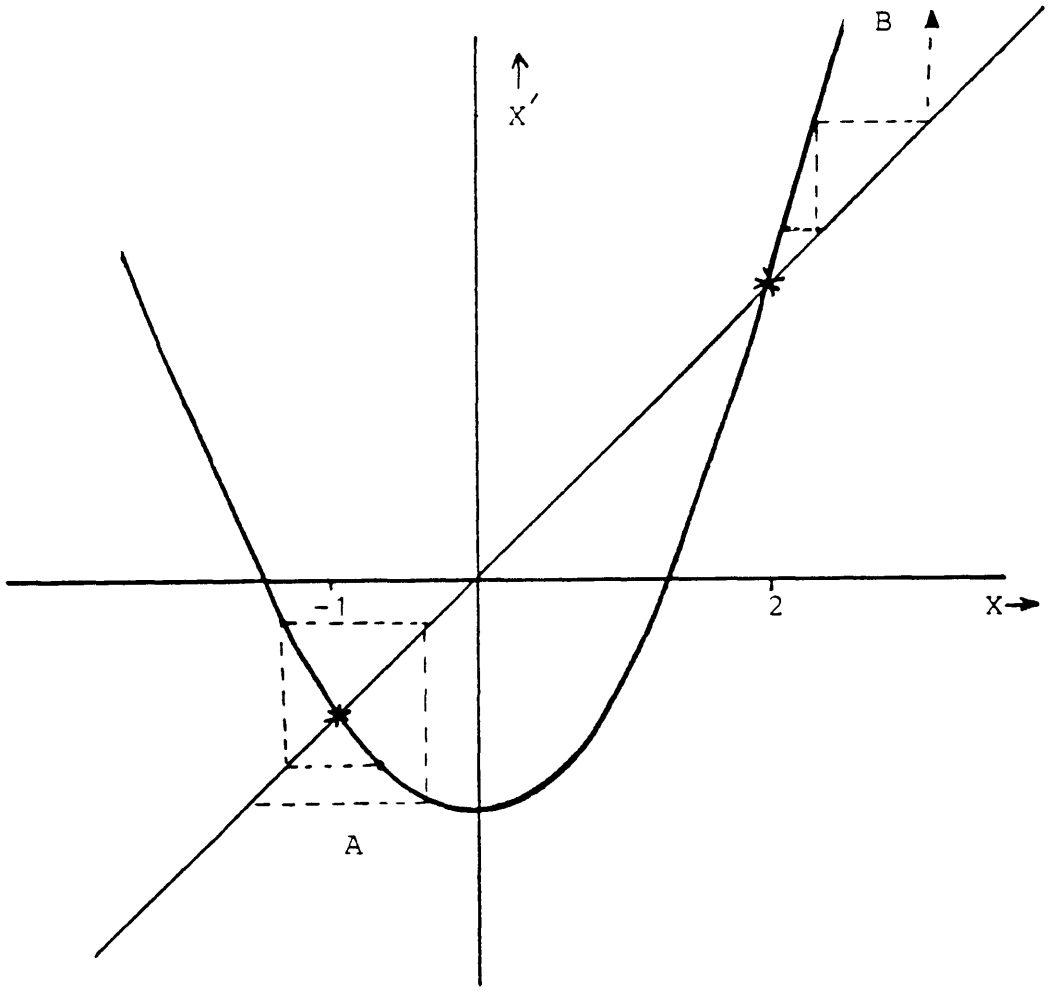


Fig 7.10 The standard map. Two typical trajectories are illustrated; A) a trajectory which starts within the band and cycles and B) a trajectory which starts outside the band and escapes.

and

$$V \dashrightarrow V^2$$

Thus on decimating every other site the form of the Hamiltonian remains invariant, and the couplings iterate in a simple manner. Defining $X = (E - \varepsilon)/V$ eqn's 4 and 5 can be combined to give the much studied standard map,

$$X' = X^2 - 2 \qquad \{28.7\}$$

This has two fixed points $X = 2$ and $X = -1$, which are both unstable. The existence of two repulsive fixed points can lead to a interesting dynamical structure, such as the existence of limit cycles. See Fiegenbaum(1979) . It is easy to see from fig[7.10] that if we start within the allowed energy band ie $-2 \leq X \leq 2$ then on iteration X remains in the interval -2 to 2, whilst if we start outside the band $|X| > 2$ we move off to infinity. Within the band we either end up at one of the fixed points, execute limit cycles of various length, or end up in essentially chaotic trajectories. In fact the map is known to be ergodic so that almost all initial conditions lead to a chaotic behaviour, except those that start with a value of $k = p/q$ that are irreducible with q odd, which lead to cycles of length q. This method does not distinguish between gaps or localized states, so we have to have some knowledge about the spectrum in order to check whether we have a state at an allowed energy or not.

The quasicrystal

In section 7.2 we saw that in the deflation algorithm, the n^{th} generation can be obtained from the $n+1^{th}$ by simply replacing all the sequences LS by L' and all the remaining L's by S'. This is clearly equivalent to decimating every atom between a long bond and a short bond, and the structure of the quasicrystal is preserved under this transformation. There are three different situations that have to be considered depending upon the three different local bond arrangements that can occur

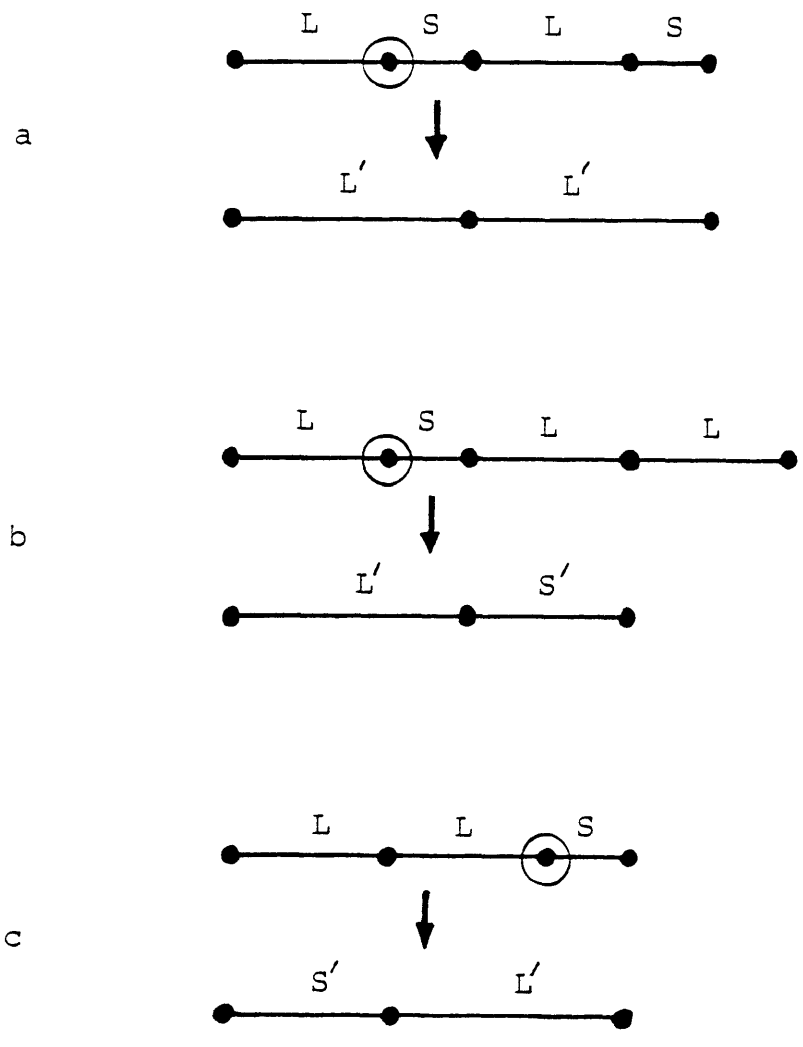


Fig 7.11 Decimating the quasicrystal. The three different situations are illustrated and the site to be decimated is circled in each case.

around a site that is to be decimated. This is illustrated in fig[7.11]. Thus a LS sequence can have another LS to its right in which case it decimates to an L'L'. It can have a L to its left in which case it decimates to a S'L' or it can have an LL to its right whereby it decimates to a L'S'. It is easily checked that these are the only three possibilities. If we denote a site by the sort of bonds that are to its immediate left and right then decimation leads to the following set of relations

$$X' = XY - V_S^2$$

$$Y' = XZ - V_L^2$$

$$Z' = XY - V_L^2 - V_S^2 \qquad \{29.7\}$$

$$V_S' = XV_L$$

$$V_L' = V_L V_S$$

where $X = E-\varepsilon_{LS}$, $Y = E-\varepsilon_{SL}$ and $Z = E-\varepsilon_{LL}$
Thus even if we start with a model with all site energies equal we will under iteration end up with a more generalised model in which there are three different kinds of masses. It is the structure of this more general model which is preserved under decimation and our model is a special case of it. Hence the properties of this more general model will be the same as those of the quasicrystal. Now under decimation we expect that the long bond will vanish first, if states are localized or if we lie in a gap, so we shall examine the quantities $(E-\varepsilon)/V_L$. Defining P, Q, T and R by

$$P = X/V_L \quad Q = Y/V_L \quad T = Z/V_L \quad \text{and} \quad R = V_S/V_L$$

the set of relations {29.7} can be transformed into a set in terms of these new variables.

$$P' = PQR - 1/R$$

$$Q' = PTR - R$$

$$T' = PQR - R - 1/R \qquad \{30.7\}$$

$$R' = 1/RP$$

These define a four parameter map in contrast to the one parameter map obtained for the ordered system. The important quantities are P, Q, and T. If they diverge on iteration then the Fermi level lies in gap or we have localized states. If they remain finite or exhibit some sort of cyclic behaviour then we have extended states.

Fixed points

As in the case of the perfect system the set of equations {30.7} lead to two fixed points

$$\begin{matrix} P \\ Q \\ T \\ R \end{matrix} = \begin{matrix} 1/\tau^2 \\ 1/\tau^2 \\ 2 \\ -\tau \end{matrix} \quad \text{and} \quad \begin{matrix} \tau^2 \\ \tau^2 \\ 2 \\ 1/\tau \end{matrix} \qquad \{31.7\}$$

Where τ is the golden ratio

Linearising the mapping around these leads to identical eigenvalues (τ^2, τ, -1 , $1/\tau^2$). Thus the fixed points are repulsive in two directions, marginal in one and attractive in the other. If we iterate to any of these fixed points we have extended states. It is found that in practice all initial conditions lead to diverging P, Q and T, which is consistent with the observation that the spectrum is empty. ie has a Cantor set structure. To check whether states are extended or localized, using this mapping we must pick an energy at which we know a state exists. In section 7.5.2 we found that the band centre E = 0 is always in the spectrum. Unfortunately at this energy the mapping is at its most unstable point and tends to oscillate between 0 and ∞, because of eqn{31.7}. These extreme oscillations may be characteristic of the unusual

behaviour of the band centre wavefunction (section 7.5.1), and are caused by the negative eigenvalue.

In conclusion, although we cannot say anything definite about the nature of the eigenstates, using this mapping, the existence of two fixed points which are partially repulsive seems to suggest that a bounded 'cyclic' behaviour could be possible for some initial conditions. Thus there could be extended states in the system.

Appendix 7.1 Properties of the transfer matrices for a quasicrystal

Consider the Schrödinger equation in its transfer matrix form

$$M_n U_n = U_{n+1}$$

where

$$M_n = \begin{bmatrix} E/V_n & -V_{n-1}/V_n \\ -1 & 0 \end{bmatrix} \qquad \{A1.7.1\}$$

and

$$U_n = \begin{bmatrix} a_n \\ a_{n-1} \end{bmatrix}$$

Let us construct a periodic system by taking a word W_1 and repeating it. For diagonal disorder the transfer matrices T_1 corrosponding to the word W_1 satisfy a similar recursion relation to that satisfied by the words W_1, as each transfer matrix depends only upon the site energy at a single point. All the V's are identical.

From 7.2 we have $W_n = W_{n-1}W_{n-2}$

Transfer matrices act to the right and so they obey the relation

$$T_n = T_{n-2}T_{n-1} \qquad \{A2.7.1\}$$

For off diagonal disorder this is no longer true as the transfer matrices depend upon the previous as well as present bond eqn{A1.7.1}. This means for example $T_5 = T_3T_4$. However a relation similar to {A2.7.1} can be obtained if one inverts all the words W_1.

L		L
LS		SL
LSL	--->	LSL
LSLLS		SLLSL

The rule for generating successive inverted words W_n' is now

$$W_n' = W_{n-2}'W_{n-1}' \qquad \{A3.7.1\}$$

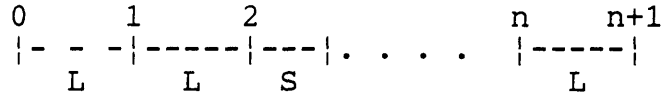
The effect of this is that all the transfer matrices for the inverted words T_n' can now be calculated assuming a long bond to the left, and will thus satisfy the relation

$$T_n' = T_{n-1}'T_{n-2}' \qquad \{A4.7.1\}$$

Thus $$U_{n+1} = T_n'U_1 \qquad \{A5.7.1\}$$

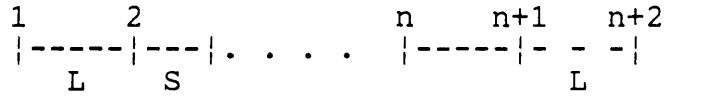
with $U_1 = (1,0)$ if we have free boundaries.

This corresponds for example to the situation



fig[A1.7.1]

Where there is a fictitious L bond to the left. The situation we really wish to describe is the inverse one, in which we transfer from n+1 ->1 as this corresponds to the original word. ie



fig[A2.7.1]

Where we now need to introduce a fictitious L bond to the right.

This is easily done by adding a fictitious L bond to the right of fig[A1.7.1] to extend the system to the site n+2 and then inverting {A5.7.1}.

Thus $$U_{n+2} = M_L T_n' U_1 \qquad \{A6.7.1\}$$

where $$M_L = \begin{bmatrix} 0 & -1 \\ 1 & 0 \end{bmatrix} \qquad \{A7.7.1\}$$

Hence $$U_1 = T_n'^{-1} M_L^{-1} U_{n+2} \qquad \{A8.7.1\}$$

where we must choose $U_{n+2} = (0,1)$. $M_L^{-1} = -M_L$ and simply inverts the initial vector. This solves the problem of describing the original word.

If we denote $T_n = T_n'^{-1}$ then the recurrence relation {A4.7.1} becomes

$$T_n = T_{n-2} T_{n-1} \qquad \{A9.7.1\}$$

The matrices T_n satisfy a six cycle in analogy to those of Kohmoto and Banavar(1986).

ie $$T_{n+6} = T_n \qquad \{A10.7.1\}$$

The first six matrices T_n are given by

$$T_1 = \begin{bmatrix} 0 & 1 \\ -1 & 0 \end{bmatrix} \qquad T_2 = \begin{bmatrix} -1/r & 0 \\ 0 & -r \end{bmatrix}$$

$$T_3 = \begin{bmatrix} 0 & -r \\ 1/r & 0 \end{bmatrix} \qquad T_4 = \begin{bmatrix} 0 & 1 \\ -1 & 0 \end{bmatrix} \qquad \{A11.7.1\}$$

$$T_5 = \begin{bmatrix} r & 0 \\ 0 & 1/r \end{bmatrix} \qquad T_6 = \begin{bmatrix} 0 & 1/r \\ -r & 0 \end{bmatrix}$$

where $r = V_S/V_L$

Appendix 7.2 Trace mapping for the quasicrystal

Consider constructing periodic systems with a unit cell corresponding to successive approximants to the Quasicrystal. The spectrum of these systems consists of a set of bands and Bloch's theorem tells us that if we pick an energy E which lies in a band the eigenvalues of the transfer matrix T_1 for a unit cell must be of modulus unity. Since we have a 2 by 2 matrix the trace satisfies

$$X_1 = 1/2|\mathrm{Tr}\ T_1| < 1 \qquad \{A1.7.2\}$$

If $X_1 > 1$ we are in a gap. Thus the spectrum can be examined by studying X_1. Now the matrices T_1 satisfy the relation eqn{A4.7.1}

$$T_n' = T_{n-1}' T_{n-2}' \qquad \{A4.7.1\}$$

for the inverted words. It does not matter that the words are inverted since we have periodic boundary conditions.

Kohmoto et al(1983) have shown that this relation can converted into one for the traces of these matrices.

$$X_{l+1} = 2X_l X_{l-1} - X_{l-2} \quad \text{where } X_l = 1/2\mathrm{tr}\ T_l \qquad \{A2.7.2\}$$

This remarkable relation allows one to study the problem as a discrete dynamical map. A point which lies in an allowed energy state of the final system would presumably cycle between -1 and +1, whilst those that do not, will diverge on iteration. They were also able to show that the map had an invariant Γ^2 given by

$$X_n^2 + X_{n-1}^2 + X_{n-2}^2 - 2X_n X_{n-1} X_{n-2} - 1 = \Gamma^2 \qquad \{A3.7.2\}$$

This defines a surface in the three dimensional space (X_n, X_{n-1}, X_{n-2}) upon which the trace mapping moves. The major difference from the model of Kohmoto et al comes in the initial conditions for this mapping. For our model these become

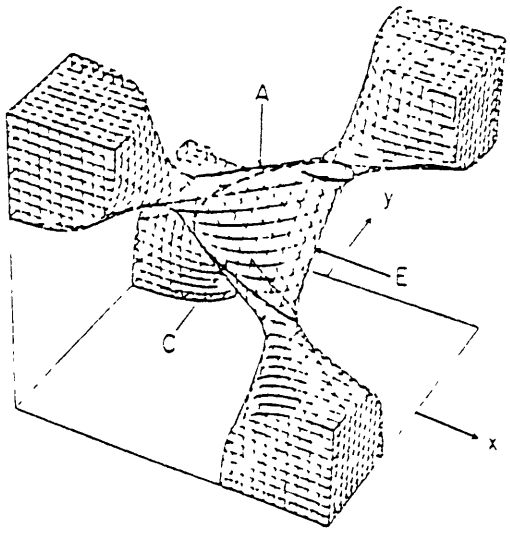


Fig A2.7.1 The manifold upon which the trace mapping moves (from the paper of Kohmoto).

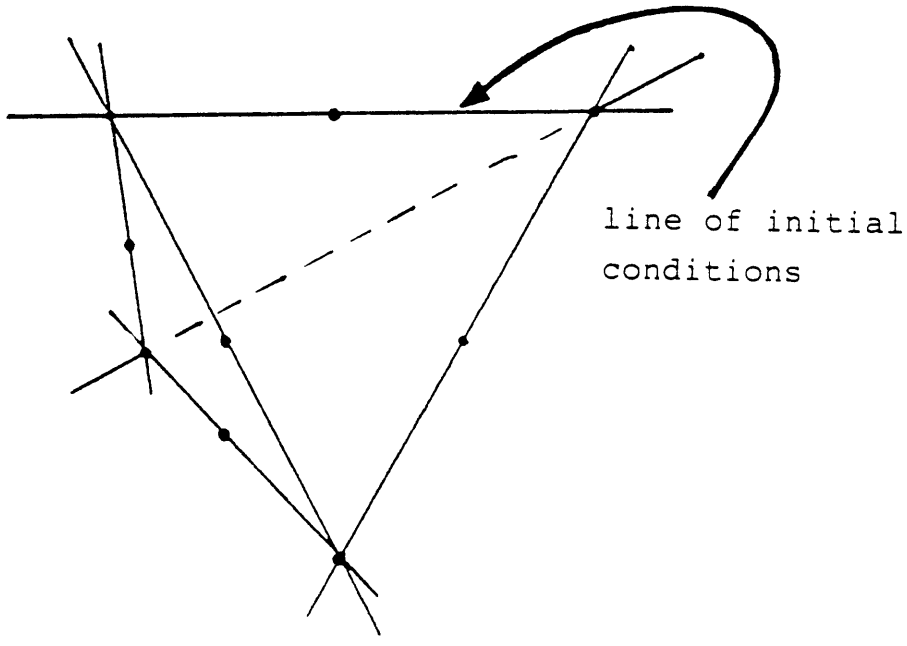


Fig A2.7.2 The manifold for a perfectly ordered system.

$$X_{-1} = 1/2(V_L/V_S + V_S/V_L)$$

$$X_0 = E/2V_S \qquad \{A4.7.2\}$$

$$X_1 = E/2V_L$$

which lead to

$$\Gamma^2 = 1/4(V_L/V_S + V_S/V_L)^2 - 1 \qquad \{A5.7.2\}$$

This surface is shown in fig[A1.7.2]. It is instructive to look at the ordered case $V_L = V_S = 1$, $\Gamma^2 = 0$. Now the open part of the manifold fig[A2.7.2] is essentially pinched off so that all points which start in a band remain in a band.

If the V's differ then the manifold opens up, and escaping orbits are possible. Numerically for the quasicrystal the mapping is found to escape everywhere which implies that the measure of the spectrum is zero.

Kohmoto and Oono(1984) have shown that for their model the scaling of the spectrum is governed by a six cycle of the mapping which visits the saddle points of the manifold. The positions of these saddle points are given by (0,0,a), (-a,0,0), (0,-a,0), (0,0,-a), (0,0,-a), (a,0,0) and (0,a,0).

where $a = (1 + \Gamma^2)^{\frac{1}{2}} = \frac{1}{2}(V_L/V_S + V_S/V_L)$ $\{A6.7.2\}$

For our model this implies that at E = 0 the initial conditions eqn{A4.7.2} fall onto the first of these saddle points, so that the band centre is always an allowed energy. Since most of the spectrum is gap it is important that we can identify a point which is always in the spectrum, if we are going to examine the properties of the electronic wavefunctions.

The proof that the spectrum is self similar and a Cantor set is related to the properties of the manifold,

which are rather complex. There is essentially an embedded horseshoe dynamics in the map. The reader is referred to the original paper for more details.

References

Abrahams E, P. W. Anderson, D. C. Licciardello, and T. V. Ramakrishnan(1979) Phys. Rev. Lett. 42, 673.

Altshuler B. L. (1985) JETP Lett 41, 648.

Anderson P .W.(1958) Phys. Rev. 109, 1492.

Anderson P. W.(1978) Rev. Mod. Phys. 50(2), 191.

Anderson P. W., E. Abrahams and T. V. Ramakrishnan(1979) Phys. Rev. Lett. 43, 718.

Anderson P. W., D. J. Thouless, E. Abrahams and D. S. Fisher(1980) Phys. Rev. B22 3519.

Anderson P. W. (1981) Phys. Rev. B23, 4828.

Anderson P. W. and P. A. Lee(1981) Supp. of Prog. of Theo. Phys 69, 212.

Aubry S. and S. Andre(1980) Ann Israel Phys. Soc.

Aubry S. (1986) J.Phys. Colloques. Proc. Les Houches workshop on Quasicrystals.

Azbel M. Ya. (1983) Phys. Rev. B28, 4106.

Bell R. J. and P. Dean(1970) Disc. Faraday Soc. 50, 51.

Bergmann G. (1984) Phys. Rep. 107, 1.

Brezin E. and G. Parisi(1980) J. Phys. C13, L307.

Bütticker M , Y. Imry, R. Landauer and S. Pinhas(1985) Phys. Rev. B31, 6207.

Chase K. S. and A. MacKinnon(1985) Festkörperprobleme/ Advances in Solid State Physics XXV, 475.

Economou E. N. and M. H. Cohen(1972) Phys. Rev. B5, 2931.

Economou E. N. and C. M. Soukoulis(1981) Phys. Rev. Lett. 46, 618.

Economou E. N. (1983) Green's functions in Quantum Physics,(Springer-Verlag).

Economou E. N. and C. M. Soukoulis(1984) Phys. Rev. Lett. 52, 565.

Edwards J. T. and D. J. Thouless(1972) J.Phys. C5, 807.

Efetov K. B. (1984) JETP Lett. 40, 738.

Efetov K. B. (1985) Sov. Phys. JETP 62(3), 605.

Erdös P. And R. C. Herndon(1982) Adv. Phy. 31, 65.

Fisher D. S. and P. A. Lee(1981) Phys. Rev. B23, 6851.

Fowler A. B. , G. L. Timp, J. J. Wainer and R. A. Webb(1986) Phys. Rev. Lett. 57, 138.

Gorkov L. P., A. I. Larkin and D. E. Khmelnitskii(1979) JETP Lett 30, 248.

Gorkov L. P., O. N. Dorokov and F. V. Prigara(1983), JETP 58(4) 852.

Hikami S. (1981) Phys. Rev. B24, 2671.

Imry Y. (1980) Phys. Rev. B24, 1107.

Ioffe L. B., I. R. Sagdeev and V. M. Vinokur(1985) J.Phys C18, L641.

Johnston R. and H. Kunz(1983) J.Phys. C16, 4565.

Jose J. V.(1982) Proc. Latin American Summer School, Cali, Columbia, ed B. Gomez(World Scientific) 1983.

Kapitulnik A. and Y. Shapir(1983) J.Phys. A16, L 243

Kirkman P. D.(1984) Phd Thesis, Imperial College.

Kirkman P. D. and J. B. Pendry(1984) J.Phys. C17, 4327.

Kirkman P. D. and J. B. Pendry(1984) J.Phys. C17, 5707.

Kohmoto M. and Y. Oono(1984) Phys. Lett. A102, 145.

Kohmoto M. , L. P. Kadanoff and C. Tang(1983) Phys. Rev. Lett. 50, 1870.

Kohmoto M. and J. Banaver(1986) Phys. Rev. B34, 563.

Kramer B. (1985) in Localization, Interaction and Transport phenomena (Springer-Verlag)

Kunz and Souillard(1980), Commun. Math. Phys. 78, 201.

Landauer R. (1970) Philos. Mag. 21, 863.

Landauer R. (1985) in Localization, Interaction and Transport phenomena (Springer-Verlag)

Langreth D. C. and E. Abrahams(1981) Phys. Rev. B24, 2987.

Lee P. A. and T. V. Ramakrishnan(1985) Rev. Mod. Phys. 57(2), 287.

Lee P. A. And A. D. Stone(1985) Phys. Rev. Lett. 55, 1622.

Levine D., and P. J. Steinhardt(1985) Preprint(to appear in Phys. rev.).

Licciardello D. C. and D. J. Thouless(1975) J.Phys. C8, 4157.

Liftshitz I. M. (1964) Adv. Phys. 13, 483.

MacKinnon A.(1980) J.Phys. C13, L1031.

MacKinnon A. and B. Kramer(1981) Phys. Rev. Lett 47, 1546.

MacKinnon A. and B. Kramer(1983) Z. Phys. B53, 1.

MacKinnon A. (1985) Z. Phys. B59, 385.

Mahan G. D. (1981) Many Particle Physics(Plenum Press).

Merlin R., K. Bajema, R. Clarke, F. T. Juang and P. K. Bhattacharya(1985) Phys. Rev. Lett. 55, 1768 .
Mott N. F. and W. D. Twose(1961) Adv. Phys. 10, 107.
Nozières and Pines, The theory of interacting Fermi systems (Academic press).
Castellani C. and L. Peliti(1986) J.Phys. A19, L249.
Pendry J. B. (1982) J.Phys. C15, 4821, and C15, 5773.
Pendry J. B.(1984) J.Phys. C17, 5317.
Pichard J. L. and G. Sarma(1981) J.Phys. C14, L127.
Rivier N.(1986) J.Phys. Colloques. Proc. Les Houches workshop on Quasicrystals.
Sak J. and B. Kramer(1981) Phys. Rev. B24, 1071.
Schreiber M. (1985) Phys. Rev. B31, 6146.
Sokoloff J. B.(1985) Phys. Rep. 126(4), 189.
Sharvin D. Y. and Y. V. Sharvin(1981) JETP Lett. 34,272.
Shechtman D. , I. Blech, D. Gratias, J. W. Cahn(1984) Phys. Rev. Lett. 53,1951.
Thouless D. J. (1974) Phys. Rep. 13C, 3, 93.
Thouless D. J. (1979) Ill Condensed Matter I, ed. R. Balian, R. Maynard and G. Toulouse(North-Holland)
Thouless D. J. and S. Kirkpatrick(1981) J.Phys. C13, L1031.
Thouless D. J. (1981) Phys. Rev. Lett. 47, 13, 972.
Thouless D. J. (1985) Lecture notes, Ill condensed matter II, Les Houches, 1985.
Wegner F. J. (1979) ZPhys. B35, 207.
Wegner F. J. (1981) Zphys. B44, 9